DOE/NV/0000939-38

Project 57 Air Monitoring Report: January 1 through December 31, 2015

Prepared by

Steve A. Mizell, George Nikolich, Craig Shadel, Greg McCurdy, and Julianne J. Miller

Submitted to

Nevada Field Office
National Nuclear Security Administration
U.S. Department of Energy
Las Vegas, Nevada

January 2017

Publication No. 45272

Nevada System of Higher Education

DOE/NV/0000939-38

Project 57 Air Monitoring Report: January 1 through December 31, 2015

Prepared by

Steve A. Mizell, George Nikolich, Craig Shadel, Greg McCurdy, and Julianne J. Miller

Desert Research Institute
Nevada System of Higher Education

Publication No. 45272

Submitted to

Nevada Field Office
National Nuclear Security Administration
U.S. Department of Energy
Las Vegas, Nevada

January 2017

The work upon which this report is based was supported by the U.S. Department of Energy under Contract #DE-NA0000939. Approved for public release; further dissemination unlimited.

THIS PAGE INTENTIONALLY LEFT BLANK

EXECUTIVE SUMMARY

On April 24, 1957, the Atomic Energy Commission (AEC, now the Department of Energy [DOE]) conducted the Project 57 safety experiment in western Emigrant Valley north east of the Nevada National Security Site (NNSS, formerly the Nevada Test Site) on lands withdrawn by the Department of Defense (DOD) for the Nevada Test and Training Range (NTTR). The test was undertaken to develop (1) a means of estimating plutonium distribution resulting from a non-nuclear detonation; (2) biomedical evaluation techniques for use in plutonium-laden environments; (3) methods of surface decontamination; and (4) instruments and field procedures for prompt estimation of alpha contamination (Shreve, 1958). Although the test did not result in the fission of nuclear materials, it did disseminate plutonium across the land surface. Following the experiment, the AEC fenced the contaminated area and returned control of the surrounding land to the DOD. Various radiological surveys were performed in the area and in 2007, the DOE expanded the demarked Contamination Area by posting signs 200 to 400 feet (60 to 120 meters) outside of the original fence.

Plutonium in soil attaches preferentially to smaller particles (Tamura, 1985; Friesen, 1992; Murarik *et al*., 1992; and Misra *et al*., 1993). Therefore, redistribution of soil particles by wind (dust) is the mechanism most likely to transport plutonium beyond the boundary of the Project 57 Contamination Area. Monitoring was implemented in 2011 by Desert Research Institute (DRI) to determine if radionuclide contamination was detectable in samples of airborne dust and characterize meteorological and environmental parameters that influence dust transport. Collected data also permits a comparison of radiological conditions at the Project 57 monitoring stations to conditions observed at Community Environmental Monitoring Program (CEMP) stations around the NTTR that are operated by DRI for the Department of Energy (DOE). Initially, two monitoring stations consisting of radiological, meteorological, and dust sampling equipment were installed near the southeast and northeast corners of the Contamination Area. In January 2015, the original monitoring stations were dismantled and moved further to the west along the Contamination Area boundary. This move was made to place the monitoring stations downwind of the ground zero and High Contamination Area during the dominant northerly and southerly winds.

Biweekly samples of particles suspended in the air are submitted for laboratory assessment of gross alpha and gross beta radioactivity and for determination of gamma-emitting radionuclides. The mean gross alpha concentration at Project 57 monitoring station 3 (P57-3) is slightly higher than, but on the same order of magnitude as, the mean concentrations at surrounding CEMP stations. The mean gross alpha concentration for P57-4 is notably higher than the mean concentration for surrounding CEMP stations. The mean gross beta concentration for the Project 57 stations is essentially the same as the mean concentrations determined for the CEMP stations. Gamma spectroscopy analyses identified only naturally occurring radionuclides in all but one sample. Americium 241 was reported in the sample from P57-4 collected June 23, 2015. The subsequent sample collected on July 7, 2015, was determined to have a gross alpha concentration somewhat higher than the mean. Both samples were analyzed further to determine the concentration of plutonium 238 and plutonium 239+240.

The June 23, 2015, sample from P57-4 and the sample collected from P57-3 on April 15, 2015, also had higher than average gross alpha concentrations. Both samples were determined to be associated with unique wind conditions. On April 14, 2015, a major dust storm

was observed approaching the monitoring stations. Samples were collected on April 15th to ensure the radiological data was associated with the observed dust storm. This storm front was observed in the meteorological data by a sharp change in wind direction and a rapid increase in wind speed. There was no evidence of a significant wind event in the 10-minute average data normally used for analysis. However, when the 3-second instantaneous wind condition observations were analyzed, it appeared that several dust devils had passed almost directly across the monitoring station. The above normal radionuclide values are associated with wind conditions representing the extreme of conditions observed at the monitoring stations.

Soil material is also transported by saltation, a wind driven phenomena that bounces soil particles, too heavy to be suspended in air, across the land surface. Samples of particles transported by saltation were collected downwind and upwind of the Contamination Area at both monitoring stations. The mass of collected material was greater in traps facing the northerly winds suggesting that although saltation material may be moving back and forth under the two dominant wind directions, there is a net trend for saltation material to be transported toward the south. Radionuclide concentrations for material transported by saltation were 2 to 4 times higher in samples collected in traps facing the Project 57 Contamination Area compared to samples collected in traps facing away from the Contamination Area. This result suggests that saltation may not be transporting radionuclide-contaminated soil material significant distances but that the opposing dominant wind directions are moving the saltation material back and forth over a limited area.

Thermoluminescent dosimeters (TLDs) indicated that the average annual external radioactivity dose at the monitoring stations is higher than the dose determined at surrounding CEMP stations (NSTec, 2016) but approximately half of the estimated national average dose received by the general public as a result of exposure to natural sources. The TLDs at the Project 57 monitoring stations are exposed to both natural sources (terrestrial and cosmic) and radioactive releases from the Project 57 Contamination Area.

Winds in excess of approximately 15 mph (24.1 km/hr) begin to generate dust movement by saltation (migration of sand at the ground surface) or suspension in the air. Saltated sand, PM_{10} (inhalable) dust, and $PM_{2.5}$ (fine particulate dust) exhibit an approximately exponential increase with increasing wind speed. The greatest concentrations of dust occur for winds exceeding 20 mph (32.2 km/hr). When the wind/dust analysis is performed for winds separated into the dominant wind directions, northerly and southerly, it is evident that at wind speeds above 25 mph (40.2 km/hr) the northerly winds generate more PM_{10} dust than the southerly winds.

A preliminary assessment of individual wind events suggests that dust generation is highly variable, likely because of the influence of other meteorological and environmental parameters. Additionally, during the reporting period, winds in excess of 20 mph (32.2 km/hr) occurred a little more than 3 percent of the time at station P57-3 and a little less than three percent of the time at station P57-4. Although winds sufficient to generate significant amounts of dust occur at the Project 57 site, they are infrequent and of short duration. Additionally, the potential for wind transport of dust is dependent on other parameters whose influence have not yet been assessed.

CONTENTS

LIST OF FIGURES

LIST OF TABLES

LIST OF ACRONYMS

AEC	Atomic Energy Commission
Am-241	americium 241
Be-7	beryllium 7
BSNE	Big Spring Number Eight
CA	Contamination Area
CAS	Corrective Action Site
CAU	Corrective Action Unit
CEMP	Community Environmental Monitoring Program
cfm	cubic feet per minute
cps	counts per second
CY	calendar year
DOD	U.S. Department of Defense
DOE	U.S. Department of Energy
DRI	Desert Research Institute
HCA	High Contamination Area
K-40	potassium 40

lpm	liters per minute
mph	miles per hour
mR	millirem
NAFR	Nellis Air Force Range
NFO	Nevada Field Office
NNSA	National Nuclear Security Administration
NNSS	Nevada National Security Site
NSTec	National Security Technologies
NTTR	Nevada Test and Training Range
P57-1	Project 57 monitoring station 1
P57-2	Project 57 monitoring station 2
P57-3	Project 57 monitoring station 3
P57-4	Project 57 monitoring station 4
Pb-210	lead 210
$PM_{2.5}$	particulate matter less than 2.5 µm
PM_{10}	particulate matter less than 10 µm
Pu-238	plutonium 238
Pu-239+240	plutonium 239+240
Pu-241	plutonium 241
RCT	radiological control technician
RMA	radiological material area
TLD	thermoluminescent dosimeter
µCi/ml	microcurie per milliliter
$\mu g/m^3$	microgram per cubic meter
µm	micrometers

THIS PAGE INTENTIONALLY LEFT BLANK

INTRODUCTION

During the late 1950s, the Atomic Energy Commission (AEC) (now the U.S. Department of Energy [DOE]) conducted a series of safety experiments to determine if a nuclear device subjected to a large conventional explosives detonation would result in a nuclear yield. The AEC obtained temporary use of a large portion of western Emigrant Valley from the U.S. Department of Defense (DOD) for one of these experiments, Project 57. Following the Project 57 safety experiment, the AEC fenced the contaminated area and returned control of the surrounding land to the DOD.

Emigrant Valley is part of the Nevada Test and Training Range (NTTR, formerly the Nellis Air Force Range [NAFR]). For safety and security reasons, access to the NTTR is controlled through the use of both physical (i.e., fences) and administrative (e.g., signs and postings) controls. Therefore, the public cannot access the Project 57 site and there are no known human receptors with routine access to the site.

Project 57 was detonated on April 24, 1957, in Emigrant Valley approximately 13 miles (21 kilometers) northeast of the north end of Yucca Flat (Figure 1). This test was undertaken to develop (1) a means of estimating immediate distribution and long-term redistribution of plutonium dispersed during a non-nuclear detonation; (2) biomedical evaluation techniques for use in likely plutonium-laden environments; (3) methods of decontamination of ground areas, pavements, and building materials; and (4) alpha survey instruments and field monitoring procedures to promptly estimate contaminant deposition (Shreve, 1958). Data collection stations were distributed on a variable-scale rectangular grid pattern that extended approximately 9.5 mi (15.3 km) north of the ground zero detonation point and encompassed a total of approximately 64.5 mi^2 (167 km^2). Although the test did not result in the fission of nuclear materials, it did disseminate plutonium across the ground surface.

Various radiological surveys have been performed in the area since Project 57 was conducted. The original fence constructed by the AEC to control access to Project 57 (Figure 2) delineated the initial Contamination Area and was located based on radioactivity surveys performed shortly after the Project 57 test was conducted. The distribution of americium 241 (Am-241) in the area was determined in a 1997 flyover (written communication from Navarro to Desert Research Institute [DRI], 2010) and showed Am-241 concentrations ranging from as much as 70,000 counts per second (cps) at ground zero to background values. This survey documented Am-241 concentrations on the ground surface beyond the east side Contamination Area fence at levels of up to 150 cps. In 2007, the DOE expanded the Contamination Area by posting “Contamination Area” signs 200 to 400 feet (60 to 120 meters) outside of the original fence, which formed a new, concentric Contamination Area boundary. Americium 241 concentrations in the range of 70 to 150 cps are observed in the 1997 airborne survey data to extend beyond the east side of the new Contamination Area boundary (Figure 2).

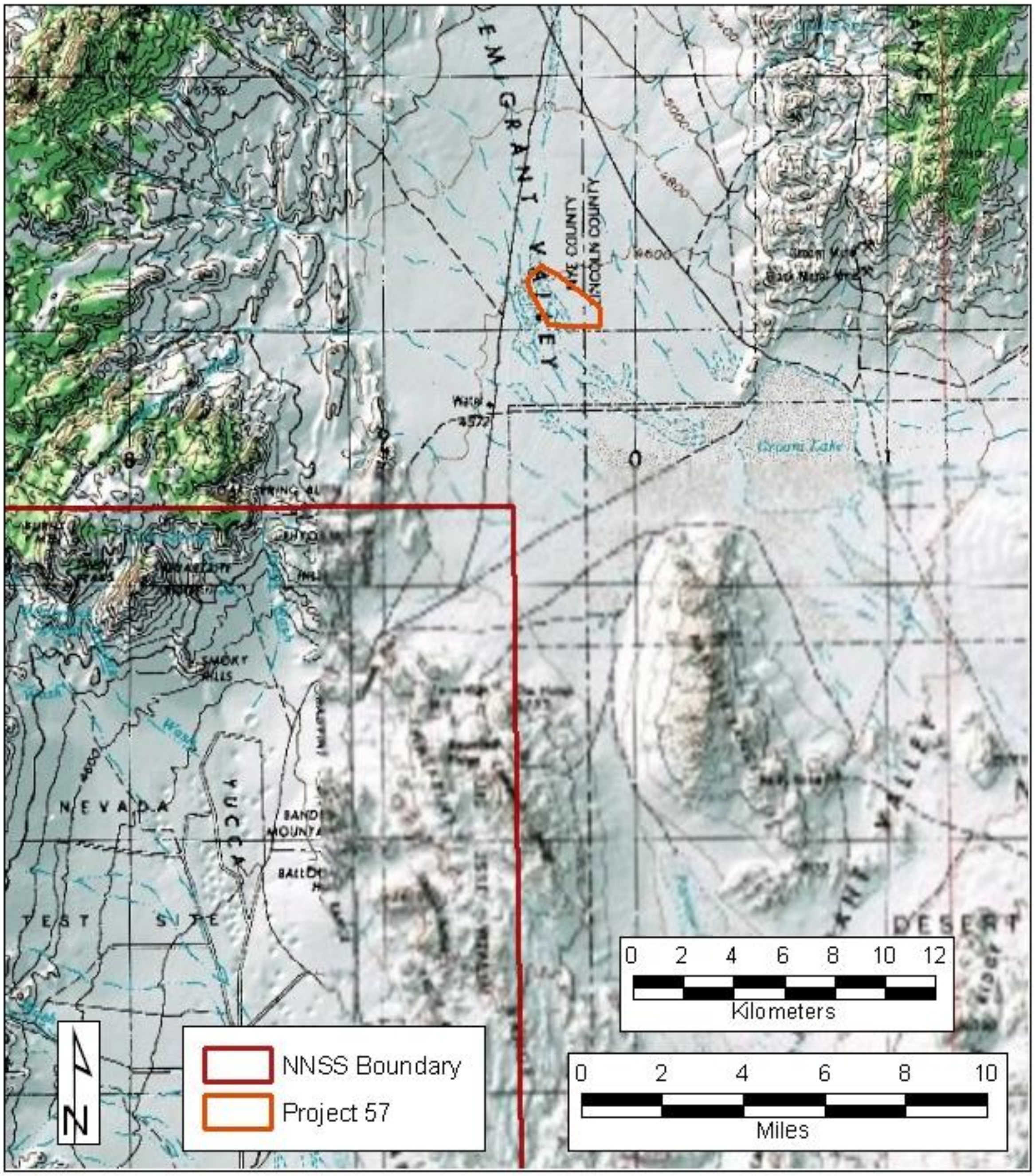

Figure 1. Project 57, outlined in orange, is off of the northeast corner of the Nevada National Security Site on the Nevada Test and Training Range at the Lincoln/Nye County border in western Emigrant Valley.

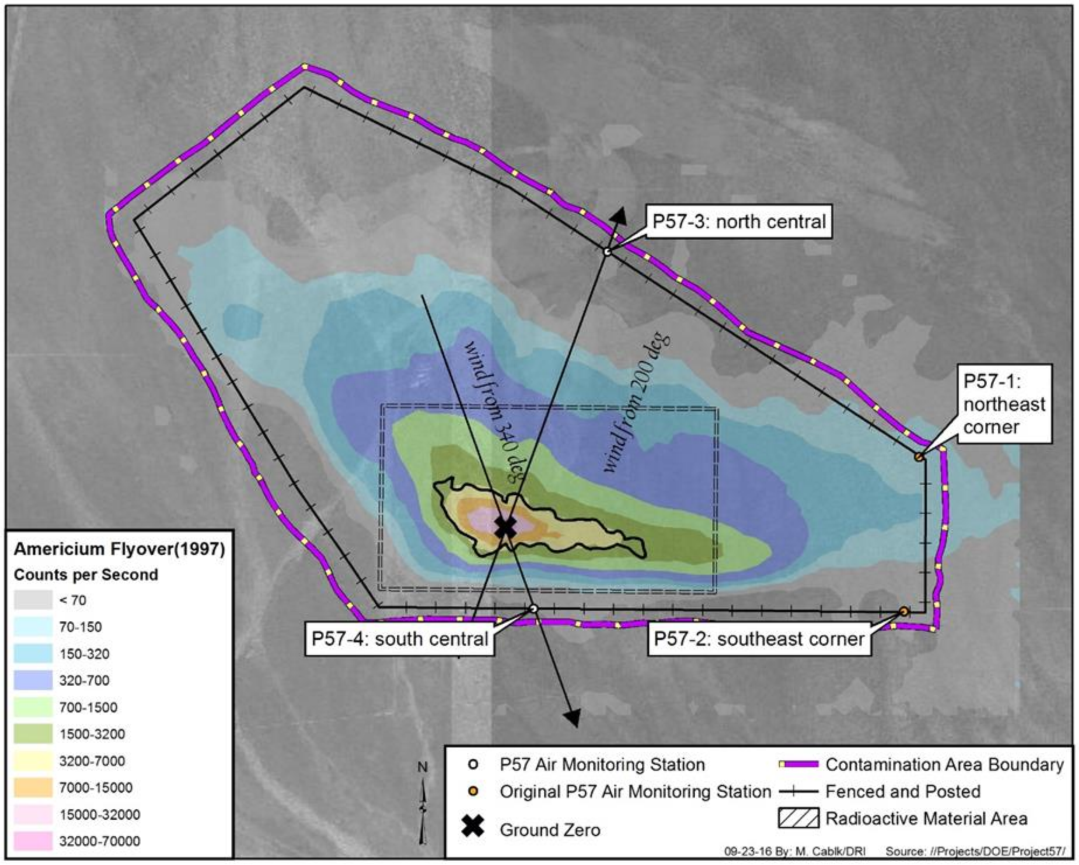

Figure 2. Locations of the original monitoring stations, P57-1 and P57-2, and those downwind of ground zero, P57-3 and P57-4 are shown in relation to the americium 241 concentrations measured during the 1997 flyover survey (from Navarro [2010]) and the original and 2007 Contamination Area boundaries.

The DOE, National Nuclear Security Administration, Nevada Field Office (NNSA/NFO) is currently working to achieve regulatory closure of radionuclide-contaminated soil sites under its purview. With respect to closure efforts, the Project 57 Contamination Area is designated Corrective Action Unit (CAU) 415, Project 57 No. 1 Plutonium Dispersion Site, which consists of one Corrective Action Site (CAS): NAFR-23-02, Pu Contaminated Soil. This CAS includes several facilities associated with Project 57 as well as the plutonium-contaminated soil.

In 2011, at the request of the NNSA/NFO, DRI constructed and deployed two environmental monitoring stations at Project 57. Data collected at these monitoring stations is used to conduct field assessments of potential wind transport of radionuclide-contaminated soil from the Project 57 site. The assessment is intended to provide site-specific information on meteorological conditions that result in airborne soil particle redistribution, as well as determine which, if any, radiological contaminants may be entrained with the soil particles and estimate their concentrations. Determining the potential for transport of radionuclide-contaminated soils will facilitate an appropriate closure design and post-closure monitoring program.

MONITORING STATION LOCATIONS AND CAPABILITIES

The Project 57 site is located near the center of the western subbasin of Emigrant Valley. Soils in the area are dominated by fine particles that are subject to transport under moderate to strong winds. Tamura (1985), Friesen (1992), Murarik *et al.* (1992), and Misra *et al.* (1993) indicate that plutonium has a tendency to bind with fine soil particles. Therefore, the particles most likely to be transported by wind are also the particles most likely to be contaminated by radionuclides. Because plutonium is likely to reside in the upper few inches (or centimeters) of soil, soil erosion by wind can potentially lead to the mobilization and redistribution of radionuclide-contaminated soil. Additionally, inhaling airborne dust raised from an area of contaminated soil is the primary risk to humans.

There were no historical site-specific data describing wind direction, speed, or other climate parameters at the Project 57 site when the monitoring stations were deployed. Regional wind data from the Community Environmental Monitoring Program (CEMP) (http://www.wrcc.dri.edu/) and the NNSS (NSTec, 2011b, Attachment A) indicated that southwest and northwest winds are predominant.

The two monitoring stations were installed at Project 57 (Figure 2) in 2011 to collect air quality, meteorological, and environmental data for a field-scale assessment of meteorological conditions that could potentially affect the transport of contaminated soil from the site. The northeast location was selected to obtain downwind data along the predominant spring through fall southwest wind direction. The southeast location was selected to obtain downwind information for the northwest winds that are common during the winter. Both stations were positioned to maximize wind fetch across the fenced Contamination Area (CA) as the winds passed over the monitoring stations. Since 2011, DRI has continued to collect data from monitoring stations at the Project 57 site.

The northeast monitoring station (P57-1) was installed on April 20, 2011, at a temporary location outside of the northeast corner of the current Contamination Area boundary (Figure 2). National Security Technologies (NSTec) Radiological Control Technicians (RCTs) surveyed two corridors from the current Contamination Area boundary to the former Contamination Area boundary at the fence and determined that the corridors could be downgraded to Radioactive Material Areas (RMAs). Radioactive Material Areas can be accessed by Radiological Worker II–trained personnel without RCT support. On August 11, 2011, P57-1 was reinstalled within the RMA at the fence line on the northeast side of the Contamination Area. The southeast monitoring station (P57-2) was installed in the southern RMA corridor at the fence boundary on November 18, 2011. Table 1 lists the coordinates and elevations of both monitoring stations. Figures 3 and 4 show the P57-1 and P57-2 monitoring stations, respectively, as deployed at the fence boundary. These locations were selected in an effort to maximize the fetch over the Contamination Area as winds approached the monitoring stations.

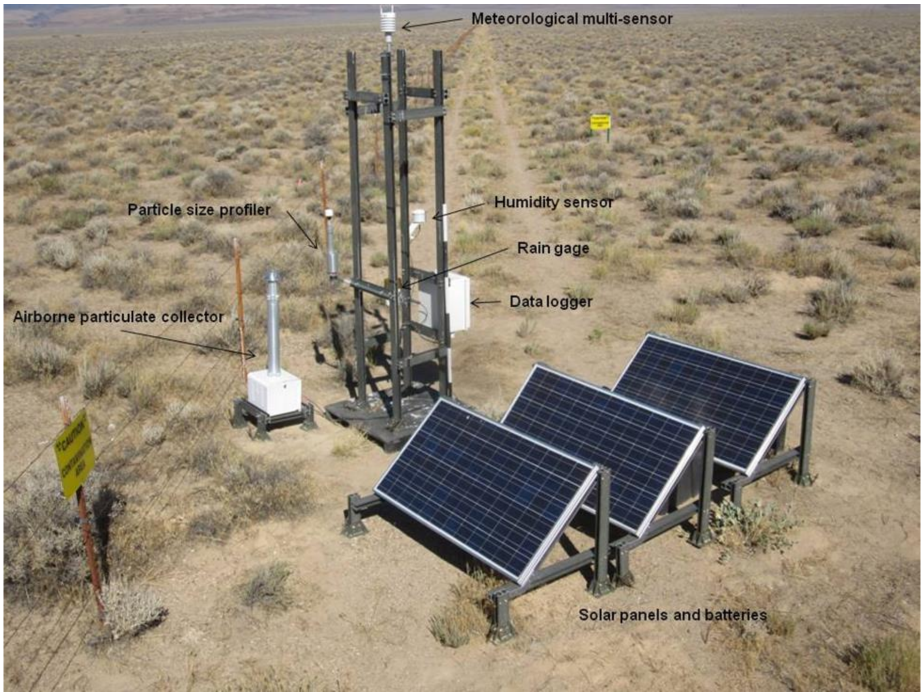

Figure 3. Project 57 monitoring station #1 (P57-1) was installed at the northeast corner of the Project 57 fenced boundary in August 2011. The associated saltation sensor (not pictured) was installed in January 2012.

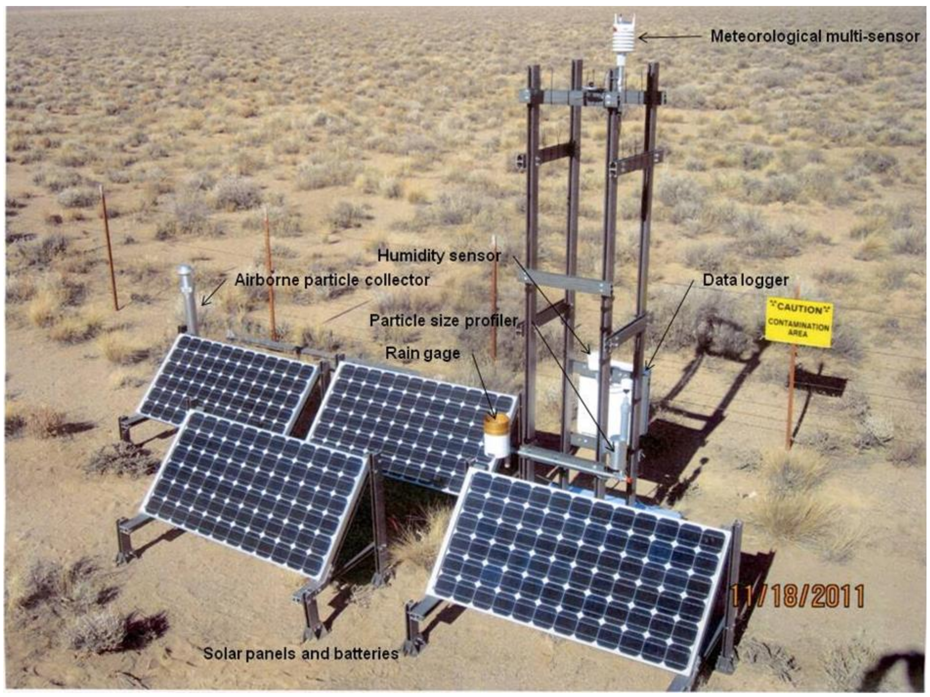

Figure 4. Project 57 monitoring station #2 (P57-2) was installed at the southeast corner of the Project 57 fence boundary in November 2011. The associated saltation sensor (not pictured) was installed in December 2011.

Table 1. Project 57 meteorological stations are located in Emigrant Valley, Nevada, at the coordinates and elevations given.

Meteorological Station	Latitude	Longitude	Elevation (ft [m])
P57-1	37º 19’ 19”	115º 53’ 20”	4,590 (1,399)
P57-2	37º 18’ 53”	115º 53’ 21”	4,575 (1,394)
P57-3	37º 19’ 47”	115º 54’ 5”	4,618 (1,408)
P57-4	37º 18’ 57”	115º 54’ 17”	4,586 (1,398)

Wind direction data collected from the P57-1 and P57-2 stations provided site-specific information. These data indicated that the dominant winds passing over the monitoring stations were not traversing the Project 57 ground zero. The site specific data were used to select new monitoring locations, which are directly downwind of the Project 57 ground zero during the predominant southwest and northwest winds. Stations P57-1 and P57-2 were decommissioned and the equipment was relocated to establish new monitoring stations, P57-3 and P57-4, on January 7, 2015 at locations directly downwind of ground zero when winds were blowing in the predominant directions. This report reviews and analyzes data collected from the P57-3 and P57-4 stations for calendar year (CY) 2015.

The fundamental design of these stations is similar to that used in the CEMP (DeSilva, 2004; NSTec, 2011a). The equipment deployed provides data on radiological, meteorological, and environmental conditions. Table 2 lists the parameters measured. The Quality Assurance Program is also patterned after that used by the CEMP (Appendix C).

Plutonium was the principal radionuclide released into the environment during the Project 57 experiment. It attaches to small soil particles and may be suspended in the air and transported from the site along with windblown dust. Continuous flow, low-volume air samplers (flow rate is approximately 2 ft^3 [0.05663 m^3] per minute) are used to collect airborne particulate matter at each station. The air is drawn through filters that collect particles and are retrieved every two weeks and delivered to the Radioanalytical Services Laboratory (RSL) at the University of Nevada, Las Vegas, for analyses. Gross alpha, gross beta, and gamma spectroscopy analyses are performed in an effort to assess the magnitude of radionuclides associated with the suspended dust. Gamma spectroscopy is performed to determine if Am-241, the daughter product of plutonium 241 (Pu-241), is present. If Am-241 is detected, then alpha spectroscopy is performed to determine the quantity of Pu-241 present.

Table 2. Radiological, meteorological, and environmental sensors deployed at the Project 57 air monitoring stations. Dates refer to the first occurrence of data collection for the specified parameter at the P57-1 and P57-2 stations.

Instrument/Measurement[1]	**P57-1**	**P57-2**	**Data Collection Interval**
Wind speed	8/11/2011	11/18/2011	3 seconds
Wind direction	8/11/2011	11/18/2011	3 seconds
Precipitation	8/11/2011	11/18/2011	3 seconds
Temperature	8/11/2011	11/18/2011	3 seconds
Relative humidity	8/11/2011	11/18/2011	3 seconds
Solar radiation	not installed	11/18/2011	3 seconds
Barometric pressure	8/11/2011	11/18/2011	3 seconds
Soil temperature	8/11/2011	11/18/2011	3 seconds
Soil moisture content	8/11/2011	11/18/2011	3 seconds
Airborne particle size profiler	8/11/2011	11/18/2011	1 minute
Saltation sensor	1/09/2012	1/09/2012	3 seconds
Datalogger	8/11/2011	11/18/2011	Monthly
Airborne particle collector	8/11/2011	11/18/2011	Biweekly
Thermoluminescent dosimeters	1/09/2012	1/09/2012	Quarterly
BSNE Saltation Sand Traps	4/14/2014	4/14/2014	TBD[2]

[1] See Appendix H for instrument make, model, and manufacturer.

[2] The data collection interval for the BSNE saltation sand traps has not been determined.

BSNE = Big Spring Number Eight.

Suspension and transport of dust is controlled by local meteorological and other environmental conditions, such as wind speed and soil moisture content. Electronic sensors measure these parameters at the stations every three seconds. The three-second measurements are averaged or totaled as appropriate and stored in the on-site datalogger every 10 minutes. The maximum and minimum values of each parameter observed during the 10 minute interval are also saved so they can be used to evaluate data quality or for future analysis. The dataloggers are downloaded during site visits once each month. The retrieved data are quality checked and archived by the Western Regional Climate Center for later interpretation.

Thermoluminescent dosimeters (TLDs) were installed at both stations in November 2011 and are collected on a quarterly basis for laboratory analysis. Saltation sensors, which are used to measure the occurrence and frequency of soil particle transport by saltation, were installed at the P57-2 and P57-1 stations in December 2011 and early January 2012, respectively.

On April 14, 2014, DRI installed Big Spring Number Eight (BSNE) saltation sand traps to collect dust and soil transported by saltation at the Project 57 monitoring stations. The BSNE saltation sand traps are isokinetic wind aspirated samplers (Figure 5) that collect a large portion of the airborne sand that enters the opening regardless of wind speed. Three replicate BSNE saltation sand traps, each with two collectors, were installed along the fence line at the Project 57 monitoring stations. The inlet height is set at 6 in (15 cm) to collect the maximum amount of erodible soil material. The two collectors at each mounting rod are installed so that one is pointed toward, that is, downwind of, the Contamination Area to collect material moving across the contaminated ground. The other collector is pointed in the opposite direction, that is, upwind of the Contamination Area, to collect material moving across the uncontaminated soil. The BSNE saltation sand traps will allow a radiological assessment of soil material transported near the ground surface, an estimation of net movement of soil material to and from the contaminated area, and perhaps an assessment of the spatial variability in soil transport. The BSNE saltation sand traps were collected on March 3, 2015, after the P57-1 and P57-2 stations were decommissioned, and again on January 4, 2016, after being deployed for approximately a year.

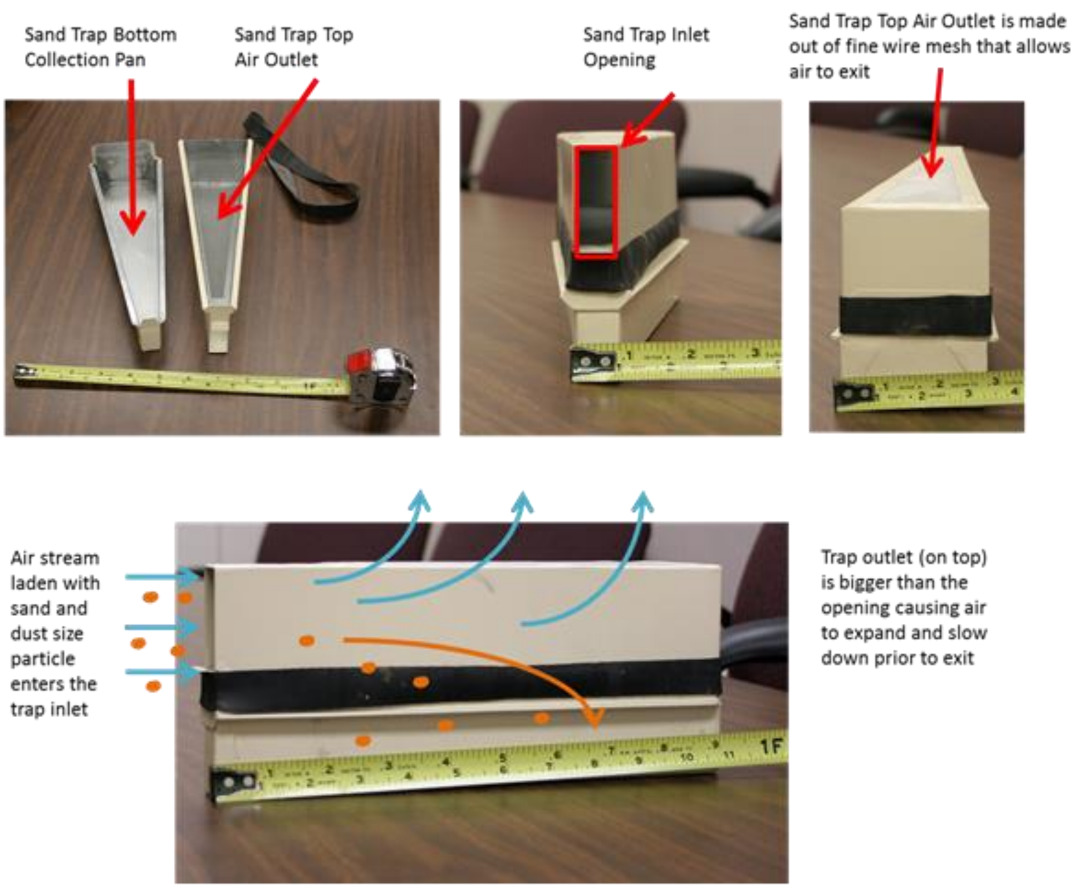

Figure 5. Sand and dust particles are carried into the BSNE Saltation Sand Trap by fast moving air. As the air slows down, momentum is lost and the particles settle on the bottom of the collection pan.

OBSERVED METEOROLOGICAL AND ENVIRONMENTAL CONDITIONS

Meteorological and environmental sensors (Table 2) operated continuously and a complete record of observations were collected at P57-3 and P57-4 during the reporting period, January 1, 2015, through December 31, 2015. Tables 3 and 4 show monthly average/total values, as appropriate, of the observed meteorological and environmental parameters for the year. Monthly average wind speed was less than 10 mph throughout the year (Tables 3 and 4). Monthly average wind directions varied from southwest to northwest. Average monthly air temperature ranged from 32 ^oF (0 ^oC) in December to 77 ^oF (25 ^oC) in August. Extreme air temperatures ranged from near 7 ^oF (-13.9 ^oC) in December to 104 ^oF (40 ^oC) in June. The minimum average monthly relative humidity was approximately two or three percent. Daily average air temperature follows the expected annual cycle (Figure 6). Over the reporting period, the seasonal variations in the daily average temperature ranged from approximately 25 ^oF (-3.9 ^oC) to near 90 ^oF (32.2 ^oC) at both monitoring stations.

Charts displaying daily observations of the parameters are presented in Appendices A, B, and C. Both stations are exposed to large diurnal temperature ranges with infrequent precipitation and seasonally directional winds. The general conditions observed are typical of a Great Basin Desert location.

Total precipitation for the reporting period was 4.43 in (112.52 mm) and 4.83 in (122.68 mm) at P57-3 and P57-4, respectively. No precipitation was observed between about the middle of August and the end of September (Figure 7). The majority of the precipitation received occurred during three different storms. The first major storm occurred late February through early March 2015 (Figure 7). It was a typical springtime storm that produced light to moderate rainfall intervals (< 0.1 in/10 min [2.5 mm/10 min]) over a five day period. This storm produced a total of approximately one inch of rain at both sites. The second and third major storms occurred in October and were characterized by several moderate (~0.1 in/10 min [2.5 mm/10 min]) intensity showers that lasted 30-60 minutes with little to no rainfall between the showers. Total precipitation during each of these storms was less than one inch. Nevertheless, the October storms produced nearly half of the observed annual precipitation. The October storms produced the maximum precipitation amounts for a month, day, hour, or 10-min interval during the year (Table 5). Although some precipitation was measured at both P57-3 and P57-4 during each rainfall event, station P57-4 appears to receive slightly more precipitation than station P57-3 throughout the year (Figure 7).

Table 3. Monthly average or total meteorological and environmental observations at station P57-3 for CY2015.

		Date (mm-yy)											
		Jan-15	Feb-15	Mar-15	Apr-15	May-15	Jun-15	Jul-15	Aug-15	Sep-15	Oct-15	Nov-15	Dec-15
Solar Radiation (Ly)	Total	-9,999[1]	-9,999	-9,999	-9,999	-9,999	-9,999	-9,999	-9999	-9,999	5,457	9,498	7,579
Mean Wind Speed (mph)	Ave.	8.433	8.019	7.989	9.709	8.196	7.677	7.833	7.589	7.709	7.537	9.89	8.03
Mean Wind Direction (Deg.)	Vector Ave.	354.8	346.7	341.3	329.1	223.1	243	208	264	203.6	337.1	346.1	347.9
Maximum Wind Gust (mph)	Max.	46.9	39.5	33.5	52.9	43.3	47.8	51.1	48	40.8	39.3	50.6	38.2
Average Air Temperature (Deg. F)	Ave.	42.04	46.23	50.96	52.58	59.87	76.02	75.12	77.06	70.75	58.71	39.41	31.98
	Ave. Daily Max.	57.85	63.71	68.77	68.97	74.35	93.28	90.63	94.51	88.57	73.35	54.38	46.86
	Max.	69.49	74.44	81.68	82.44	91.54	104	100.8	101.4	97.95	89.19	72.73	63.52
	Ave. Daily Min.	29.2	30.4	33.73	34.2	42.77	54.14	56.8	58.28	51.61	46.66	26.42	19.52
	Min.	14.14	23.07	22.49	20.4	29.46	39.64	43.99	49.19	40.59	35.75	9.986	7.34
Average Soil Temperature - 4 Inches (Deg. F)	Ave.	41.75	46.32	51.18	56.73	64.18	79.2	81.49	81.24	76.18	59.78	41.94	33.85
	Max.	51.4	58.46	68.74	71.13	82.85	97.61	100.9	94.15	92.68	78.67	62.67	45.08
	Min.	32.51	35.83	34.14	44.68	50	62.89	66.36	67.93	62.44	46.81	28.74	25.94
Average Relative Humidity (%)	Ave.	55.54	42.84	37.65	27.72	38.53	19.53	28.48	27.22	24.41	53.38	46.67	55.8
	Max.	100	100	100	98.4	98.5	86	97.2	91.3	73.39	96.2	98.2	99.7
	Min.	11.03	7.582	6.46	6.88	7.127	3.158	4.658	4.055	5.939	10.88	7.431	9.66
Barometric Pressure (in Hg)	Ave.	25.51	25.42	25.44	25.31	25.27	25.33	25.39	25.4	25.37	25.41	25.38	25.37
Precipitation (in)	Total	0.35	0.63	0.32	0.15	0.3	0.01	0.08	0.24	0	2.26	0.31	0.04

[1] The value -9,999 means signals from the instrument were not recorded by the datalogger. The solar radiometer was not installed at P57-3 until October 2015.

Table 4. Monthly average or total meteorological and environmental observations at station P57-4 for CY2015.

		Date (mm-yy)											
		Jan-15	**Feb-15**	**Mar-15**	**Apr-15**	**May-15**	**Jun-15**	**Jul-15**	**Aug-15**	**Sep-15**	**Oct-15**	**Nov-15**	**Dec-15**
Solar Radiation (Ly)	Total	6,351	10,152	14,821	17,935	17,676	19,817	19,249	17,853	15,838	10,677	9,230	7,434
Mean Wind Speed (mph)	Ave.	7.428	7.162	7.098	8.909	7.681	7.15	7.321	7.054	7.077	6.782	8.812	7.148
Mean Wind Direction (Deg.)	Vector Ave.	22.23	12.01	5.745	350	267.6	278.7	256.8	294.9	261.1	348	350.5	350.3
Maximum Wind Gust (mph)	Max.	31.6	39.6	40.3	47.8	43.9	43.3	39	43.6	40.8	36.9	47.7	38.2
Average Air Temperature (Deg. F)	Ave.	42.38	46.13	50.95	52.83	59.92	75.96	75.18	77.07	70.68	58.86	39.61	32.04
	Ave. Daily Max.	59.02	64.47	69.45	69.84	75.37	94.07	91.56	95.43	89.18	73.91	55.37	47.82
	Max.	70.29	75.51	82.27	83.26	92.52	104.7	101.4	102	97.43	88.38	73.83	64.65
	Ave. Daily Min.	28.29	29.12	32.67	33.22	41.35	52.54	55.5	57.4	50.29	46.03	25.42	18.62
	Min.	12.51	21.34	21.98	20.32	26.7	37.86	42.61	49.48	39.54	32.89	9.23	6.782
Average Soil Temperature - 4 Inches (Deg. F)	Ave.	41.7	47.52	54.36	60.6	68.13	83.62	84.37	84.11	78.1	60.7	41.61	33.15
	Max.	66.47	66.15	78.62	82.62	95.22	108	110.9	104.3	99.05	84.11	64.27	49.15
	Min.	28.16	32.96	31.86	41.18	47.59	61.41	60.62	64.83	58.26	43.16	23.17	21.34
Average Relative Humidity (%)	Ave.	56.37	44.48	39.55	28.69	40.16	20.83	30.76	29.83	26.51	56.37	48.37	57.27
	Max.	100	99.5	99.7	98.5	99.3	88	99.4	93.4	73.08	99	96.7	97.1
	Min.	11.8	7.032	5.594	6.067	6.934	1.608	3.971	3.183	5.564	12.33	7.373	10.98
Barometric Pressure (in Hg)	Ave.	25.54	25.45	25.48	25.34	25.31	25.38	25.43	25.44	25.41	25.44	25.4	25.38
Precipitation (in)	Total	0.39	0.75	0.3	0.12	0.19	0.01	0.23	0.43	0	2.03	0.32	0.06

Table 5. Precipitation extremes observed during calendar year 2015.

Station	Minimum Monthly (in)	Maximum Monthly (in)	Maximum Daily (in)	Maximum Hourly (in)	Maximum 10 min (in)
P57-3	0.00 Sept. 2015	2.26 Oct. 2015	0.85 Oct. 18, 2015	0.21 Oct. 18, 2015	0.18 Oct. 4, 2015
P57-4	0.00 Sept. 2015	2.03 Oct. 2015	0.82 Oct 18, 2015	0.24 Oct. 18, 2015	0.11 Oct. 18, 2015

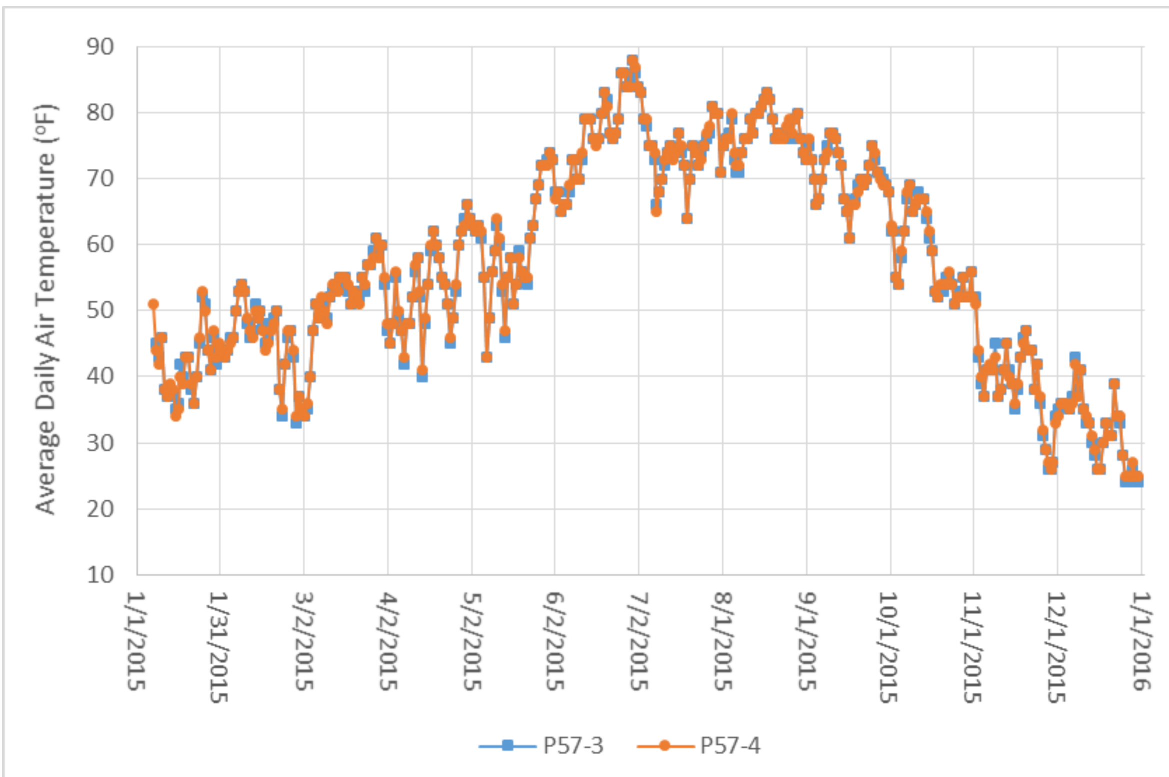

Figure 6. Daily average air temperature during the period January 6, 2015, through December 31, 2015, shows the anticipated annual trends.

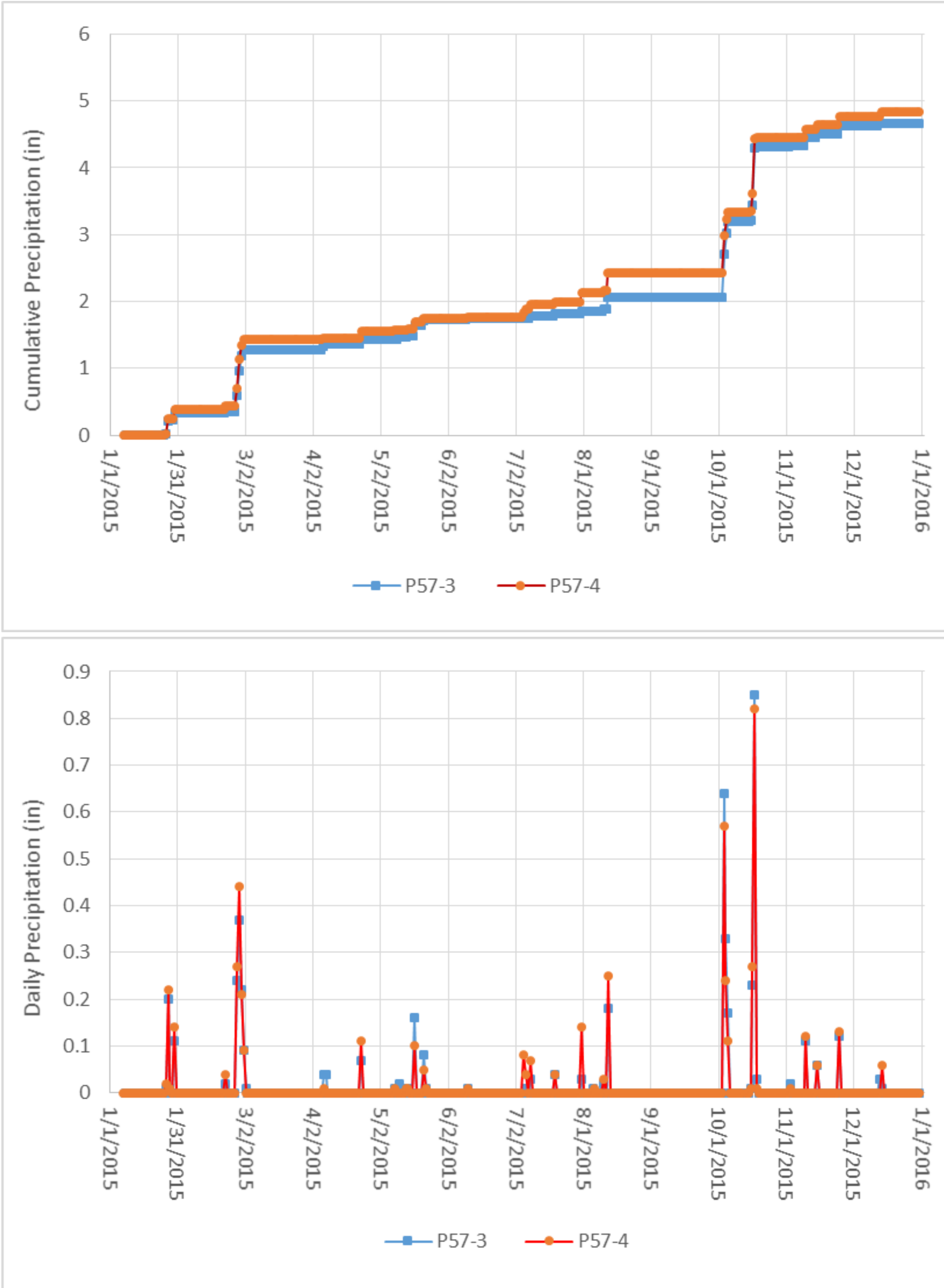

Figure 7. Daily (top) and cumulative (bottom) precipitation for January through December 2015 are shown. Precipitation patterns at the P57-3 and P57-4 monitoring stations are similar, although there are slight differences in intensity.

Soil temperature and soil moisture are also collected at the P57 stations. Like the average daily air temperature, the average daily soil temperature exhibits an annual seasonal pattern (Figure 8, B-1, and B-3). The soil temperature is typically warmer at P57-4 than at P57-3, especially during the spring and summer. During CY2015, soil moisture is typically approximately 10 percent of soil volume (Figure B-2 and B-4). As a result of the October rains, soil moisture rose from approximately 7 percent to approximately 22 percent at P57-3 and from approximately 10 percent to approximately 30 percent at P57-4. Generally, soil moisture at P57-4 appears to be slightly higher, and is slower to drop, than at P57-3.

Peak wind speeds during 2015, 53 mph (85.3 km/hr) in April and 51 mph (82.1 km/hr) in November, were observed at P57-3. The peak wind speed observed at P57-4, 48 mph (77 km/hr), was also measured in April and November. Wind rose diagrams for all 10-minute average wind conditions observed during 2015 (Figures 9, A-6, and A-15) indicate that winds were predominantly from either the northeast-to-northwest or the south-to-southwest at both Project 57 monitoring stations.

To evaluate seasonal differences in wind conditions, wind roses were constructed for spring/summer (March 1 to August 31) season winds (Figures A-7 and A-16) and fall/winter (September 1 to February 28) season winds (Figures A-8 and A-17). These diagrams indicate that winter winds are dominantly from northerly directions, whereas both northerly and southwesterly winds are common during the summer. The seasonal winds come from the same predominant directions identified for all winds. However, winds from the south to southwest appear somewhat more common during the summer, whereas winds from the northeast to northwest were more common during the winter.

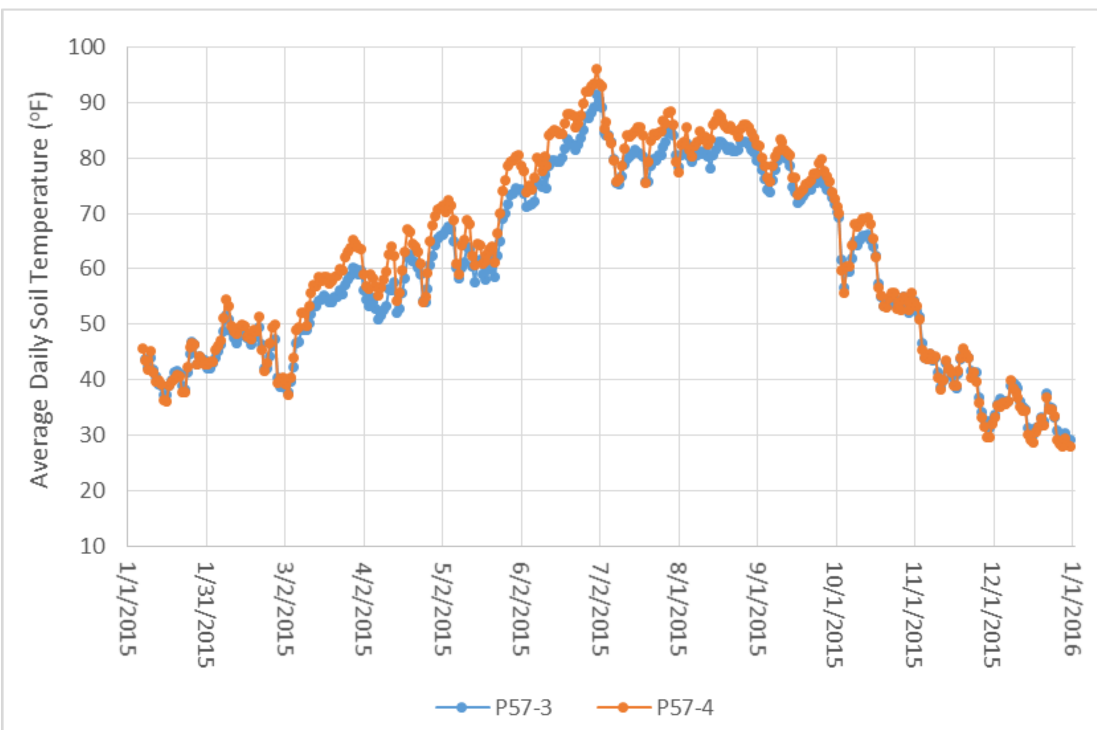

Figure 8. The average daily soil temperature at P57-4 is typically slightly warmer than at P57-3. This is especially noticeable during the spring, summer, and fall.

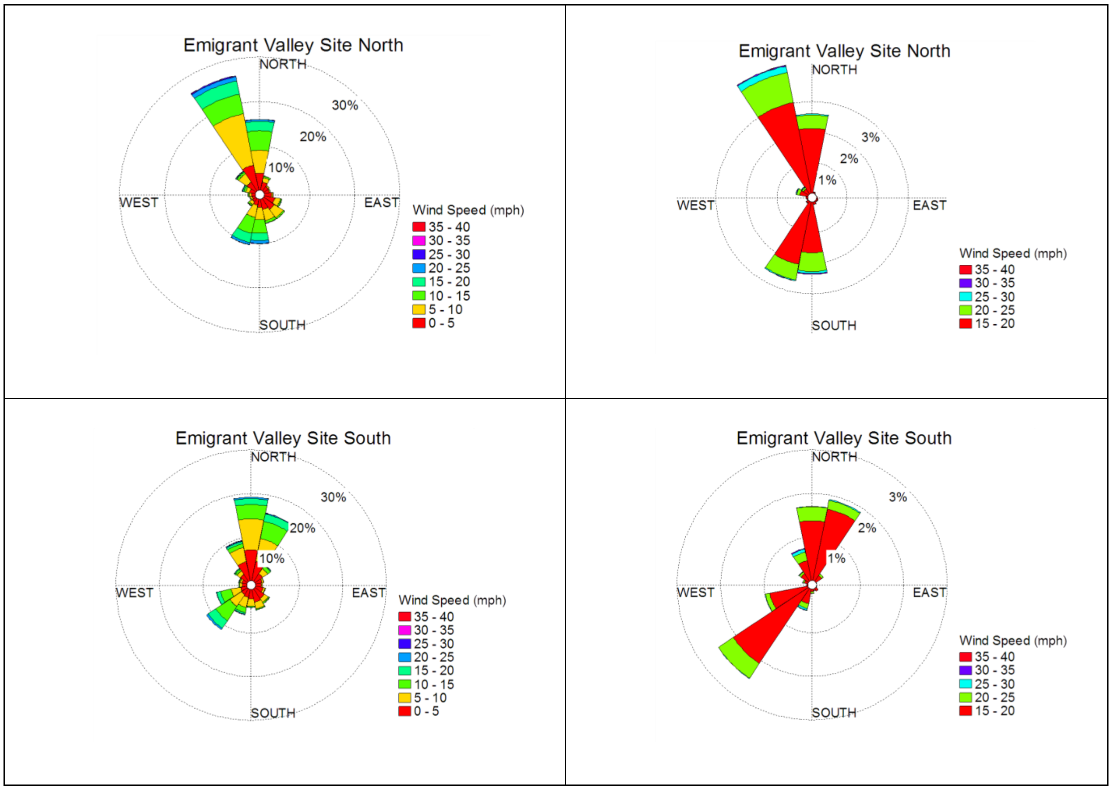

Figure 9. Wind roses for all wind speeds (left column) and for wind speeds in excess of 15 mph (24.1 km/hr) (right column) at P57-3 (top) and P57-4 (bottom) monitoring stations.

Generally, wind speeds must exceed 15 mph (24.1 km/hr) to produce dust by saltation or suspension (see discussions in the section on dust transport that follows). At the Project 57 stations, wind speed exceeded 15 mph (24 km/hr) approximately 13 percent of the time at P57-3 and nine percent of the time at P57-4. Wind roses for winds in excess of 15 mph (24.1 km/hr) (Figure 9) show the same dominant directions seen in the analysis of all winds. Two dominant wind directions account for 97.5 percent of all winds over 15 mph (24 km/hr) at P57-3 and 98.6 percent of all winds over 15 mph (24 km/hr) at P57-4. At P57-3, winds from the northeast-to-northwest quadrant are most common, they occur approximately 57.5 percent of the time, whereas the south-to-southwest winds occur approximately 40 percent of the time. At station P57-4, the two dominant wind directions are slightly more balanced. Winds from the northeast-to-northwest occur approximately 53.7 percent of the time, whereas winds from the south-to-southwest occur approximately 44.9 percent of the time (Figures 9 and 10, and Figures A-3 and A-8).

The wind direction data were assigned to bins representing 10-degree direction intervals and bin counts were expressed as percentage of all observations. Figure 10 shows the wind direction frequency distribution for the wind direction bins. This chart shows that winds from the south-to-southwest are bounded by 160 degrees and 260 degrees and that winds from the northeast-to-northwest are bounded by 300 degrees to 60 degrees. An analysis of dust transport conditions associated with these two predominant wind directions will be performed to determine if there are major differences.

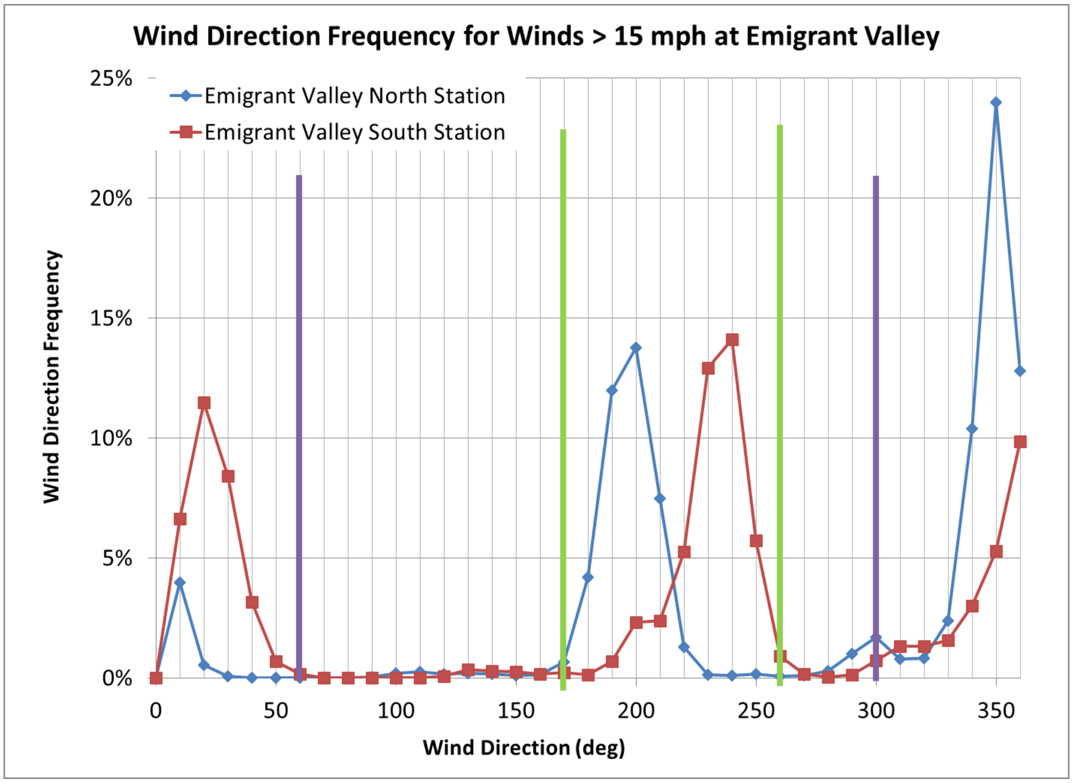

Figure 10. Wind direction frequency for 10-minute average wind direction observations at the Project 57 monitoring stations. The wind direction data were assigned to bins representing 10-degree direction intervals and bin counts expressed as percentage of all observations. In later analyses the southerly winds (bounded by the green lines) and northerly winds (bounded by the purple lines) were separated for comparison.

Both sites are exposed to large diurnal temperature ranges with infrequent precipitation events and seasonally directional winds, which is typical of a Great Basin Desert location. A comparison of the data from both stations shows only minor differences in temperature, precipitation, humidity, and barometric pressure. Wind patterns distinctly show two dominant directions. Soil temperature and moisture show strong similarities to meteorological patterns.

OBSERVATIONS OF SOIL/DUST TRANSPORT BY WIND

Soil movement initiated by wind forces is characterized as surface creep, saltation, and suspension (Figure 11). Surface creep is a process by which particles are rolled across the ground surface by wind and impacts from saltating particles. Creep particles are generally over 0.02 in (500 µm) in aerodynamic diameter and are too heavy to be lifted into the air. Saltation is the mechanism by which soil particles in the range of 0.002 in (50 µm) to 0.02 in (500 µm) are transported. These particles are dislodged and carried a small distance in the air before falling to the ground. Their transport paths usually follow a parabolic trajectory, so the particles essentially bounce across the ground surface. The amount of time the particles are in the air and the distances they travel are functions of wind speed and particle mass. Saltation is important because the impact of saltated particles may push creep particles and may dislodge smaller particles that are ejected into the air where they are transported

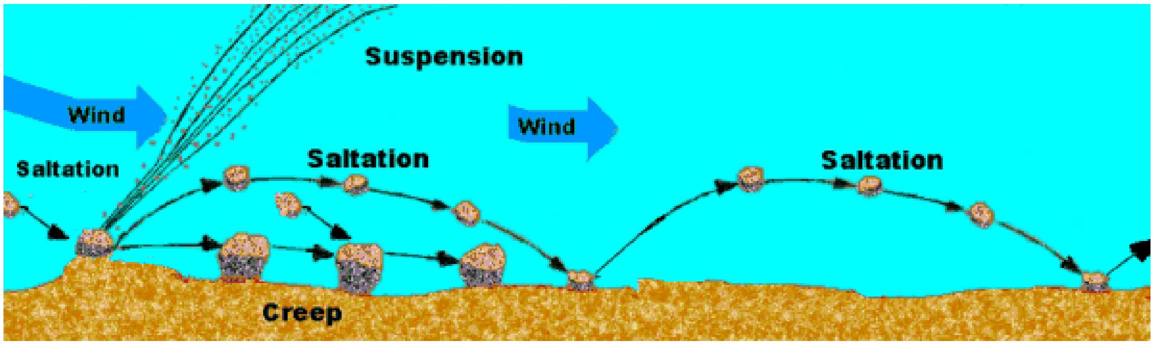

Figure 11. Illustration of the saltation process. (The Weather Doctor, http://www.islandnet.com/~see/weather/elements/dustwind.htm, accessed December 7, 2015.)

in suspension. Suspended particles are usually smaller than 0.002 in (50 µm). Particles less than 0.0008 in (20 µm) in diameter can be entrained in the air by wind or from impact with saltation-sized particles. Once these particles are suspended in the air, they can be transported over extremely long distances. Fine particles, which are particles with an aerodynamic diameter less than 0.0004 in (10 µm) (PM_{10}), are small enough to be inhaled by humans and are called respirable suspended particles. At the Project 57 monitoring stations suspended particles are counted using the Met One™ Ambient Particulate Profiler Model 212 and saltated particles are counted using the Sensit H11-LIN™.

The Sensit sensor impact area is made of piezoelectric material that wraps completely around the vertically oriented instrument. The sensor registers impacts from all directions and converts them to electrical impulses. The impact surface is centered 4 in (10 cm) above the ground surface based on the recommendation of the manufacturer (http://www.sensit.com/images/Tech_Note_5.pdf, accessed December 7, 2015). Particle counts are summed over 10-minute intervals and stored on the station datalogger. Currently, the saltation sensors are located near the metrological towers at each station in areas that are free of vegetation and recent disturbances, which might interfere with their operation.

Because raindrop impact dislodges and ejects soil particles into the air, counts on the saltation sensors increase during precipitation events. This phenomenon does not result in the same type of particle trajectory or dust emission associated with wind-driven saltation described above. Raindrops can also be carried by wind and hit the saltation sensor and register as false saltation counts. The saltation sensor cannot distinguish between raindrop or soil particle impacts. Therefore, even though rain plays an important role in soil mechanics in desert environments, counting periods that are coincident with precipitation are removed from the data set to ensure that the analyses focus on wind driven saltation.

Suspended particles are counted using a Met One™. The Met One™ detects and counts the suspended particle concentration in eight different size groups that range from 0.00002 in (0.5 µm) to 0.00039 in (10 µm) in diameter. These particle count concentrations are used to calculate PM_{10} and $PM_{2.5}$ concentrations. Particle counts are reported every minute and the average for each 10-minute interval is recorded in the datalogger. The Met One™ instruments are mounted so that the air inlet of the instrument is between 4.9 ft (1.5 m) and 5.6 ft (1.7 m) from the ground, which is the respirable zone for most people.

Dust Transport by Saltation

Saltated particle counts are strongly dependent on wind speed. The relationship between wind speed and saltation particle counts was investigated by determining the average number of particle counts/10-minute interval for wind speeds categorized in 5-mph (8-km/hr) wind speed classes (Table 6) after removing those intervals influenced by rainfall. Figure 12 shows that the relationship between wind speed and saltation particle count is approximately exponential for wind speeds between 0 and 35 mph (0 to 56.3 km/hr) and this is especially true for the P57-3 station where there is a strong saltation activity for winds over 30 mph (48.3 km/hr). The P57-4 station indicates a somewhat similar trend in saltation counts for speeds of up to 30 mph (48.3 km/hr) but shows a supply limitation of saltation activity for winds over 30 mph (48.3 km/hr) when compared to the P57-3 station. The monitoring period covered in this report lasted for almost the entire CY2015 and winds over 30 mph (48.3 km/hr) lasted for total of 7.3 hours and 1.8 hours at P57-3 and P57-4, respectively. This is equivalent to approximately 0.089 percent and 0.026 percent of total monitoring (Table 6) time during 2015, respectively. This is considerably longer for P57-3 station compared to approximately 2.33 hours in 2014 (Mizell, 2016) but still not statistically significant in order to formulate a good predictive model for saltation activity for sustained winds over 30 mph (48.3 km/hr).

Table 6. Average saltation particle counts by wind speed class at Project 57 monitoring stations.

Wind Speed Class (mph)	Duration (hours)	Frequency (%)	Average Wind Speed (mph)	Average Particle Counts (count/10-min)
P57-3				
0 – 5	2,691.17	32.703	3.48	0.00
5 – 10	2,905.33	35.306	6.95	0.02
10 – 15	1,560.67	18.965	12.35	0.12
15 – 20	803.17	9.760	17.12	0.14
20 – 25	228.83	2.781	21.88	0.88
25 – 30	32.50	0.395	26.70	5.46
30 – 35	7.33	0.089	31.95	46.61
Total	8,229.0	--	--	--
P57-4				
0 – 5	2,917.83	40.101	3.56	0.35
5 – 10	2,413.67	33.172	7.01	0.41
10 – 15	1,313.67	18.054	12.23	0.48
15 – 20	518.50	7.126	16.97	0.34
20 – 25	97.33	1.338	21.59	1.19
25 – 30	13.33	0.183	26.96	9.40
30 – 35	1.83	0.025	30.70	10.64
Total	7,276.17	--	--	--

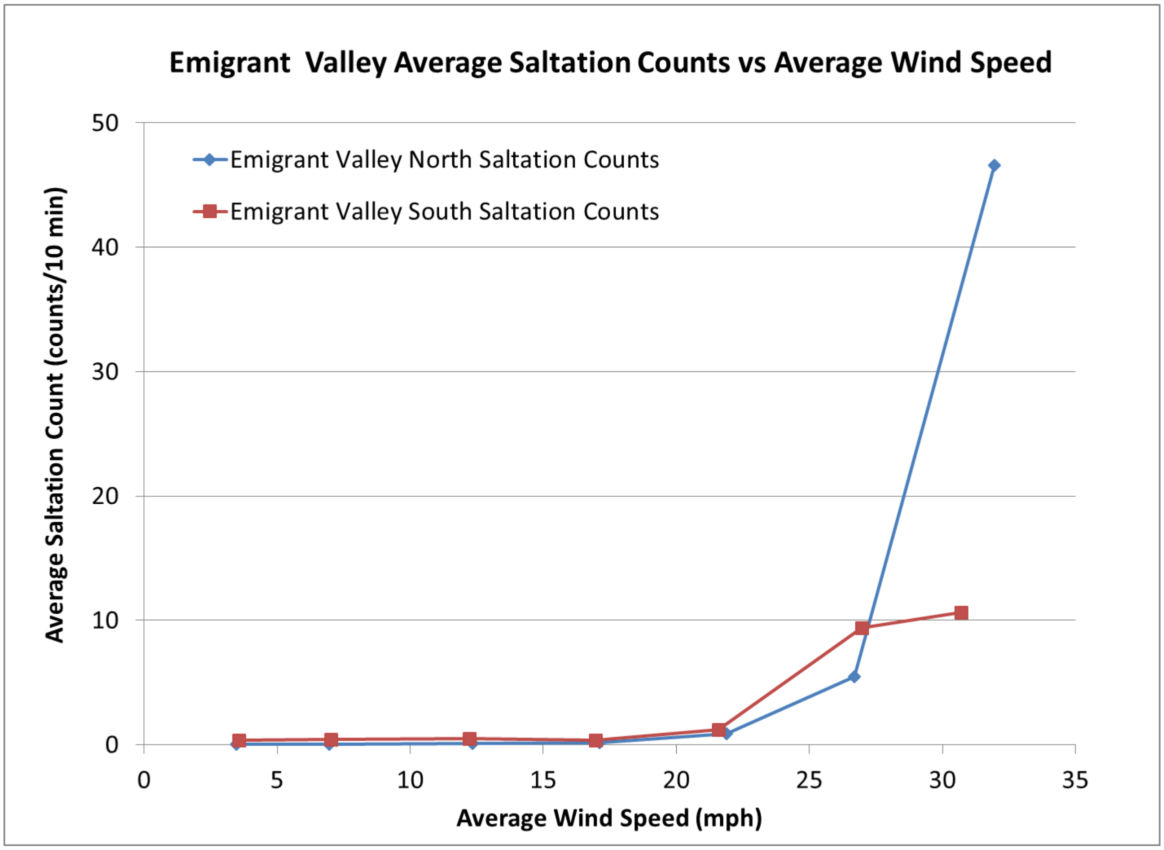

Figure 12. Average saltation counts for Emigrant Valley North (P57-3) and South (P57-4) stations. The saltation counts generally increase exponentially as the wind speed increases.

Dust Transport by Suspension

Table 7 summarizes wind speed and the corresponding PM_{10} concentration by wind-speed class for Emigrant Valley monitoring stations. Approximately 87-90 percent of the time, the wind speed at both stations is below 15 mph (24 km/hr) and the corresponding average PM_{10} concentrations are below 9 x 10^{-9} oz/ft^3 (9 µg/m^3). Only 10-13 percent of the time is wind speed above 15 mph (24 km/hr), and even though PM_{10} concentrations generally increase as wind speed increases, the PM_{10} concentrations remain fairly low until winds exceed about 25 mph (40 km/hr), which occurs less than 0.5 percent of the time. At P57-3, PM_{10} concentrations increase with increasing wind speed and exceed 2.66 x 10^{-7} oz/ft^3 (266 µg/m^3) for the strongest winds between 30 and 35 mph (48.3 and 56.3 km/hr). At P57-4, PM_{10} concentrations also increased consistently with increasing wind speed and similarly exceeds 4.2 x 10^{-7} oz/ft^3 (420 µg/m^3) for wind speeds between 30 and 35 mph (48.3 and 56.3 km/hr). However, high wind and correspondingly high PM_{10} events are relatively rare and generally last for short periods of time. Wind speed exceeds 48 km/hr (30 mph) only 0.089 percent (< 8 hrs) at P57-3 and 0.026 percent (< 3 hrs) at P57-4 for the twelve month period covered in this report.

Table 7. Summary of wind and PM_{10} data for Project 57 Stations P57-3 and P57-4 during the period from January 6, 2015, to December 31, 2015.

Wind Speed Class (mph)	Duration (hours)	Frequency (%)	Cumulative Frequency (%)	Average Wind Speed (mph)	PM_{10} (µg/m^3)
P57-3					
0 – 5	2,691.17	32.697	32.697	3.48	11.19
5 – 10	2,905.50	35.301	67.998	6.95	11.97
10 – 15	1,561.33	18.970	86.967	12.35	8.87
15 – 20	804.00	9.768	96.736	17.12	13.18
20 – 25	228.83	2.780	99.516	21.88	40.54
25 – 30	32.50	0.395	99.911	26.70	266.54
30 – 35	7.33	0.089	100.000	31.95	4,478.51
Total	8,230.67	--	--	--	--
P57-4					
0 – 5	3,289.00	39.900	39.900	3.53	9.59
5 – 10	2,666.67	32.350	72.250	7.03	9.01
10 – 15	1,528.00	18.537	90.786	12.26	9.21
15 – 20	617.00	7.485	98.271	16.96	17.18
20 – 25	125.83	1.527	99.798	21.60	50.00
25 – 30	14.50	0.176	99.974	26.87	420.47
30 – 35	2.17	0.026	100.000	30.84	2,152.24
Total	8,243.17	--	--	--	--

Various wind speeds occur with similar frequency at both stations (Figure 13). Light winds (0 to 5 mph [0 to 8 km/hr]) were most common at P57-4 and moderate winds (5 to 10 mph [8 to 16 km/hr]) were most common at P57-3. Wind speeds in excess of 15 mph (24 km/hr) occur less than four percent of the time and wind speeds in excess of 20 mph (32 km/hr) occur less than one percent of the time (Table 7).

The average PM_{10} concentrations at P57-3 and P57-4 increase in an approximately exponential pattern with linear increases in wind speed (Figure 14). The two monitoring stations, as expected, show very similar trends. Values for average PM_{10} concentrations are nearly identical for wind speeds below 25 mph (40.2 km/hr) (Table 7). For wind speeds over 25 mph (40.2 km/hr) the PM_{10} shows an exponential-like increase and concentration for those high wind speeds exceed 2.5 x 10^{-7} oz/ft^3 (250 µg/m^3). The lower graph in Figure 14 is plotted on a log scale to highlight the exponential rise in PM_{10} concentration for wind speeds over 20 mph (32.2 km/hr). Although the PM_{10} concentration increases approximately exponentially at high wind speeds, this does not imply that large volumes of soil material are moving. The wind speeds necessary to generate the higher PM_{10} concentrations occur less than about two percent of the time, which limits the net soil transport.

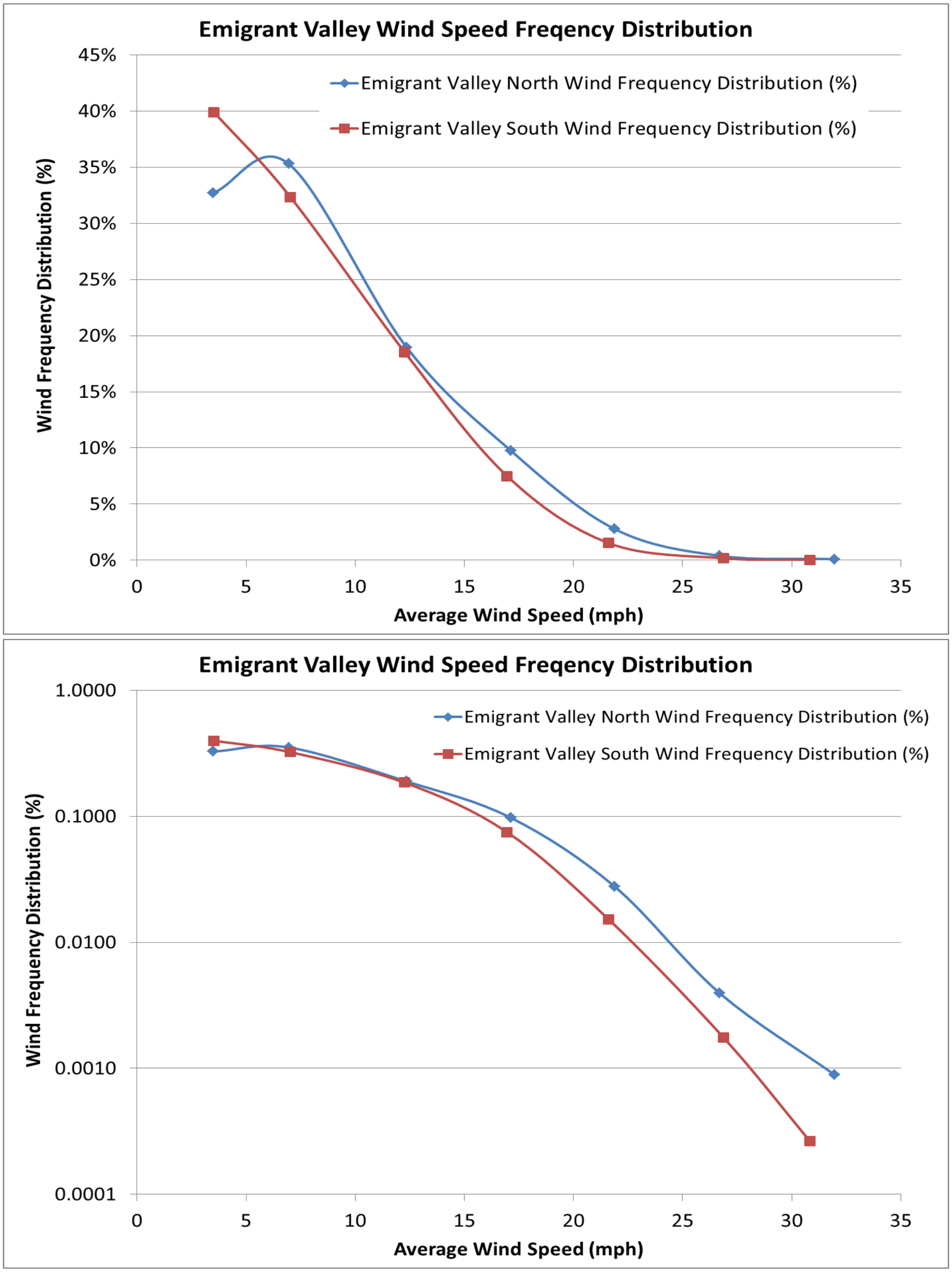

Figure 13. Wind speed frequency by wind class for Project 57 monitoring stations during the period January 2015 through December 2015. A logarithmic scale is used in the lower graph to give a better sense of the dynamic range and low frequency of high winds.

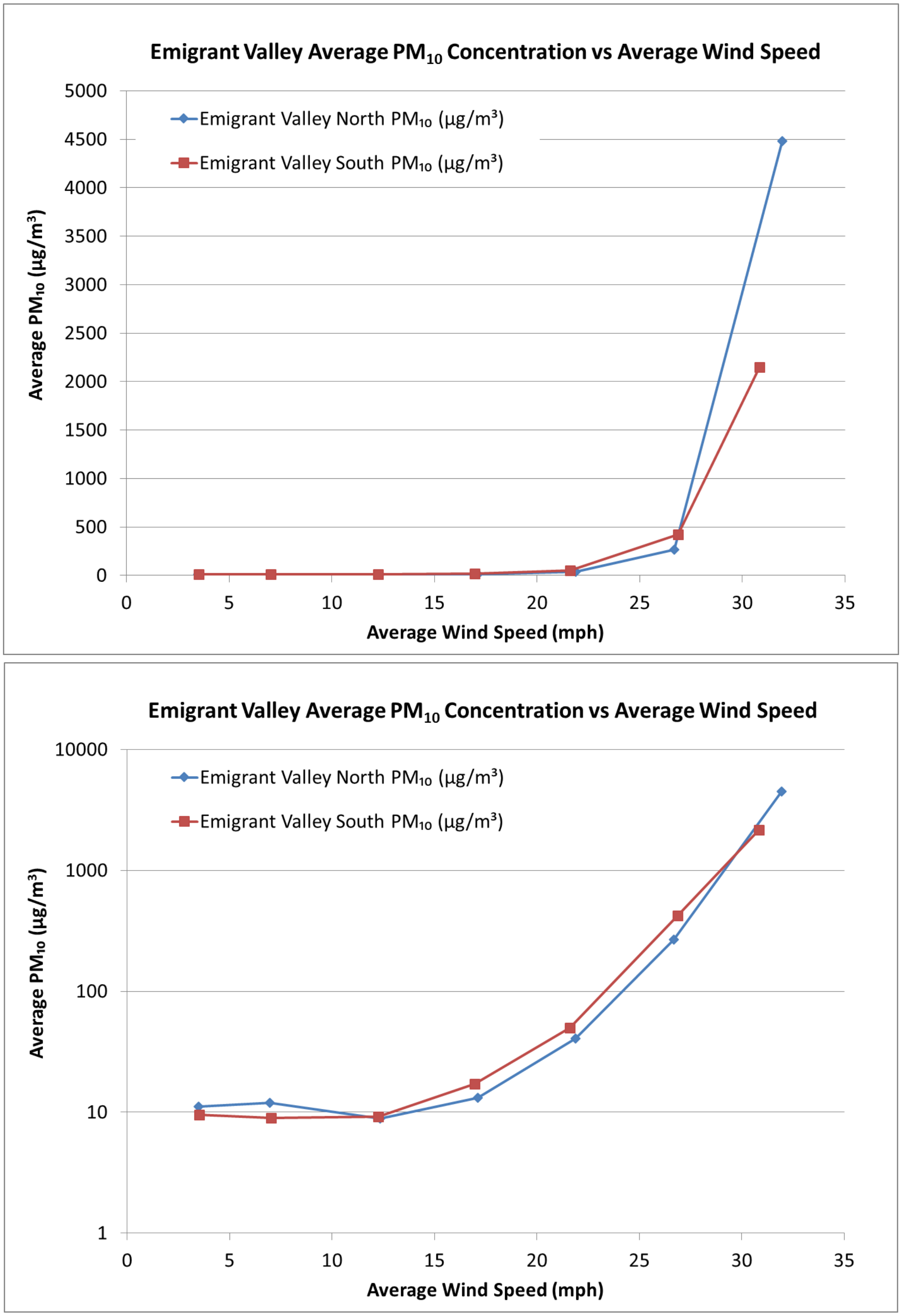

Figure 14. PM_{10} trends as a function of wind speed for P57-3 and P57-4. A logarithmic scale is used in the lower graph to illustrate the wide dynamic range of PM_{10} concentrations.

Because saltating particles are likely to dislodge and eject smaller particles from the soil surface, the relationship between saltation particle counts and PM_{10} concentrations is important. In addition to PM_{10} transported from upwind locations some PM_{10} is generated locally because of saltation. A correlation analysis was performed to investigate this relationship. Strong correlation between high saltation values and high PM_{10} values would indicate that strong winds are driving the saltation activity, which in turn contributes to the fine dust emissions. Figure 15 shows the correlation between saltation counts and PM_{10} concentration at Emigrant Valley North Station. At this station there is a linear correlation between saltation counts and PM_{10} concentration. However, the slope of the relationship shown is affected by the saltation counts and PM_{10} at the highest wind speed. There is a similar relationship and response between saltation counts and PM_{10} concentration at both P57-3 and P57-4 stations, which suggests that for strong winds over 25-30 mph (40.2-48.2 km/hr), local saltation activity has a strong contribution to PM_{10} emissions.

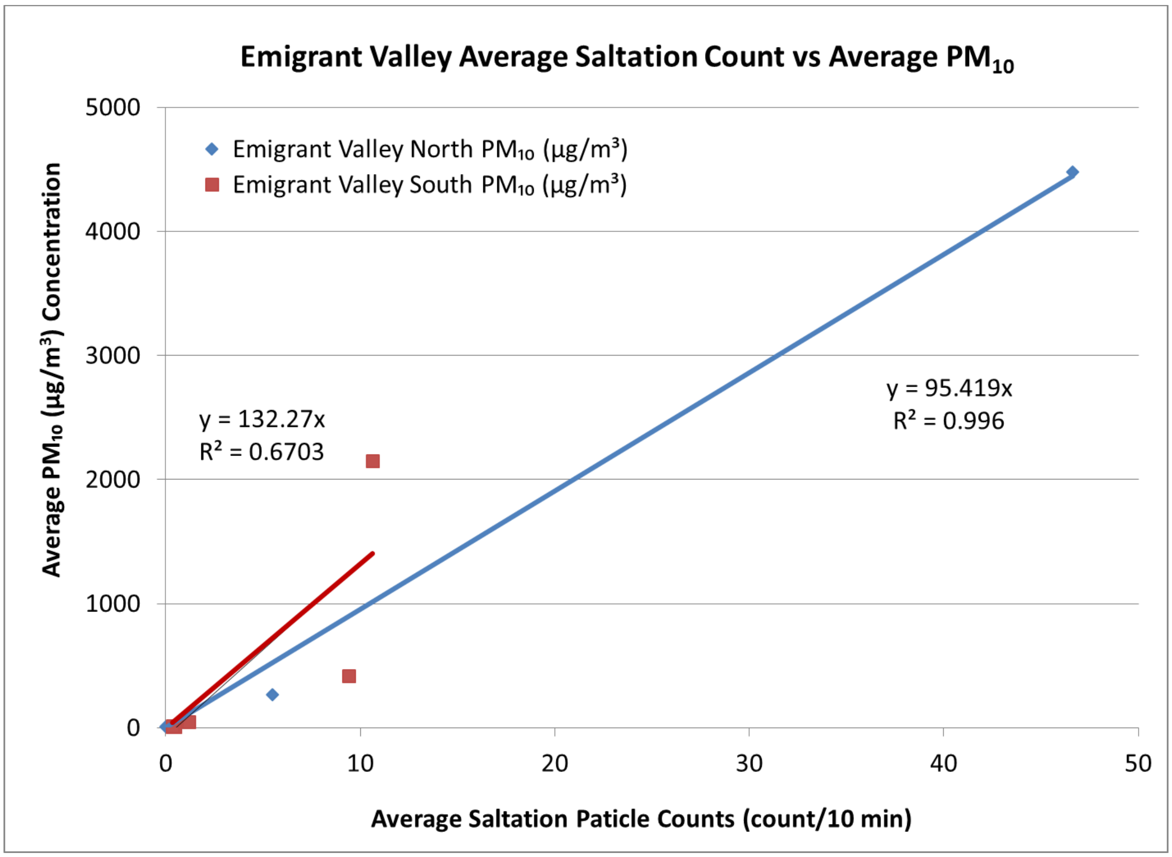

Figure 15. Regression of PM_{10} against saltation counts for wind speed class shows a linear relationship.

Comparison of Predominant Northly and Southly Winds

Winds over 15 mph (24.1 km/hr) are predominantly from northwest to northeast and from south to southwest as it was shown in Figure 10. Because there are two major wind directions from which strong winds blow, it is important to determine which winds are stronger and potentially result in more dust transport. Tables 8 and 9 summarize the wind frequency based on 5 mph (8 km/hr) wind classes and give the corresponding average PM_{10} concentration for all winds and for winds from the northwest to northeast and from south to southwest at the P57-3 and P57-4 monitoring stations, respectively. Figure 16 shows the relationship between average wind speed and PM_{10} concentration for the predominant wind directions for each of the monitoring stations. These figures clearly indicate that for winds over 20 mph (32.2 km/hr) there is greater PM_{10} transport for winds from the northerly directions compared to winds from the southerly directions. The PM_{10} concentration for winds over 20 mph (32.2 km/hr) from all directions is dictated by northerly winds. This implies that net dust transport is driven by the winds from the north. It is important to remember that winds over 20 mph (32.2 km/hr) from all directions occur less than three percent of total time, so transport events are relatively rare and short in duration. However, these winds still result in net dust transport in the southerly direction because transport during northerly winds dominate transport.

Table 8. Summary of wind and PM_{10} data for the two predominant wind directions at station P57-3.

Wind Speed Class (mph)	Duration (hours)	Frequency (%)	Cumulative Frequency (%)	Average Wind Speed (mph)	PM_{10} (µg/m^3)
		P57-3 All Winds			
0 – 5	2,691.17	32.697	32.697	3.48	11.19
5 – 10	2,905.50	35.301	67.998	6.95	11.97
10 – 15	1,561.33	18.970	86.967	12.35	8.87
15 – 20	804.00	9.768	96.736	17.12	13.18
20 – 25	228.83	2.780	99.516	21.88	40.54
25 – 30	32.50	0.395	99.911	26.70	266.54
30 – 35	7.33	0.089	100.000	31.95	4,478.51
Total	8,230.67	--	--	--	--
		P57-3 Northwest to Northeast Winds			
0 – 5	1,334.17	29.690	29.690	3.65	13.34
5 – 10	1,726.50	38.421	68.111	6.82	13.17
10 – 15	825.33	18.367	86.477	12.36	7.35
15 – 20	452.67	10.073	96.551	17.15	10.79
20 – 25	127.00	2.826	99.377	21.85	38.53
25 – 30	23.33	0.519	99.896	26.81	287.33
30 – 35	4.67	0.104	100.000	31.63	6,506.21
Total	4,493.67	--	--	--	--
		P57-3 South to Southwest Winds			
0 – 5	526.50	23.079	23.079	3.38	10.06
5 – 10	693.17	30.384	53.463	7.38	9.56
10 – 15	633.33	27.762	81.224	12.41	10.09
15 – 20	322.83	14.151	95.376	17.08	16.15
20 – 25	95.00	4.164	99.540	21.93	44.98
25 – 30	8.00	0.351	99.890	26.41	97.69
30 – 35	2.50	0.110	100.000	32.55	124.16
Total	2,281.33	--	--	--	--

Table 9. Summary of wind and PM_{10} data for the two predominant wind directions at station P57-4.

Wind Speed Class (mph)	**Duration (hours)**	**Frequency (%)**	**Cumulative Frequency (%)**	**Average Wind Speed (mph)**	**PM_{10} (μg/m^3)**
		P57-4 All Winds			
0 – 5	3,289.00	39.900	39.900	3.53	9.59
5 – 10	2,666.67	32.350	72.250	7.03	9.01
10 – 15	1,528.00	18.537	90.786	12.26	9.21
15 – 20	617.00	7.485	98.271	16.96	17.18
20 – 25	125.83	1.527	99.798	21.60	50.00
25 – 30	14.50	0.176	99.974	26.87	420.47
30 – 35	2.17	0.026	100.000	30.84	2,152.24
Total	8,243.17	--	--	--	--
		P57-4 Northwest to Northeast Winds			
0 – 5	1,587.50	41.318	41.318	3.77	11.21
5 – 10	1,353.50	35.228	76.545	6.86	8.56
10 – 15	615.83	16.028	92.574	12.19	7.05
15 – 20	231.83	6.034	98.608	16.93	12.07
20 – 25	42.67	1.110	99.718	21.61	40.72
25 – 30	9.33	0.243	99.961	26.68	500.35
30 – 35	1.50	0.039	100.000	30.79	2,947.50
Total	3,842.17	--	--	--	--
		P57-4 South to Southwest Winds			
0 – 5	675.67	27.210	27.210	3.51	10.12
5 – 10	826.83	33.298	60.507	7.31	11.30
10 – 15	645.33	25.988	86.496	12.31	12.11
15 – 20	276.67	11.142	97.637	16.99	24.76
20 – 25	54.33	2.188	99.825	21.57	76.37
25 – 30	4.00	0.161	99.987	27.60	319.81
30 – 35	0.33	0.013	100.000	30.32	329.53
Total	2,483.17	--	--	--	--

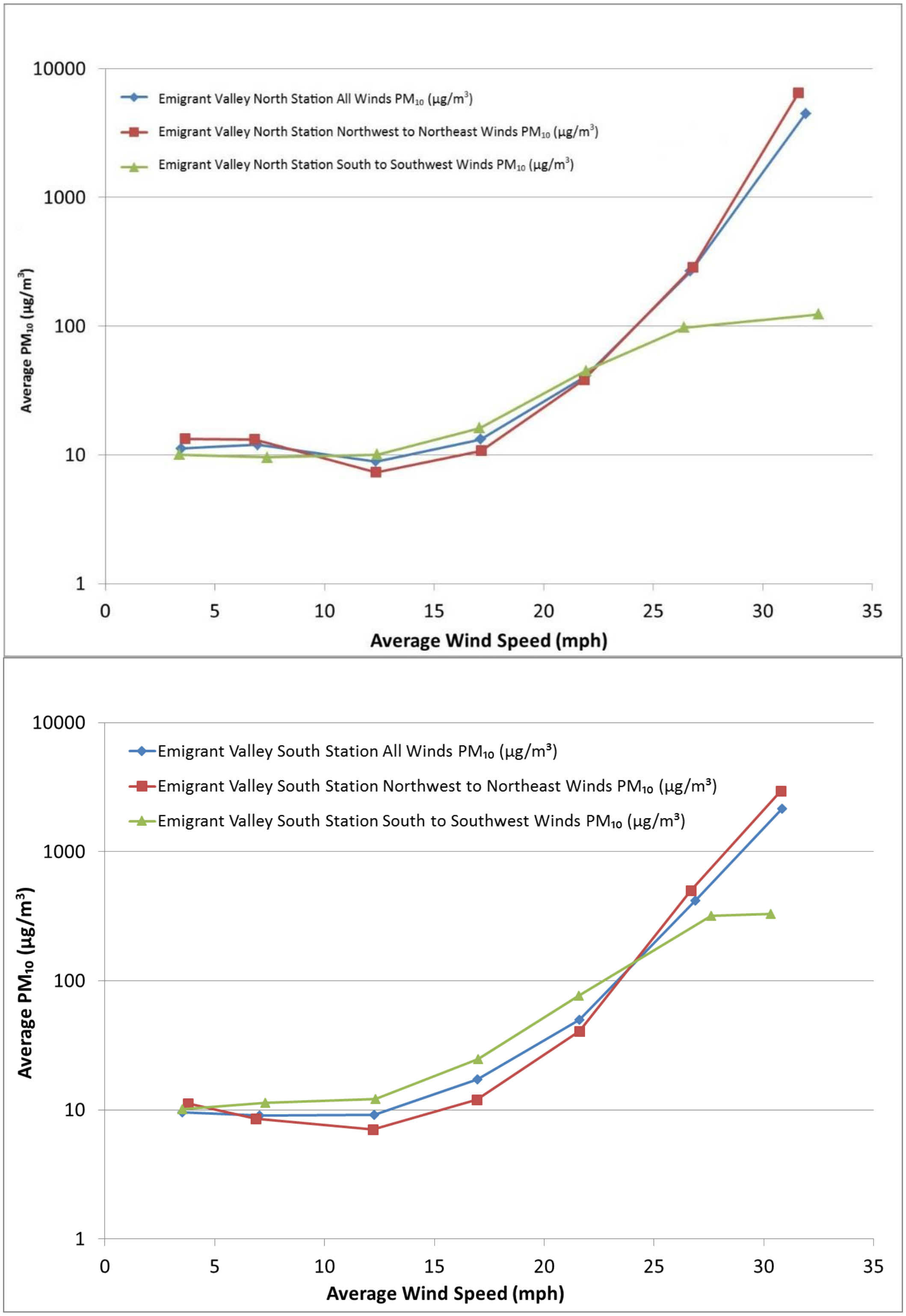

Figure 16. Average PM_{10} concentrations for 5 mph (8 km/hr) wind speed intervals at P57-3 (top) and P57-4 (bottom) for winds from all directions and for winds from the two predominant wind directions.

Dust Source Proximity Analysis

Wind is the driving mechanism for transport of dust, soil, and potentially contaminated material, but the difficulty in data analysis is to decouple and identify dust generated locally from the Project 57 site versus dust transport from the surrounding areas that exhibit the same or similar dust emission potential. Native, undistributed desert areas in the arid southwest are well-known to emit dust under strong winds. To try and determine the dust contribution between near and far sources at the Project 57 monitoring stations the data analysis will include calculation of $PM_{2.5}$ concentration. The $PM_{2.5}$ concentration contains smaller size particles than PM_{10}. Because of the smaller size, $PM_{2.5}$ particles have a considerably lower settling velocity. Therefore, they have a longer residence time in the atmosphere resulting in longer transport distances. Under normal atmospheric conditions the PM_{10} concentration is 4-8 times higher than the $PM_{2.5}$ concentration. However, that ratio can be exceeded when there are local resuspension sources and windy conditions. The ratio between PM_{10} and $PM_{2.5}$ can be used to make a qualitative estimate of how far the aerosol has traveled from the source areas relative to the observation location. Higher PM_{10} to $PM_{2.5}$ ratios indicate aerosol closer to the source area.

The $PM_{2.5}$ concentration as a function of average wind speed class is shown in Figure 17 and exhibits a trend similar to the trend of PM_{10} concentration shown in Figure 14. Figure 18 shows the ratio between PM_{10} and $PM_{2.5}$ for increasing wind speed classes. Both stations show a significant increase in this ratio from around 6-8 for wind speeds under 20 mph (32.2 km/hr) to over 12 for wind speeds over 20 mph (32.2 km/hr). At speeds over 20 mph (32.2 km/hr) winds at the Project 57 monitoring stations are strong enough to result in local saltation activity (Table 6, Figure 12). The increase in saltation contributes to a significant increase in both $PM_{2.5}$ and PM_{10} concentration; however, the increase in PM_{10} is greater than the increase in $PM_{2.5}$ suggesting that these stronger winds are raising dust from the local area.

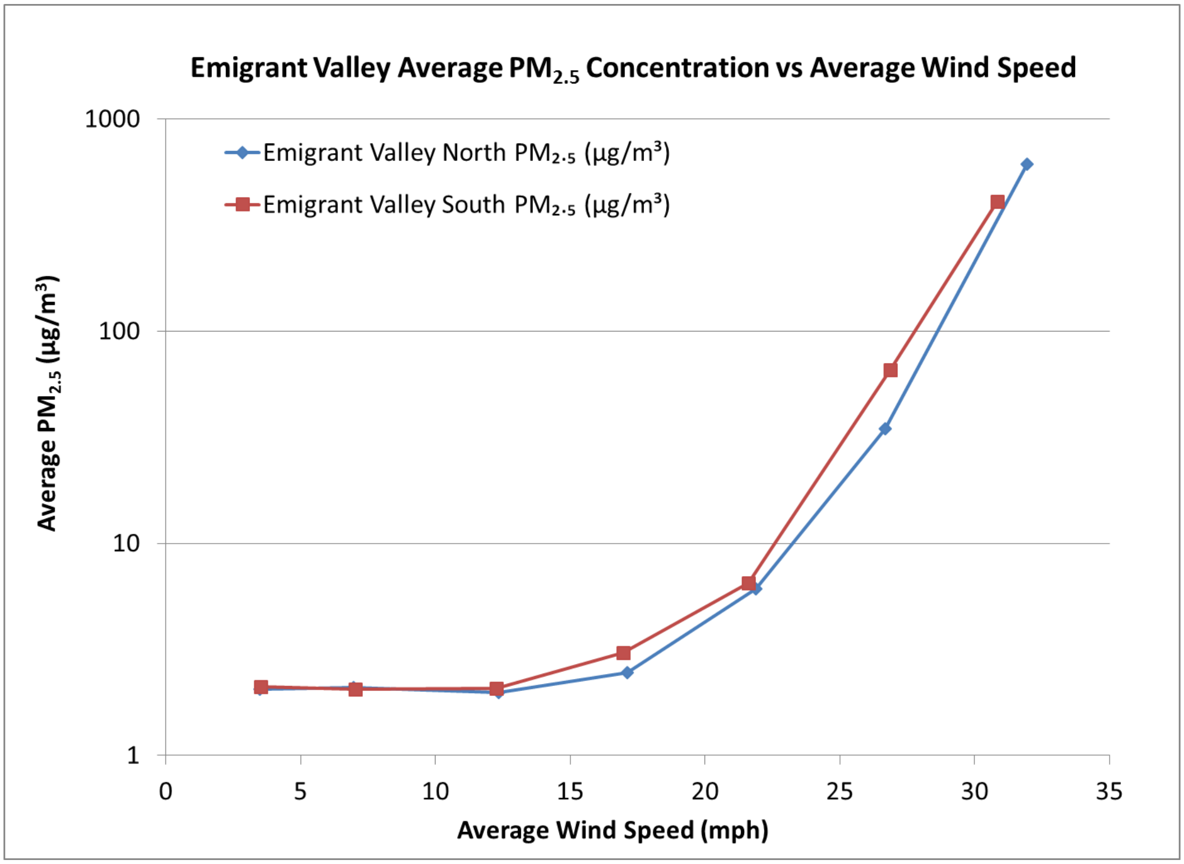

Figure 17. $PM_{2.5}$ trends as a function of wind speed for the P57-3 and P57-4 monitoring stations at Project 57.

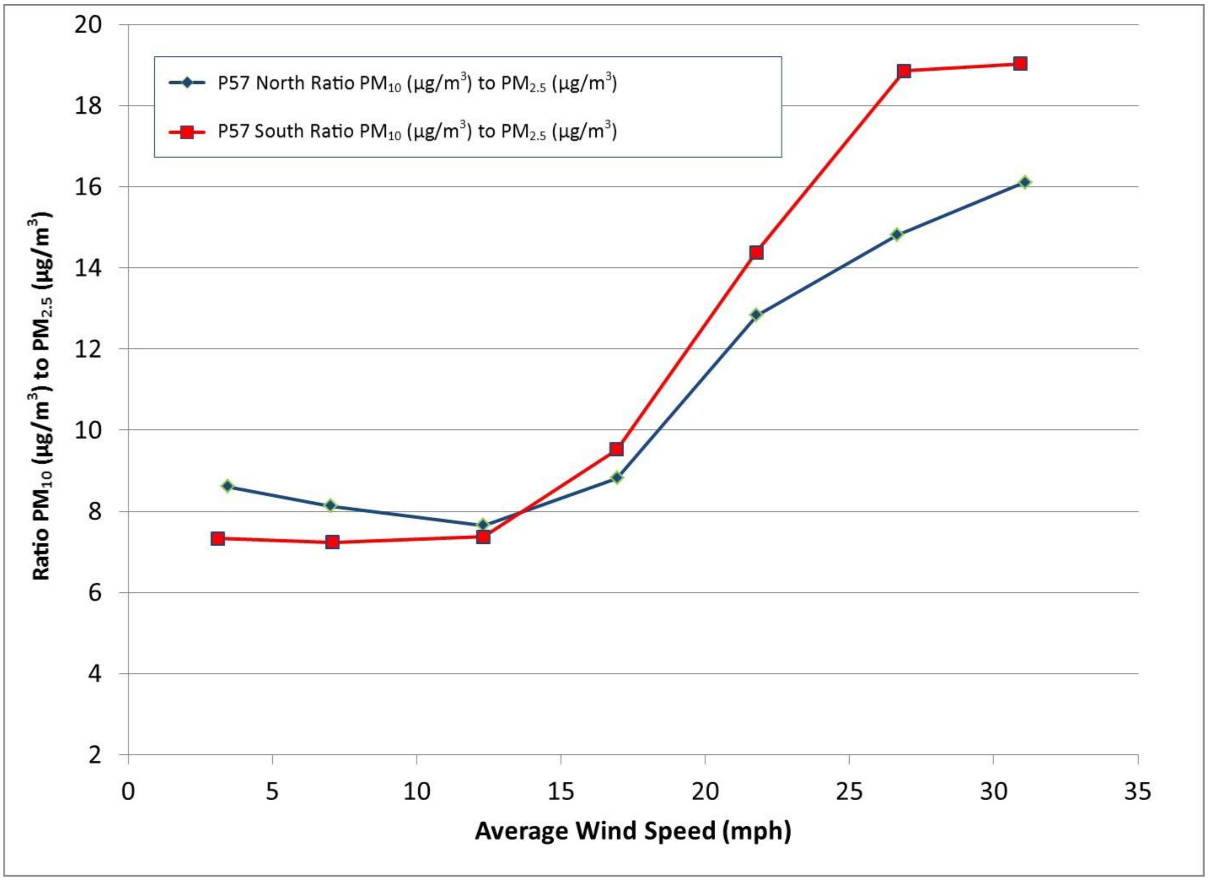

Figure 18. Ratio of PM_{10} to $PM_{2.5}$ trends as a function of wind speed for Project 57 monitoring statoins P57-3 and P57-4.

MAJOR SUSPENSION AND SALTATION DUST TRANSPORT EPISODES

Most dust transport occurs during high-wind events that are usually short in duration. Eight significant wind/dust events were identified, on the basis of elevated PM_{10} counts, during CY2015 (Table 10). Six occurred during the summer season, March through August, and two occurred during the winter season, September through February.

Table 10 summarizes the wind and dust conditions associated with the most notable wind episodes. Appendix Figures E-1 through E-8 show the wind speed and PM_{10} concentration and saltation counts observed during these wind episodes.

Table 10. Description of wind and dust conditions during selected high-wind episodes observed during the reporting period.

Date	Wind Speed (mph)	Wind Direction	PM_{10} (µg/m^3)	Saltation (#/10 min)	Figure	Comments
Feb 24, 2015	15 to 30	Northerly	300	0	E-12	PM_{10} concentration fell below 20 µg/m^3 as wind speed dropped below 20 mph; no saltation activity indicates the dust source was not local.
Mar 31, 2015	15 to 20	Northerly changing to Southwesterly	125	5	E-13	Saltation, even though minor, peaks coincidentally with PM_{10} indicating some local soil suspension and transport. In the evening, after winds dropped below 15 mph, PM_{10} remained relative high suggesting transport from other areas.
Apr 1, 2015	15 to 20	Northerly	780	20	E-14	The 10-minute average wind speeds were generally below 20 mph. The high PM_{10} and occasional high saltation counts may have been facilitated by fresh fine dust deposited during the dust event on March 31. The PM_{10} concentrations above 200 µg/m^3 only lasted about 2 hours indicating a limited dust supply left by the previous dust event.
Apr 5, 2015	15 to 22	South-southwesterly	240	0	E-15	Sustained winds were not adequate to generate saltation activity. Short duration PM_{10} peaks aligned with short duration wind peaks implying some local resuspension before the limited dust supply was depleted.
Apr 7, 2015	15 to 25	South-southwesterly	270	6	E-16	The minimal saltation activity in conjunction with notable PM_{10} concentrations suggest the dust event was principally long-range transport with some local contribution.
Apr 14, 2015	15 to 35	South-southwesterly changing to Northerly	30,000	100	E-17	The strongest dust event of CY2015. Sustained winds remained above 15 mph for approximately 12 hours. The PM_{10} dust concentration closely mirrored the wind speed pattern. Peak PM_{10} concentrations were accompanied by strong saltation counts. This wind/dust event was observed at other regional monitoring stations on the TTR and NNSS.
Aug 6, 2015	15 to 32	Northerly changing to South-southwesterly	850	80	E-18	Sudden increase in wind speed from 15 to 30 mph was accompanied by a sharp increase in PM_{10}, from near zero to more than 850 µg/m^3 and an increase in saltation counts from zero to approximately 100. Illustrating the effect of short duration summer winds during dry soil conditions.
Sep 13, 2015	15 to 23	Northerly changing to South-southwesterly changing to Northerly	880	30	E-19	Sudden increase in wind speed form less than 10 mph to 22 mph was accompanied by a sharp increase in PM_{10}, from near zero to 880 µg/m^3 and an increase in saltation counts from zero to approximately 30.

RADIOLOGICAL ASSESSMENT OF AIRBORNE PARTICULATE MATTER

Airborne dust particles are collected using Hi-Q™ air samplers located at each of the monitoring stations. These collectors draw ambient air through a 4 in (10 cm) diameter glass- fiber filter (pore size 0.00001 in [0.3 µm]) at a rate of 2 cfm (56.6 lpm). The collector is designed to maintain a constant flow rate as dust accumulates on the filter. The total volume of air passed through the filter and the total hours of operation are recorded when the filters are collected. The deployed filters are collected and replaced with new filters every two weeks. Filters are weighed before and after deployment to determine the mass of the particles collected. Accumulated filters are submitted to the Radiological Services Laboratory at the University of Nevada, Las Vegas, for gross alpha, gross beta, and gamma spectroscopy assessment.

During the operational period covered in this report, sample filters were deployed for approximately 14-day periods from January 7, 2015, through December 23, 2015. In the two weeks between April 13, 2015, and April 28, 2015, two samples were collected at both P57-3 and P57-4: one two-day sample associated with a dust storm observed in the field was collected between April 13 and 15, 2015, and one 13-day sample collected during the balance of the two week period (April 15 through April 28, 2015). Discussion of the April 15 samples and the associated meteorological conditions is presented later in the section titled "April 15, 2015 2-day Airborne Particulate Matter Samples". At P57-3, a total of 23 samples were collected, including the two-day sample, because three samples (September 14 to 27, 2015; September 28 to October 13, 2015; and November 9 to 23, 2015) were lost because the sampler failed to operate or was repeatedly knocked over in the field. It is not known exactly why the air sampler was knocked over, winds or animal contact may have been the cause; the sampler has been well-tethered to prevent a recurrence. Each time the sampler was turned over it continued to run while the air intake lay on the ground. The samples for these collection periods were rejected because they were not considered representative of airborne particulate matter because of the potential for contamination by particles drawn in directly from the soil surface. At P57-4 a total of 26 samples of airborne particulate matter were collected because no samples were lost. The gross alpha and gross beta observations for the reporting period are summarized in Tables 11 and 12, respectively.

Table 11. Gross alpha results for Project 57 sampling stations during CY2015.

Sampling Location	**Number of samples**	**Concentration (x 10^{-15} µCi/mL [3.7 x 10^{-5} Becquerel (Bq)/m^3])**			
		Mean	**Standard Deviation**	**Minimum**	**Maximum**
P57-3	23	1.88	2.53	0.45	15.43
P57-4	26	2.78	4.32	0.47	23.08

NOTES: Bq = Becquerel; m^3 = cubic meter; µCi/ml = microcurie per milliliter.

The statistics include the results for nine laboratory analysis replicates run on P57-3 samples and two replicates run on P57-4 samples.

Table 12. Gross beta results for Project 57 sampling stations during CY2015.

Sampling Location	Number of samples	Concentration (x 10^{-14} µCi/mL [3.7 x10^{-4} Becquerel (Bq)/m^3])			
		Mean	Standard Deviation	Minimum	Maximum
P57-3	22	1.96	0.70	0.73	4.75
P57-4	26	1.92	0.41	1.30	3.10

NOTES: Bq = Becquerel; m^3 = cubic meter; µCi/ml = microcurie per milliliter.

Table 13 gives the CY2015 gross alpha and gross beta concentrations reported for CEMP stations surrounding the northern ranges of the NTTR (NSTec, 2016). Sampling procedures at the Project 57 and CEMP stations are similar, which allow general comparisons to be made for the region.

The mean gross alpha concentration at P57-3 is slightly higher than, but on the same order of magnitude as, the gross alpha mean concentrations at the surrounding CEMP stations. This difference is driven primarily by one sample that exceeded the maximum value observed at the surrounding CEMP stations during CY2015 (Table 14). The P57-4 mean gross alpha concentration is notably higher than the mean gross alpha concentration values at surrounding CEMP stations. The minimum gross alpha concentration reported for the Project 57 stations are near the low end of the range of minimum values observed at the CEMP stations. The higher mean gross alpha concentration for P57-4 results because of four individual sample values that exceeded the maximum value observed (Table 13, Sarcobatus Flat) at the surrounding CEMP stations (Table 14). Three of the four high gross alpha concentration values at P57-4 were between 1.0 and 1.6 times the maximum gross alpha concentration observed at the surrounding CEMP stations. The fourth high gross alpha concentration was almost 4.5 times the highest gross alpha concentration observed at the surrounding CEMP stations.

Mean gross beta concentrations at the Project 57 stations are essentially the same as those determined for the CEMP stations. The minimum and maximum gross beta concentration values for P57-3 are outside the range of minimum and maximum values for the CEMP stations. Minimum and maximum values for P57-4 fall within the range of minimum and maximum values for the CEMP stations.

Table 13. Mean annual gross alpha and gross beta concentrations for CY2015 reported at CEMP stations that surround the Tonopah Test Range (NSTec, 2016).

Sampling Location	Gross alpha (x 10^{-15} µCi/mL)			Gross beta (x 10^{-14} µCi/mL)		
	Mean	Minimum	Maximum	Mean	Minimum	Maximum
Alamo	1.79	0.46	3.98	2.12	1.56	3.27
Beatty	1.05	0.49	1.76	1.94	1.34	3.23
Goldfield	1.05	0.59	1.77	1.85	1.18	3.06
Rachel	1.07	0.53	2.10	1.94	1.14	3.20
Sarcobatus Flat	1.81	0.58	5.16	2.05	1.22	3.09
Tonopah	1.02	0.42	1.82	1.78	1.16	3.14

Table 14. Gross alpha concentrations for individual Project 57 samples that exceed the maximum concentrations observed at the surrounding CEMP stations in CY2015.

Sampling Location	Collection Date	Concentration (x 10^{-15} µCi/mL [3.7 x 10^{-5} Bq/m^3])	Exceedance Factor
P57-3	April 15, 2015	15.43	2.99
P57-4	January 22, 2015	6.67	1.29
P57-4	April 15, 2015	5.39	1.04
P57-4	June 23, 2015	23.08	4.47
P57-4	July 7, 2015	7.99	1.55

NOTES: Bq = Becquerel; m^3 = cubic meter; µCi/ml = microcurie per milliliter.

The statistics include the results for nine laboratory analysis replicates run on P57-3 samples and two replicates run on P57-4 samples.

Environmental monitoring on the NNSS collects airborne particulate matter samples at 16 stations for gross alpha and gross beta concentration analyses. For 2014 (results of the 2015 samples are not available), the mean annual gross alpha concentration values range from 1.73 x 10^{-15} µCi/mL to 3.59 x 10^{-15} µCi/mL and average 2.37 x 10^{-15} µCi/mL and the gross beta concentration values range from 1.95 x 10^{-14} µCi/mL to 2.34 x 10^{-14} µCi/mL and average 2.14 x 10^{-14} µCi/mL (NSTec, 2015). The mean gross alpha concentration value for P57-3 is in the low end of values observed at the NNSS stations. The P57-4 value exceeds the mean gross alpha concentration for the NNSS samples but is less than the maximum observed NNSS value. The mean gross beta concentration values for the Project 57 stations are at the low end of the values observed for the 2014 NNSS samples.

The naturally occurring radionuclides, beryllium 7 (Be-7), lead 210 (Pb-210), and potassium 40 (K-40) were detected in the particulate matter samples with varying frequency by gamma spectroscopy analyses (Table 15). Gamma spectroscopy also identified americium 241 (Am-241) in the June 23, 2015, sample from P57-4. Am-241 is an anthropogenic radionuclide that is not naturally occurring. It indicates the presence of plutonium 241 (Pu-241), which is a minor yet easily detected component of the material used for the Project 57 plutonium dispersal test. When Am-241, in any concentration, is detected by gamma spectroscopy, the sampling protocol stipulates that the sample be analyzed for plutonium 238 and plutonium 239+240. These results of these analyses are discussed in the following section of this report.

Two TLDs are deployed at each of the Project 57 monitoring stations to determine the radiation exposure external dose, whether from natural environmental sources or radiation transported from Project 57 Contamination Area. The TLDs are collected and replaced quarterly. Tables 16 and 17 give the observed quarterly exposure external dose and the estimated equivalent annual external dose at the Project 57 monitoring stations. The estimated annual external dose at the P57-3 and P57-4 monitoring stations is 156.9 millirem (mR) and 163.0 mR, respectively. The millirem (0.001 rem) is a measure of the dose equivalence pertaining to the human body and takes into account both the absorbed energy and the biological effect on the body because of the different types of radiation.

Table 15. Gamma spectroscopy analysis of the airborne particle samples collected during CY2015 detected four radionuclides. Except for Am-241, all detected radionuclides are naturally occurring. The frequency of detection varied by radionuclide and location.

Radionuclide	**Number of samples showing detectable concentrations**	
	P57-3	**P57-4**
Beryllium (Be-7)	20	23
Lead 210 (Pb-210)	13	16
Potassium 40 (K-40)	3	1
Americium 241 (Am-241)	0	1

People are constantly exposed to radiation emitted by both the natural environment and anthropogenic sources. Natural environmental sources include cosmic radiation, radiation emitted by the soil and geology of the Earth's surface, radiation ingested in food and water, and radiation from radon gas. The magnitude of natural radiation exposure varies from place to place primarily as a result of differences in local geology and elevation. The general public is also exposed to anthropogenic sources of radiation associated with tobacco products, medical services, and consumer goods. The average annual radiation dose to the general public is estimated to be 620 mR (NRC, 2011), half of which is from natural sources and half of which is from anthropogenic sources (NRC, 2011). At the Project 57 monitoring stations, exposure to natural sources of radiation and any radiation transported from the Contamination Area is significantly less than (approximately half) the average annual dose experienced by the general public as a result of exposure to natural sources.

The estimated annual radiation dose at the Project 57 monitoring stations, 156.9 mR and 163 mR, (Tables 16 and 17) is slightly greater than the dose amounts reported for the CEMP stations surrounding the NTTR, which range from 112 mR at Alamo to 144 mR at Sarcobatus Flat (Table 18). These differences are likely because of differences in local geology and elevation.

Table 16. Annual radiological dose rate estimated from TLDs deployed at the P57-3 monitoring station.

Fiscal Year	**Quarter**	**Days Deployed**	**Observed Dose (mR)**	**Estimated Daily External Dose (mR)**	**Estimated Annual External Dose (mR)**
2015	1	91	36	0.4000	156.9
			37	0.4111	
	2	91	38	0.4176	
			36	0.3956	
	3	92	40	0.4565	
			40	0.4347	
	4	88	40	0.4545	
			41	0.4659	

Table 17. Annual radiological dose rate estimated from TLDs deployed at the P57-4 monitoring station.

Fiscal Year	Quarter	Days Deployed	Observed Dose (mR)	Estimated Daily External Dose (mR)	Estimated Annual External Dose (mR)
2015	1	91	38	0.4176	163.0
			39	0.4286	
	2	91	39	0.4286	
			39	0.4286	
	3	92	43	0.4674	
			41	0.4456	
	4	88	42	0.4773	
			42	0.4773	

Table 18. Estimated annual radiological dose (mR) determined from TLDs deployed at CEMP stations surrounding the NTTR.

Station	CY2013	CY2014	CY2015
Alamo	115	119	119
Beatty	139	147	150
Goldfield	122	127	130
Rachel	126	134	131
Sarcobatus Flat	144	144	1
Tonopah	133	137	140

June 23, 2015 P57-4 Sample (Am-241 detection)

Americium 241 reported in the gamma spectroscopy analysis of the June 23, 2015, sample from P57-4 triggered an alpha spectroscopy analysis for plutonium isotope concentrations in accordance with the project sampling and analysis protocol. This sample was collected between June 9 and June 23, 2015, a 13.91 day deployment. A second sample, collected at P57-4 on July 7, 2015, (deployed between June 23 and July 7, 2015, a 13.93 day period) was also submitted for alpha spectroscopy analysis although it did not test positive for Am-241 by the gamma spectroscopy analysis. The July 7 sample was submitted for analysis because of a higher than average gross alpha result and because it was obtained during the collection period immediately following the Am-241 detection. Test America performed the alpha spectroscopy analyses.

For the sample taken June 23, 2015, the Am-241 result by alpha spectroscopy (Table 19) is in good agreement with the gamma spectroscopy result of 6.6×10^{-15} µCi/mL. Although Am-241 was not detected by gamma spectroscopy for the sample taken July 7, 2015, it was detected by alpha spectroscopy because of the better sensitivity of the technique. The highest alpha spectroscopy result was for Pu-239+240 at 3.4×10^{-14} µCi/mL for the June 23 sample. The overall results for the July 7 sample are an order of magnitude less than results for the June 23 sample.

Table 19. Alpha spectroscopy results for selected airborne particle samples collected from P57-4.

Sample Date	Radionuclide ($x 10^{-15}$ µCi/mL)		
	Am-241	Pu-238	Pu-239+240
June 23, 2015	7.1	0.77	34.0
July 7, 2015	1.2	0.092	5.9

There were no major wind storms during the two weeks that the sample taken from P57-4 on June 23, 2015, was collected (Figure 19). During the two-week period wind speed and direction exhibit a diurnal pattern. Overnight the 10-minute average wind speed was near 5 mph (8 km/hr) from the north. Daytime winds were from the southwest and 10-min average wind speeds commonly exceeded 15 mph (24 km/hr) but were never greater than approximately 22 mph (35 km/hr). The higher daytime wind speeds typically occurred between 09:00h and 18:00h and lasted for between 1 hour and 9 hours. (All times shown are reported in Pacific Standard Time.) With the exception of a single notable event, the 10-minute average PM_{10} concentrations were low (Figure 19) throughout the sampling period. Between 22:10h and 23:30h on the night of June 13, 2015, the PM_{10} dust concentration was elevated. Approximately 30 minutes into the event the concentration peaked at 3.0×10^{-7} oz/ft^3 (300 µg/m^3). This dust event occurred while the winds were less than 6 mph (9.7 km/hr) and rotating from the northeast to the east. These conditions are rather common and do not immediately explain why a high Am-241 detection was reported for this sample.

Review of instantaneous wind observations, collected at three-second intervals, showed additional details. A significant wind speed and wind direction change occurred at about 14:12h on June 13, 2015. In a period of approximately 20 seconds, the wind directions shifted approximately 120 degrees from southerly (190^o) to northwesterly (310^o). The wind shift was accompanied by an increase in wind speed from 7 mph (11.3 km/hr) to about 32 mph (51.5 km/hr) (Figure 20). The wind gust lasted approximately 15 seconds and declined to less than 10 mph (16.1 km/hr) over the next 15 to 20 seconds. A similar phenomena (Figure 21) occurred at about 12:02h on June 14, 2015. In this case the wind direction shifted approximately 90 degrees from (200^o) south-southwesterly to west-northwesterly (290^o) over a period of about 20 seconds. During the same time period, the wind speed jumped from about 8 mph (12.9 km/hr) to 43 mph (69.2 km/hr) (note that the upper end of the wind speed axis was artificially limited to 35 mph [56 km/hr]). Though not illustrated in this report, similar wind direction and wind speed conditions occurred during the two-week collection period for the July 7, 2015, sample.

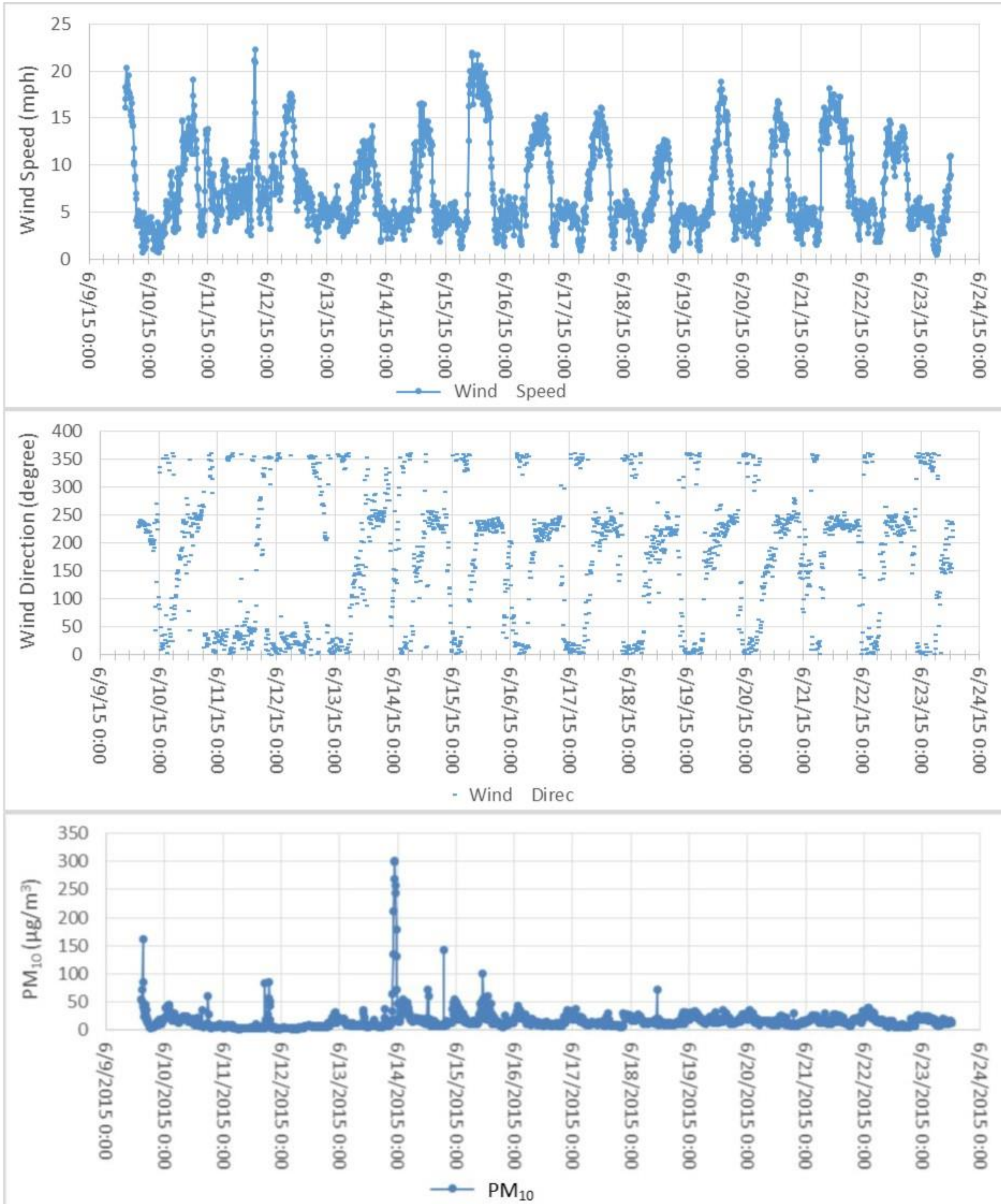

Figure 19. 10-minute average wind speed (top), wind direction (middle), and PM_{10} (bottom) observed during collection period for sample P57-4 June 23, 2015.

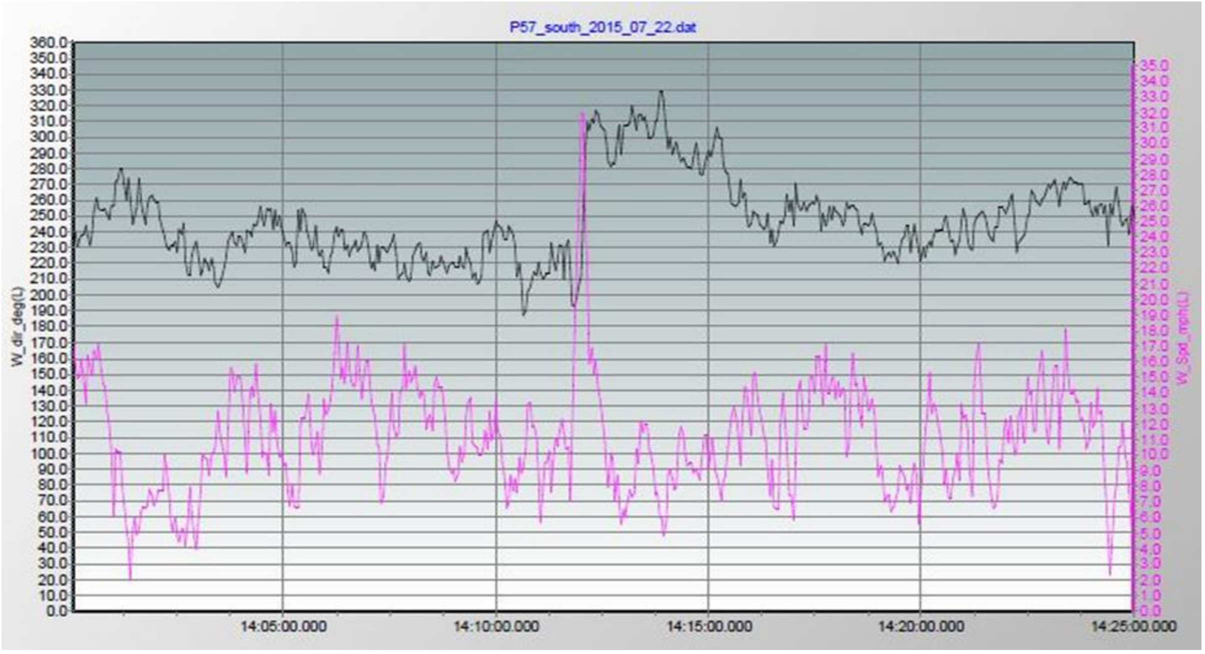

Figure 20. Wind speed and wind direction values collected every three seconds between 14:00h and 14:25h (PST) on June 13, 2015.

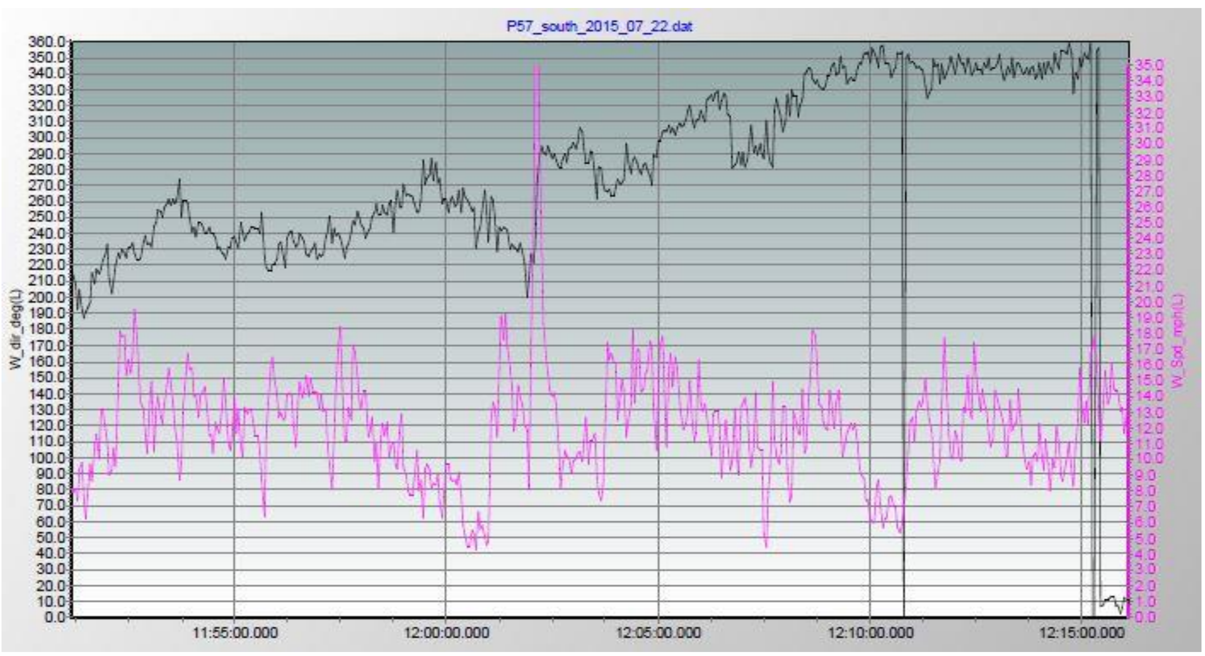

Figure 21. Wind speed and wind direction values collected at three-second intervals between 11:50h and 12:15h (PST) on June 14, 2015.

The observations described above suggest a dust devil may have passed across the monitoring station. Dust devils travel across the landscape in the direction of and at the speed of the prevailing winds. The high winds and rotational pattern of a dust devil combined with the small circumference of the phenomena would produce sudden increases in wind speed and rapid shifts in direction as the dust devil passed over recording instruments. If the dust devil passed directly over a monitoring station on a track through the center of the circulation, there would be an initial 90^o shift in wind direction as the prevailing winds are overwhelmed by the rotating winds of the dust devil, followed by a 180^o shift as the eye of the circulation passed the station, and the prevailing wind direction would return as the dust devil passed beyond the monitoring station. As the wind direction changes were observed, the wind speed would increase sharply, remain high, and then decrease sharply as the circulation passed the monitoring station. The observations described in the previous paragraph do not indicate a direct hit on the monitoring station by a dust devil, but may reflect a dust devil passing so that wind directions and speeds at the edge of the circulation were recorded.

The high wind speeds associated with the cyclonic circulation of dust devils cause the dust devil to transport large quantities of soil particles. If a dust devil passed by the P57-4 monitoring station, some of the dust it transported will be collected in the airborne particulate matter sample. The mass of material collected in the June 23, 2015, sample (0.0144 g) is approximately equal to the average mass (0.0150 g, [standard deviation = 0.0059 g]) for all samples collected from P57-4 during the year. Mass of the July 7, 2015, sample (0.0223 g) from P57-4 falls between the average plus one standard deviation and the average plus two standard deviations for all samples collected from P57-4 during the year. Although a dust devil passing across the monitoring station would likely transport more dust than the ambient winds, the short time the wind storm was over the monitoring station would limit the amount of particles collected from the dust devil. Alternatively, it is possible that the Am-241 detection is the result of a single particle with sufficient americium to be detected. If this is the case, the detection would have to be considered a rarity.

April 15, 2015 2-day Airborne Particulate Matter Samples

New sample filters were deployed on April 13, 2015, for the regular biweekly airborne particulate matter sample collection. Personnel in the area on April 14 noted a significant dust storm approaching from the north. Samples were retrieved on April 15 to obtain results specific to the observed dust storm. New filters were deployed to collect particulate matter during the balance of the regular biweekly sampling period.

The gross alpha concentration for the April 15, 2015, sample from station P57-3 (Table 20) was 8.2 times the average gross alpha concentration for all samples collected at the station during CY2015 (Table 11). At station P57-4, the April 15 sample concentration (Table 20) was approximately 1.9 times the average concentration for the year (Table 11). The gross beta concentration at P57-3 (Table 20) was 2.4 times the average concentration (Table 12) but the April 15 gross beta concentration (Table 20) and the annual average concentration (Table 12) at station P57-4 were approximately the same. Additionally, at station P57-3, the gross alpha and gross beta concentrations for the April 15 sample exceed the annual average plus two standard deviations. Clearly, the radiological concentrations for the P57-3 airborne particulate matter samples are significantly above normal; this increase is likely the result of the dust storm event.

Table 20. Radiological results for the two-day airborne particle samples. Samples were deployed on April 13, 2015, and retrieved on April 15.

Station	Start Time	End Time	Duration (minutes)	Sample Mass (g)	Gross Alpha (x 10^{-15} µCi/mL)	Gross Beta (x 10^{-14} µCi/mL)	Gamma Spec
P57-3	14:00	11:03	2703	0.1322	15.43	4.75	ND
P57-4	15:25	11:45	2650	0.0272	5.39	1.94	ND

ND = no isotopes were reported by the gamma spectroscopy analysis.

The dust storm began to be evidenced in PM_{10} values at P57-3 at about 07:50h (PST) on April 14, 2015 (Figures 22 and 23) when the PM_{10} first exceeded twice the average PM_{10} (3.0 x 10^{-8} oz/ft^3 [30 µg/m^3]) for the preceding 24 hours. (All times shown are reported in Pacific Standard Time.) The dust storm lasted until approximately 17:10 when the PM_{10} again dropped below twice the pre-storm levels. The peak PM_{10} concentration at P57-3, approximately 2.6 x 10^{-5} oz/ft^3 (26,083 µg/m^3), was recorded at 12:50h about half way through the storm. The PM_{10} dust levels at P57-4 rose above the previous 24-hour average (2.0 x 10^{-8} oz/ft^3 [19.8 µg/m^3]) at about 09:00h. The storm continued until the PM_{10} values dropped below twice the pre-storm average at about 16:50h. At P57-4, the PM_{10} concentration peaked at 4.56x10^{-6} oz/ft^3 (4025 µg/m^3) at about 13:00h. The dust storm lasted 9.3 hours at P57-3 and 7.8 hours at P57-4.

Examination of the 10-minute average wind speed and direction before, during, and after the April 14 dust storm reveal a sharp definitive change in conditions at the time of the event. Although slightly stronger at P57-3, wind speeds prior to the dust storm were less than 20 mph (32.2 km/hr) at both stations. Following the dust storm, wind speeds diminished consistently to near calm over a nine hour period, but then between 03:00h and 09:00h, wind speeds increased to the 15 to 25 mph (24.1 to 40.2 km/hr) range. These wind speeds produced a second, although very minor, increase in PM_{10} dust. During the major dust storm, 10-minute average wind speeds reached more than 34 mph (54.7 km/hr) at P57-3 and 32 mph (51.5 km/hr) at station P57-4. The change from about 15 mph (24.1 km/hr) to the peak wind speed occurred over a period of approximately five hours. Initially these winds were from the south as the winds had been during the preceding 24 hours. Over a period of about 30 minutes beginning about 11:30h the wind shifted from the south-southwest to the west-northwest. It then continued to shift to the north-northwest throughout the dust storm. Timing of the dust storm on April 14 clearly associates the dust storm with a weather front advancing north to south through the valley.

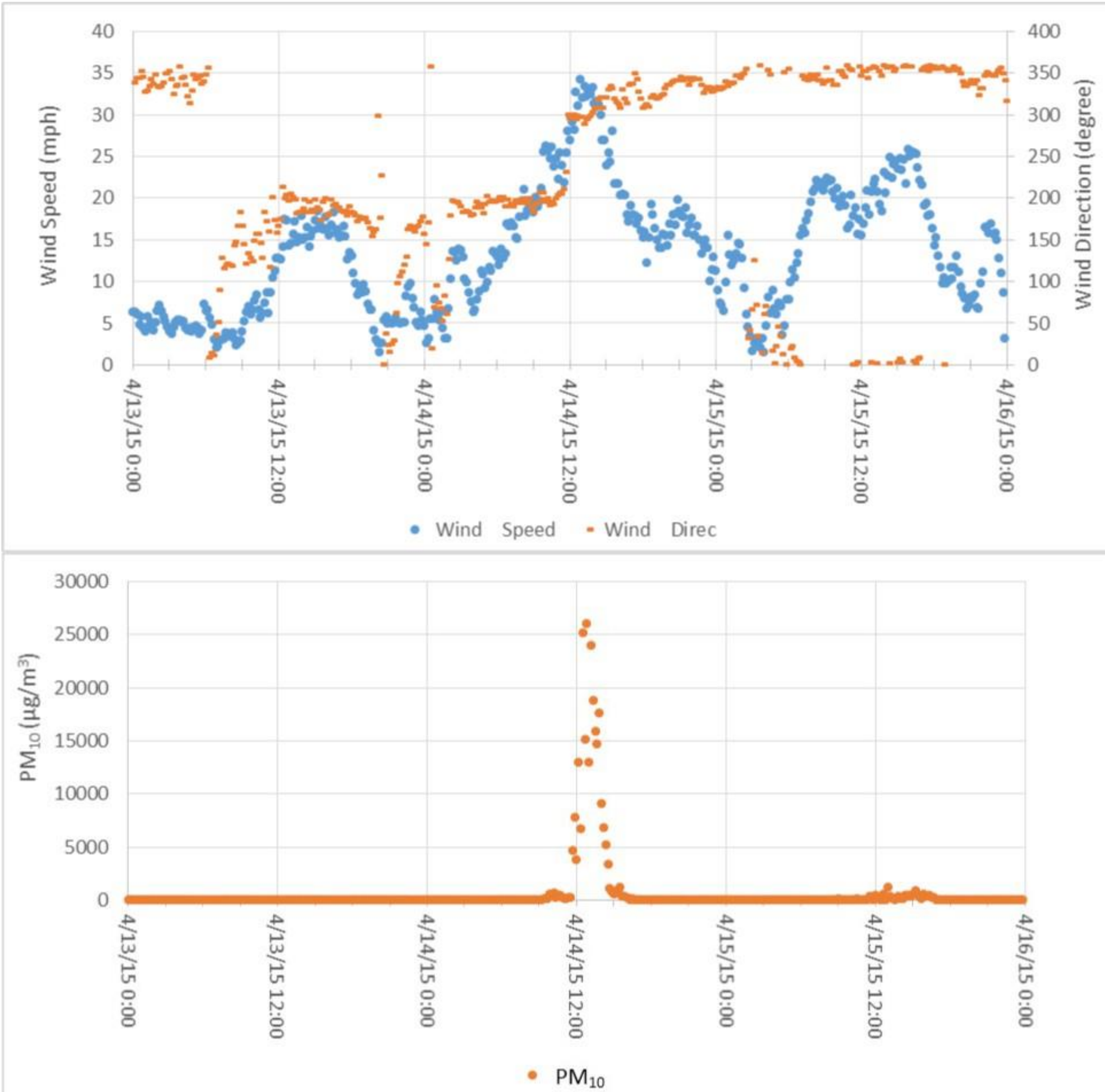

Figure 22. Wind speed and direction (top graph) and PM_{10} concentration (bottom graph) at station P57-3 immediately before, during, and immediately after the April 2015 2-day sample collection period.

The mass of particulate matter collected during the 2-day sample period is significantly greater than the average mass of all samples, most of which are 14-day samples, collected at the respective stations. Mass of the P57-3 sample is approximately six times the average for all P57-3 samples and mass of the P57-4 sample is approximately twice the average for all P57-4 samples. The additional mass of particulate matter on the 2-day sample appears to be associated with the increased PM_{10} values observed during the dust storm. The increased mass of particulate matter and the high dust concentrations during the storm are likely the cause of the higher than typical gross alpha and gross beta values in the 2-day samples. The storm passed the P57 monitoring stations from north to south and would have approached P57-3 across ground outside of the delineated Contamination Area. The increased mass of particulate matter likely resulted from the sharp increases in wind speed associated with the front. Additionally, increased wind turbulence associated with the storm front may have caused particulate matter inside the Contamination Area to become airborne and produced the higher than average gross alpha and gross beta concentration values at the P57-3 sampling station.

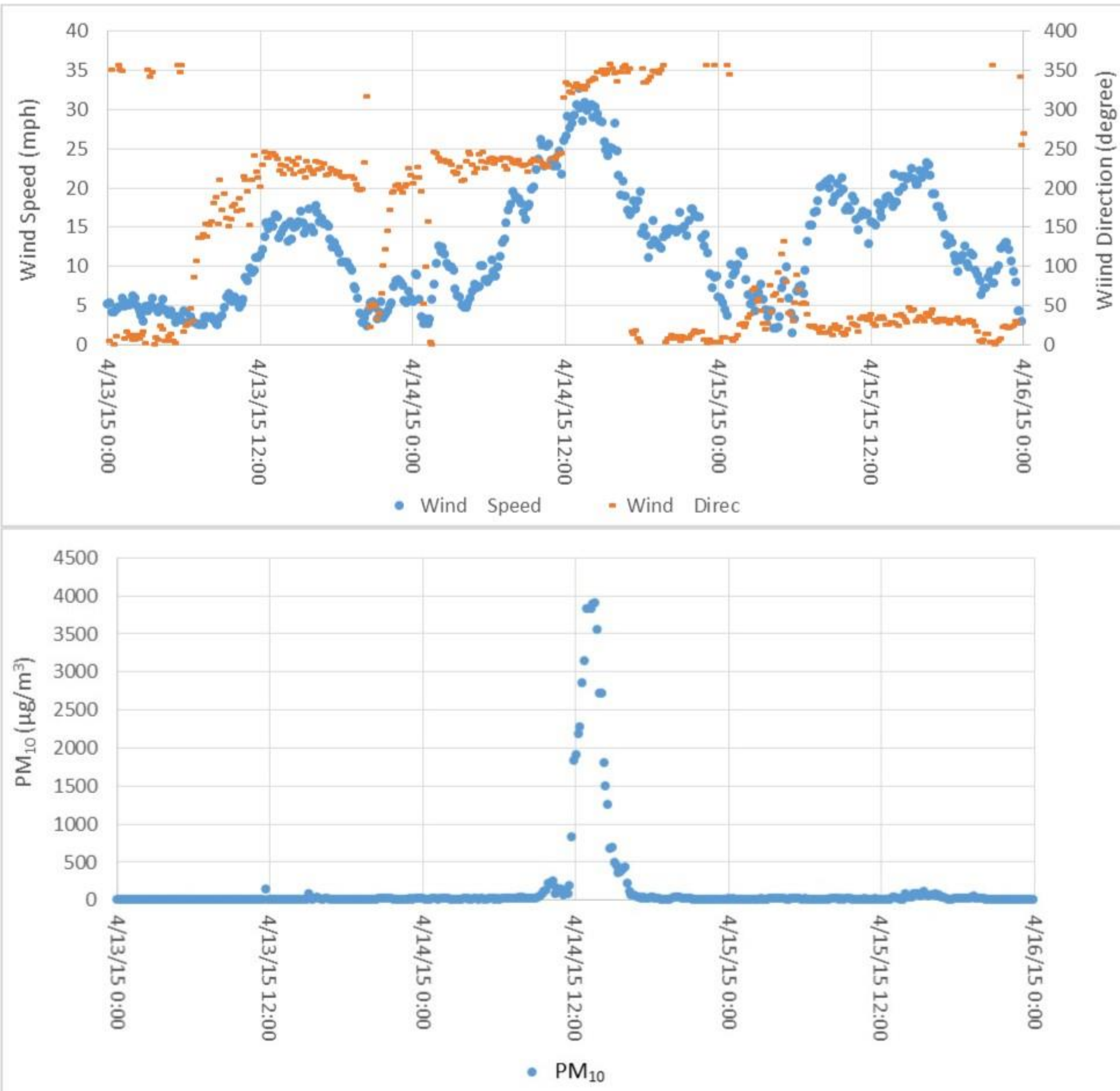

Figure 23. Wind speed and direction (top graph) and PM_{10} concentration (bottom graph) at station P57-4 immediately before, during, and immediately after the April 2015 2-day sample collection period.

RADIOLOGICAL ASSESSMENT OF SALTATION PARTICULATE MATTER SAMPLES

The BSNE saltation sand traps were installed at Project 57 to provide integrated mass samples associated with the dominant wind directions, which facilitates an estimate of the net flux of saltation material on the Contamination Area. The design and installation of the BSNE saltation sand traps is described at the end of the earlier report section titled "Monitoring Station Locations and Capabilities." In the following discussion samples are designated as upwind or downwind. Upwind samples are collected before the transporting winds have crossed the Contamination Area and downwind samples are collected after transporting winds have crossed the Contamination Area.

On April 14, 2014, six BSNE saltation sand traps were installed in three sets of paired traps at monitoring stations P57-1 and P57-2. Paired traps were oriented at 180^{o} and placed so that one opening faced the dominant wind direction coming across the Contamination Area and the other faced away from the Contamination Area (Figure 24). At P57-1, traps 25, 29, and 33 were placed downwind of the Contamination Area and were paired with traps 27, 31, and 35, respectively, which faced upwind of the Contamination Area. At P57-2, traps 37, 41, and 45 faced downwind and the paired traps 39, 43, and 47, respectively, faced upwind (Figure 25).

These saltation traps were retrieved on March 3, 2015 (Table 21). The traps were deployed for approximately 339 days. The samples were held in storage until June when they were consolidated and transferred to Navarro for shipment to Southwest Research Institute and GEL Laboratories for geotechnical and radiological analyses. In consolidating the traps, the three traps facing (i.e., downwind of) the Contamination Area at each monitoring station were intended to be combined into a single sample and the traps facing away from (i.e., upwind of) the Contamination Area at each station were intended to be combined into a single sample. Because of confusion about trap orientation at P57-1, one trap (35) facing upwind was combined with two traps (25, and 29) facing downwind and one trap (33) facing downwind was combined with two traps (27 and 31) that were facing upwind. Traps from P57-2 were correctly combined, traps 37, 41, and 45 were combined into a single sample facing downwind, and traps 39, 43, and 47 were combined into a single sample facing upwind of the Contamination Area.

When P57-3 and P57-4 were established March 3, 2015, clean BSNE saltation sand traps were installed. At P57-3, traps 38, 42, and 46 were placed downwind of the Contamination Area. They were paired with traps 40, 44, and 48, respectively, which faced upwind. At P57-4, traps 26, 30, and 34 faced downwind and the paired traps 28, 32, and 36 faced upwind (Figure 25). These traps were recovered on January 4, 2016, after approximately 307 days deployment. The samples were held in storage until February 17, 2016, when the samples were consolidated and transferred to Navarro for shipment to the Southwest Research Institute for geotechnical analysis and GEL Laboratories for radiological analysis. Multiple traps were consolidated for laboratory analysis to ensure sufficient soil material to facilitate the requested geotechnical and radiological analyses. Saltation traps 38, 42, and 46 (station P57-3) and traps 26, 30, and 34 (station P57-4) were consolidated into samples representing material collected downwind of the Contamination Area at stations P57-3 and P57-4, respectively. Similarly, traps 40, 44, and 48 (station P57-3) and traps 28, 32, and 36 (station P57-4) were consolidated into samples representing material collected upwind of the Contamination Area at stations P57-3 and P57-4, respectively. Nikolich *et al.* (2016) describe extraction of saltation samples from the traps.

The Southwest Research Institute geotechnical laboratory separated the saltation samples into three size fractions: > 0.01 in (250 µm), 0.002 in (63 µm) to 0.01 in (250 µm), and < 0.002 in (63 µm). The two smaller size fractions were submitted to GEL Laboratories for radiological analysis by alpha spectrometry to determine the concentrations of Am-241, Pu-238, and Pu-239+240.

Figure 24. Photos of the BSNE saltation sand trap installations at Project 57 are not available. However, this photograph taken at Clean Slate III on the Tonopah Test Range (Nikolich, 2016) shows a typical installation, which is essentially identical to the Project 57 installations. The BSNE saltation sand trap in the foreground is oriented with one opening facing the dominant wind direction coming across the Contamination Area, which is to the right of the fence, and one facing away from the Contamination Area.

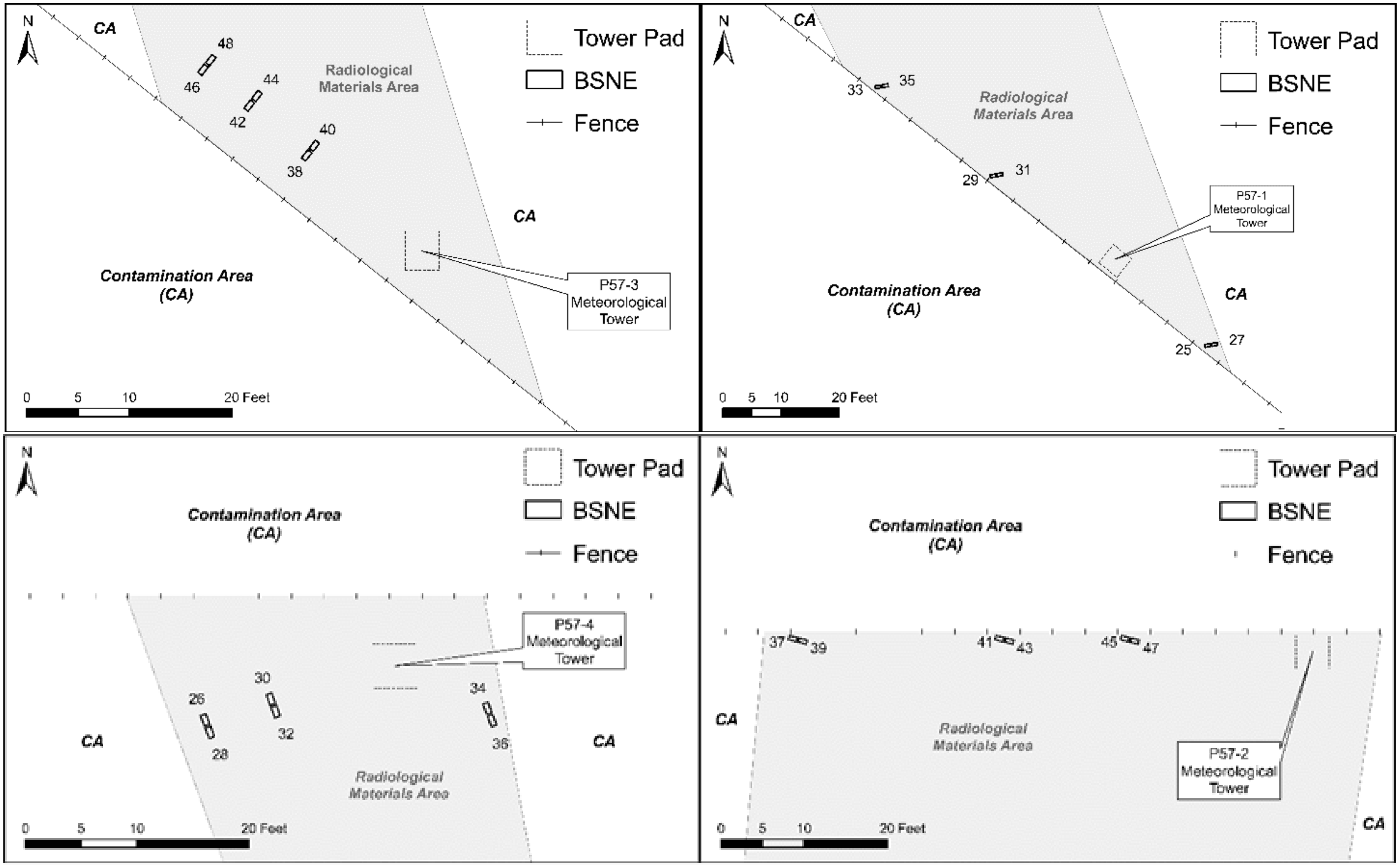

Figure 25. BSNE saltation sand trap deployment at P57-1 (upper right) and P57-2 (lower right) between April 14, 2014, and March 3, 2015, and at P57-3 (upper left) and P57-4 (lower left) between March 3, 2015, and January 4, 2016. This arrangement preserves the geographic relationships of the monitoring stations. Figure 2 shows the spatial relationships.

Table 21. Saltation samples have been retrieved twice since the traps were first installed at Project 57 on April 14, 2014.

Date	Event	Comments
April 14, 2014 March 3, 2015	Initial deployment at P57-1 and P57-2 Traps collected from P57-1 and P57-2	339 day deployment
March 3, 2015 January 4, 2016	Initial deployment at P57-3 and P57-4 Traps collected from P57-3 and P57-4	307 day deployment
January 4, 2016 October 12, 2016[1]	Traps re-deployed at P57-3 and P57-4 Traps collected from P57-3 and P57-4	281 day deployment
November 8, 2016	Traps re-deployed at P57-3 and P57-4	On-going deployment

[1] Analyses of saltation sand trap samples retrieved on October 12, 2016 are not available for this report.

The mass of sample material for each grain size fraction in each sample is reported in Table 22 and Figure 26. The mass of sample collected in the BSNE saltation sand traps deployed at P57-3 between early March 2015 and early January 2016 was three to four times greater than the mass of sample collected at any other monitoring station (Figure 26). The larger sample mass may be because a large area immediately west of station P57-3 consists of loose sandy soils that appear to have been disturbed at an unknown time in the past. Additionally, the vegetation in this area is not as large or dense as in other areas around the Contamination Area. A survey is currently underway to ascertain differences in vegetation type and density around the Contamination Area.

Although mass of the > 0.01 in (250 µm) size fraction was not determined for the samples retrieved on March 3, 2015, the mass of all material in these samples and in the < 0.01 in (250 µm) portion of the P57-4 samples retrieved on January 4, 2016, fall within the range of 0.08 oz (2.2 g) to 0.15 oz (4.3 g) (Table 22). In all samples from both years at both stations, the 0.002 in (63 µm) to 0.01 in (250 µm) size fraction appears to be the largest portion of the samples whereas the < 0.002 in (63 µm) size fraction appears to be the smallest portion of the samples (Table 22, Figure 26). This relationship can be confirmed in the January 2016 samples where the > 0.01 in (250 µm) fraction constituents approximately 20 to 30 percent of the sample, the 0.002 in (63 µm) to 0.01 in (250 µm) fraction is approximately 60 to 70 percent of the sample, and the < 0.002 in (63 µm) fraction is approximately 10 to 15 percent of the sample (Figure 26). Additionally, despite the significantly greater total mass in the P57-3 samples, the relative portions of the three size fractions in the January 2016 samples from both P57-3 and P57-4 are similar (Table 22).

Total mass collected from the downwind traps for samples from stations P57-2 and P57-4 (Figure 26) is greater than the mass collected from the upwind traps, indicating net transport is moving off the Contamination Area. Whereas, total mass collected from the upwind traps is greater at station P57-3, indicating net transport onto the Contamination Area. Comparison of the upwind and downwind sample mass at station P57-1 is not easily interpreted because upwind and downwind traps were combined in the consolidated samples analyzed by the labs. The combination of two downwind and one upwind trap resulted in slightly greater sample mass than the combination of two upwind and one downwind trap.

Because the difference between the two mass measurements for P57-1 (1.4 percent of the total mass collected) is small relative compared to the difference between the two mass measurements for P57-2 (20.32 percent), P57-3 (8.65 percent), and P57-4 (20.17 percent) and because the sample mass values obtained at P57-1 are not clearly associated with dominant wind directions, the samples from P57-1 are not considered indicative of the influence of the dominant winds.

The sample mass differences observed at P57-2, P57-3, and P57-4 are consistent with more frequent and/or stronger winds from the northwesterly direction, which would bring material moving by saltation into the upwind collector on the north side of the Contamination Area (station P57-3) and into the downwind collector on the south side of the Contamination Area (stations P57-2 and P57-4). Therefore, there appears to be a net transport of saltation material in a southerly direction driven by winds from the northwest.

Table 22. Mass (grams) of the three size fractions for saltation samples collected from Project 57 monitoring stations on March 3, 2015, and January 4, 2016.

BSNE # Orientation	Retrieval Date	Size Fraction[1]			Total
		> 250 µm	63 µm to 250 µm	< 63 µm	
P57-1 25-29-35 2 down 1 up	March 3,2015	No measurement	3.7940	0.4882	> 4.2822
P57-1 27-31-33 1 down 2 up	March 3,2015	No measurement	3.3696	0.7523	> 4.1619
P57-2 37-41-45 Downwind	March 3,2015	No measurement	2.7840	0.4874	> 3.2714
P57-2 39-43-47 Upwind	March 3,2015	No measurement	1.9527	0.2137	> 2.1664
P57-3 38-42-46 Downwind	January 4, 2016	3.3458	10.4219	1.7193	15.4870
P57-3 40-44-48 Upwind	January 4, 2016	3.7701	12.8518	1.7989	18.4208
P57-4 26-30-34 Downwind	January 4, 2016	0.9374	3.0300	0.7844	4.7518
P57-4 28-32-36 Upwind	January 4, 2016	0.8523	1.9334	0.3708	3.1565

[1] Grain size separation and sample mass measurement performed by Southwest Research Institute, San Antonio, Texas.

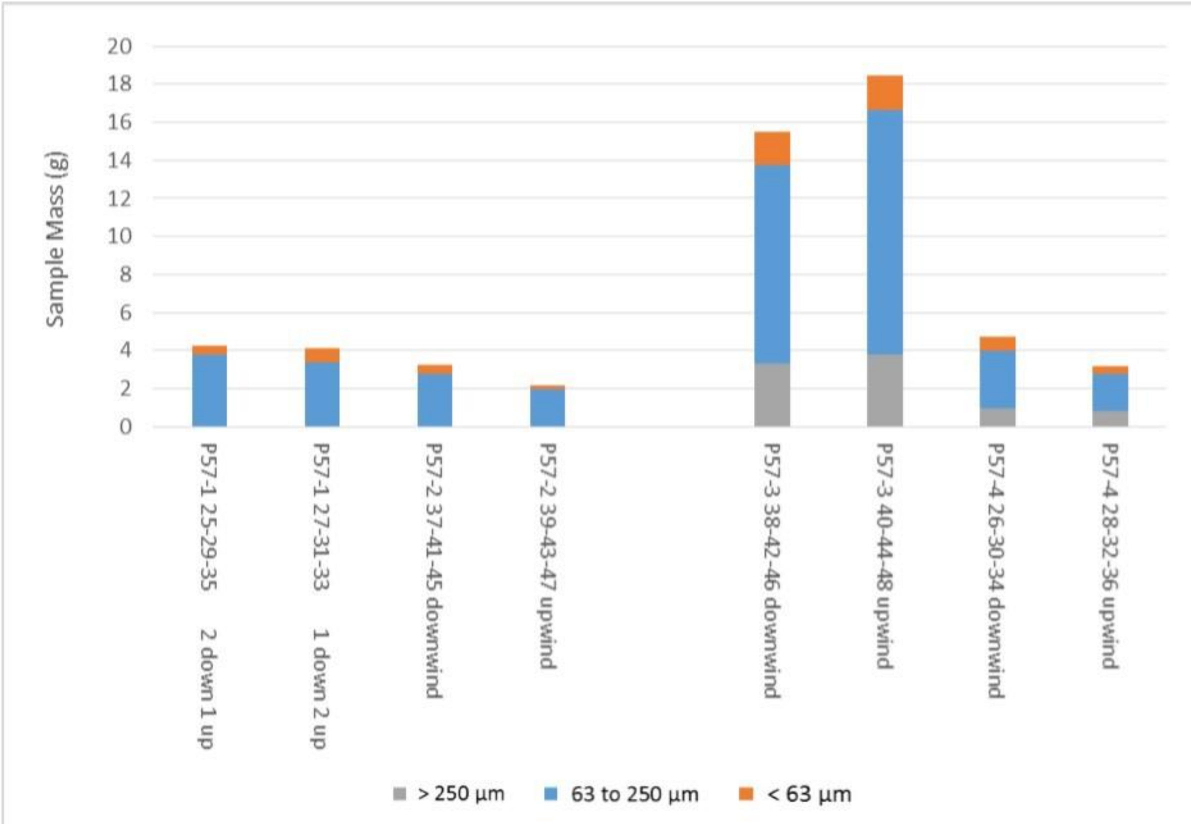

Figure 26. The 63 µm to 250 µm size fraction dominates the material collected in saltation traps deployed at the Project 57 monitoring stations in 2014 and 2015.

A preliminary assessment of the distribution of radionuclide concentrations around the Project 57 Contamination Area can be obtained by combining all results for each radionuclide concentration at each monitoring station. The lowest radionuclide concentrations occurred at station P57-2 (Figure 27) at the extreme southeastern corner of the Contamination Area (Figure 2). The highest radionuclide concentrations occurred at P57-4 (Figure 27), whereas concentrations at P57-3 are the second highest. Monitoring stations P57-3 and P57-4 were located directly downwind of the ground zero High Contamination Area when winds were blowing in the two dominant directions. Proximity to the ground zero High Contamination Area is likely the reason samples collected from these stations have the highest radionuclide concentrations.

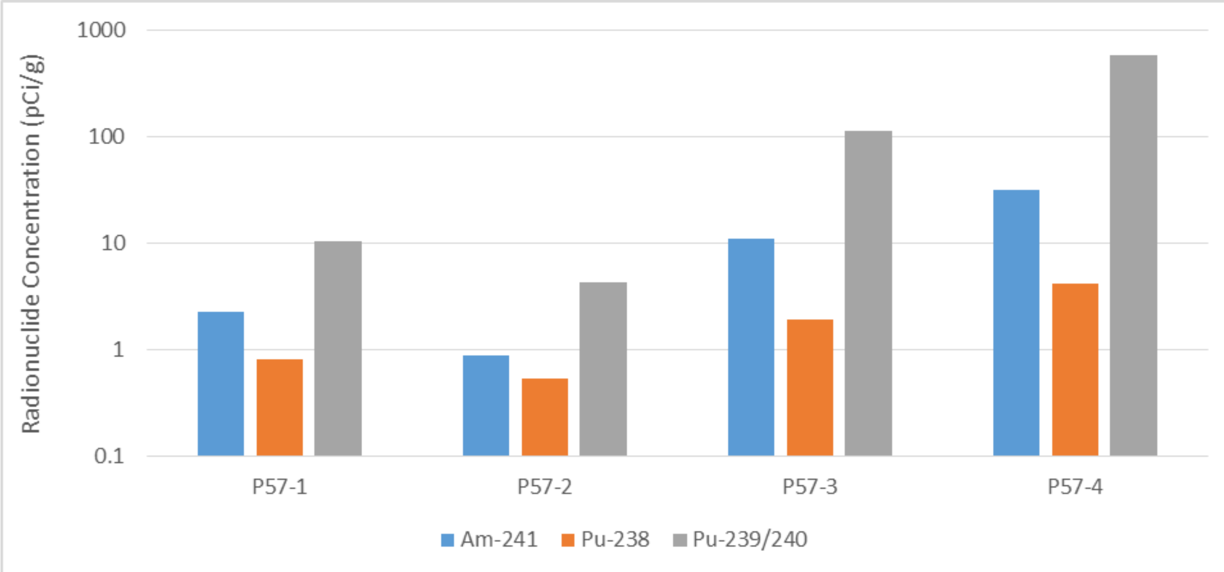

Figure 27. The concentration of radionuclide at the Project 57 monitoring stations; P57-1 and P57-3 are on the north side of the Contamination Area; P57-2 and P57-4 are on the south side. Samples at P57-1 and P57-2 were collected during 2014; samples at P57-3 and P57-4 were collected during 2015.

Radionuclide results for the saltation samples are shown in Figure 28 and Appendix D. When the two particle size fractions are compared, the Am-241, Pu-238, and Pu-239+240 concentrations are higher for the < 0.002 in (63 µm) size fraction in 23 of 24 analyses. For all samples, the difference between concentrations for the < 0.002 in (63 µm) and the 0.002 in (63 µm) to 0.01 in (250 µm) size fractions varies considerably from as little as 30 percent to as much as 260 percent.

The sample P57-1 25-29-35 is the sample for which the smaller size fraction had the lower Pu-238 concentration. This P57-1 sample is one in which the BSNE saltation sand traps were incorrectly combined making the interpretation of the radionuclide concentrations less certain. The results for all samples collected strongly suggest that the higher radionuclide concentrations will be associated with the < 0.002 in (63 µm) size fraction.

Ignoring the samples from P57-1 where directional orientation is not definitive and recognizing that the differences appear to be rather small, the < 0.002 in (63 µm) size fraction for the downwind sample from each monitoring station has higher radionuclide concentrations than the associated upwind sample for all three radionuclides (Figure 28). The downwind versus upwind difference between radionuclide concentrations for the 0.002 in (63 µm) to 0.01 in (250 µm) size fraction is not as clear. In nine of the twelve comparisons (P57-2 for Am-241, P57-4 for Am-241, and P57-3 for Pu-238), the downwind sample has a higher radionuclide concentration than the upwind sample. Higher concentrations in the downwind samples are expected because the downwind samples are transported by winds that have crossed the Contamination Area before the saltation material is collected

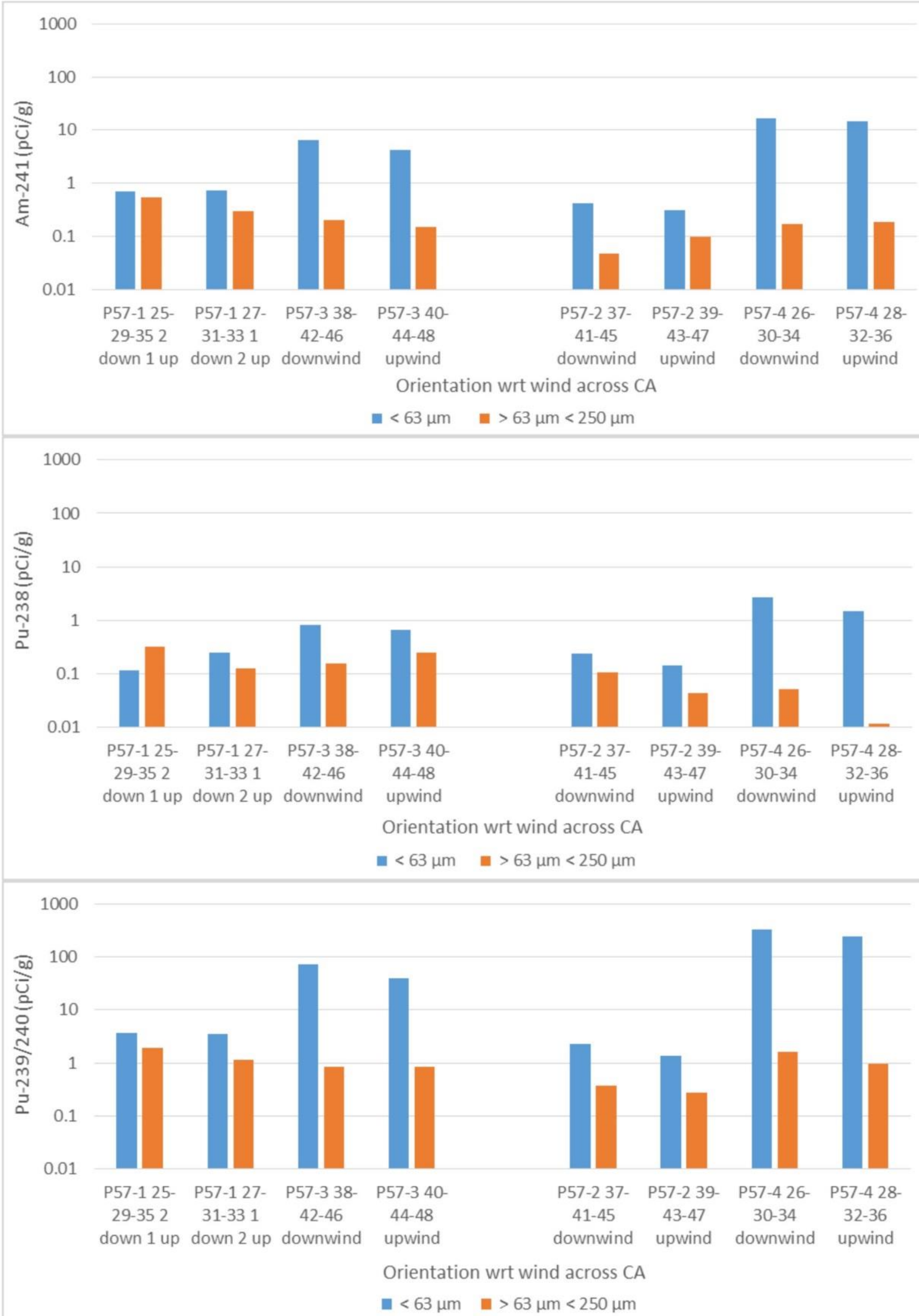

Figure 28. Am-241 (top), Pu-238 (middle), and Pu-239+240 (bottom) concentrations in saltation samples from Project 57 monitoring stations P57-1 and P57-2 collected on March 3, 2015, and P57-3 and P57-4 collected on January 4, 2016. Note concentration is shown on a logarithm scale.

in the traps. Although the radionuclide concentrations in the upwind samples are somewhat less than the concentrations in the downwind samples, the upwind and downwind concentrations are generally different by no more than a factor of two. The 0.002 in (63 µm) to 0.01 in (250 µm) size fraction of the 2016 sample from P57-4 is the only exception. There is a factor of four difference between the upwind and downwind concentrations for Pu-238 in this sample. This suggests that saltation may not be transporting radionuclide-contaminated soil material significant distances but that the opposing dominant wind directions are moving the saltation material back and forth over a limited area.

In a comparison of the radionuclide concentrations in surface soils at off-site locations upwind and downwind of the NNSS, Turner *et al.* (2003) collected upwind samples, which they presumed represented background, from an undisturbed alluvial fan near Searchlight, Nevada. The sample location was approximately 80 km south of Las Vegas, Nevada, and 99.4 mi (160 km) southeast of the southern boundary of the NNSS. Analysis of the top 0.5 inches (1.25 cm) of soil produced Pu-238 and Pu-239+240 concentrations of 0.000405 pCi/g and 0.014056 pCi/g, respectively. The Project 57 saltation samples produced values of Pu-238 that are 28 to 6,500 times the background concentration determined by Turner *et al*. (2003) and values of Pu-239+240 that are 20 to 24,000 times the background concentration indicating that soil material being redistributed by saltation is contaminated.

Turner *et al.* (2003) also noted that values of the ratio of Pu-239+240 to Pu-238 for soils in the northern hemisphere that are significantly greater than 30 might indicate possible contamination by sources other than fallout because of atmospheric testing of atomic weapons. This ratio in the Project 57 saltation samples range from 1.6 to 166. Five saltation samples from the Project 57 monitoring stations exceed the atmospheric fallout level. The Pu-239+240 to Pu-238 ratios for the < 0.002 in (63 µm) size fraction from the P57-3 and P57-4 are between 60 and 166 and the P57-4 28-23-36 upwind sample for the 0.002 in (63 µm) to 0.01 in (250 µm) size fraction is 83. These values suggest that the radionuclide contamination transported with the saltation material is derived from sources other than atmospheric fallout. The probable source of this contamination is the Project 57 test.

DISCUSSION

Airborne dust collected at the monitoring stations is analyzed for gross alpha, gross beta, and gamma spectroscopy to determine if radiological contaminants are being transported from the Project 57 Contamination Area by wind. Some gross alpha and gross beta radioactivity is expected because of natural radioactivity associated with the geologic environment and cosmic radiation. Neither background nor baseline values representing gross alpha and gross beta conditions prior to the Project 57 safety experiment are available. To determine if radioactivity at the Project 57 stations is the result of natural radiation or contamination of the area during the safety experiment, values from the Project 57 stations are compared with values for other monitoring stations in the region. The significance of gross alpha and gross beta concentrations for samples from Project 57 is determined by comparison to values obtained from CEMP stations surrounding the northern ranges of the NTTR. Radiological data from the CEMP stations are assumed to represent noncontaminated areas in the region. The mean gross alpha concentration at P57-3 is slightly higher than, but on the same order of magnitude as, the mean concentrations at surrounding CEMP stations. The mean gross alpha for P57-4 is notably higher than the mean for surrounding

CEMP stations. This is likely the result of four individual sample values that exceeded the maximum values observed at the CEMP stations. Mean gross beta concentrations at the Project 57 stations are essentially the same as those determined for the CEMP stations.

Two airborne particulate matter samples collected at Project 57 during 2015 are of special interest. The first, collected on April 15, 2015, was deployed for only 2 days. After deployment of the collection filter, field personnel noted a dust storm approaching from the north. It was decided to collect the sample after the dust storm passed in order to obtain radiological data associated with an isolated meteorological event. The gross alpha and gross beta results for the P57-3 sample were greater than the average for the year plus four standard deviations. The sample from P57-4 produced a gross alpha concentration more than twice the average for the year and a gross beta approximately equal to the average for the year. Clearly this single dust storm produced radiological conditions significantly above average. At both stations, the mass of material collected in this sample also exceeded the average for all samples collected during the year. Wind conditions changed dramatically as the dust storm approached. Light to moderate winds from the south to southwest increased in speed to peak at 32 and 34 mph (51.5 and 54.7 km/hr) over a five hour period and shifted to west to northwest in about 30 minutes and continued to shift to the north to northwest. The changes in wind conditions clearly associate the higher than average radiological conditions with a weather front moving north to south across the monitoring stations.

The second event of special interest is associated with the June 23, 2015, sample collected at P57-4, which produced an Am-241 detection by gamma spectroscopy. This led to an alpha spectroscopy analysis, which confirmed the Am-241 result and identified Pu-238 and Pu-239+240. There were no major wind storms identifiable in the 10-minute average meteorological data collected during the two-week period the sample was deployed. Therefore, the instantaneous observations of wind conditions, collected every three seconds, were reviewed. This revealed two significant wind events, during which the wind direction shifted between 200 and 300 degrees and the wind speed increased from less than 10 mph (16.1 km/hr) to more than 30 mph (48.3 km/hr). These changes occurred within a 20-second time period. Following this dramatic shift in wind conditions, there was a more gradual return to conditions similar to those existing prior to the sudden shift. These observations are similar to conditions expected if a dust devil passed over the monitoring station. A dust devil would produce a 90 degree shift in wind direction and a sharp increase in wind speed as the dust devil approached the station, followed by a 180 degree shift in wind direction as the dust devil passed across the station, then another 90 degree shift in wind direction and a decline in wind speed as the dust devil passed beyond the monitoring station. Observations at P57-4 during this event suggest that the edge of a dust devil likely clipped the monitoring station.

The observation of higher than normal radiological conditions in conjunction with strong frontal winds or dust devil winds suggests that strong wind events are the most likely mechanism of radionuclide transport adjacent to the Project 57 Contamination Area.

Saltation samples were collected at P57-1 and P57-2 during 2014 and at P57-3 and P57-4 during 2015. Total sample mass for traps facing north at each station was greater than total sample mass for traps facing south. This suggests that winds from the northerly directions are stronger and more frequent than winds from southerly directions, which is consistent with observations from analysis of 10-minute average wind conditions. It also suggests that there may be a net transport of saltation-size material from north south implying and that contaminated soil material may be transported to the south from the Project 57 Contamination Area.

In a gross assessment, the highest concentrations of radionuclides in saltation samples were observed for station P57-4. Station P57-3 had the second highest concentrations and station P57-2 had the lowest concentrations. This is an expected result because stations P57-3 and P57-4 were intentionally located to be downwind of the Project 57 ground zero, High Contamination Area, when winds are from the two predominant directions. The higher concentrations at P5-4, on the south side of the contamination, suggest that northerly winds may be stronger and more frequent than southerly wind. When the P57-3 and P57-4 saltation samples are separated by the direction the collectors face, those samples collected downwind of the Contamination Area during the predominant winds—whether northerly or southerly—have higher radionuclide concentrations than the associated upwind samples. This observation is to be expected because the downwind samples are obtained when winds cross the Contamination Area before intercepting the saltation traps. However, the difference between the radionuclide concentrations for upwind and downwind samples is small, which suggests that saltation may not be transporting contaminated soil material significant distances but that contaminated soil material may be moving back and forth over a limited area.

Saltation sample radionuclide concentrations from Project 57 stations are significantly higher than values for soil samples collected upwind of the NNSS by Turner *et al.* (2003). This indicates that the saltation samples include material transported from an area of contaminated soil. Comparing the Project 57 radionuclide concentrations to information on atmospheric fallout effects compiled and synthesized by Turner *et al.* (2003), suggests that the Project 57 saltation samples reflect contamination by sources other than atmospheric fallout.

An analysis of the relationship between wind speed and saltation particle counts, $PM_{2.5}$ concentration, and PM_{10} concentration clearly indicates that dust concentration increases as wind speed increases. When winds at the P57-3 and P57-4 stations are separated into the dominant northerly and southerly patterns, both predominant wind directions generate similar dust levels for wind speeds below 20 to 25 mph (32.2 to 40.2 km/hr). However, as wind speeds exceed the 20 to 25 mph (32.2 to 40.2 km/hr) range, the northerly winds clearly are associated with higher dust concentrations.

The wind/dust relationships show that dust concentrations remain generally low until wind speed exceeds 15 to 20 mph (24.1 to 32.2 km/hr) and that dust concentrations increase in conjunction with increasing wind speed. However, the wind observations also clearly show that wind speeds needed to transport significant dust are infrequent. Winds exceeding 20 mph (32.2 km/hr) occur less than approximately three percent of the time.

The combined results of the meteorological and particle monitoring at the Project 57 sites suggest that conditions for wind-borne contaminant migration exist but occur infrequently and for brief periods. It appears that radionuclide contaminants resulting from the Project 57 test may be transported in by wind suspension but that such transport occurs rather infrequently because the required wind conditions are quite rare.

CONCLUSIONS

The mean gross alpha concentration at station P57-3 is slightly higher than, but on the same order of magnitude as, the mean concentrations at surrounding CEMP stations. However, the mean gross alpha concentration at P57-4 is notably higher than the mean for surrounding CEMP stations. The mean gross beta concentrations at both Project 57 stations are essentially the same as the concentrations determined for the surrounding CEMP stations. The higher mean gross alpha at P57-4 is the result of several particularly high individual gross alpha observations. This comparison suggests that the Project 57 gross alpha and gross beta observations are generally caused by natural (terrestrial and cosmic) sources.

Generally, gamma spectrometry analyses of biweekly samples of airborne particulate matter collected at the Project 57 monitoring stations during the reporting period indicated only naturally occurring gamma-emitting radionuclides. However, gamma spectrometry showed Am-241 in one sample. On further testing, Pu-238 and Pu-239+240 were also shown to be present in this sample. This sample appears to have been associated with a dust devil that passed close to the monitoring station and caused a sharp increase in wind speed and change in wind direction.

A single sample produced gross alpha and gross beta concentrations that were higher than the average for the year plus four standard deviations. This sample was associated with a significant weather front that moved across the Project 57 and produced a sudden change in wind direction and a rapid increase in wind speed.

Observations of radiation dose at the Project 57 monitoring stations indicate that the dose from natural sources and transport from the Project 57 Contamination Area is approximately half of the dose that the general public is expected to receive from natural sources alone. The low natural radiation dose exposure at the Project 57 monitoring stations is likely because of lower levels of radiation emitted from the local geology.

Generally, saltation counts, PM_{10} concentrations, and $PM_{2.5}$ concentrations increase exponentially with increasing wind speed. The greatest increase in dust occurs for winds exceeding 20 mph (32.2 km/hr). Analysis of wind and dust conditions when wind conditions are separated by predominant wind direction shows that dust concentrations associated with lower wind speeds are similar for both the northerly and southerly wind directions. At wind speeds above 25 mph (40.2 km/hr), however, the northerly winds produce higher dust concentrations than the southerly winds.

Wind speeds exceed 15 mph (24.1 km/hr) only approximately nine percent of the time and 20 mph (32.2 km/hr) only approximately three percent of the time. Winds that are sufficient to generate significant dust are infrequent and generally of short duration. Therefore, significant dust events are also infrequent and short-lived. Preliminary review of the eight highest wind-speed events during the reporting period indicates that the PM_{10} concentration and the saltation count observations are highly variable.

The mass of saltation material collected in the northerly facing traps (upwind at P57-3 and downwind at P57-4) is greater than the mass of material collected in the southerly facing traps. This suggests that although saltation material may be moving back and forth under the two dominant wind directions, there is a net trend for saltation material to be transported toward the south.

The concentrations of Am-241, Pu-238, and Pu-239+240 in saltation samples collected downwind of the Project 57 Contamination Area is slightly higher than the values determined for samples collected upwind of the Contamination Area. The difference is a factor of 2 to 4. This suggests that saltation may not be transporting radionuclide-contaminated soil material significant distances but that the opposing dominant wind directions are moving the saltation material back and forth over a limited area.

RECOMMENDATIONS

1. Saltation material has been collected twice, approximately annually. This collection interval provides an integrated sample for the annual collection period. However, wind conditions have a seasonal trend in which northerly winds dominate the winter season and southwesterly and northerly winds are approximately equally common during the summer. The saltation sample retrieval timing should be adjusted to provide samples that better resolve radiological observations with wind conditions if sample volume allows. Project personnel began to implement this recommendation with collection of saltation samples in October 2016.
2. Separating the wind and PM_{10} analysis showed a significant difference in the dust transport by northerly and southerly winds. The wind/dust analysis based on the separated dominant wind directions should be expanded to $PM_{2.5}$ and saltation counts.
3. Size and radiological analyses of a representative sample of the soil material on the surface at each of the monitoring stations should be performed. This would facilitate characterization of the amount of PM_{10} and saltation material available at each site. This information would in turn be useful for interpreting the saltation and dust transport observations.
4. Establishing background/baseline conditions for the airborne particulate matter radionuclide concentrations is important for interpreting Project 57 data. Monitoring data from the surrounding CEMP stations are important for bracketing the results from the Project 57 monitoring stations. These locations should be evaluated to identify comparable and contrasting characteristics. There may also be information on uncontaminated soil sites on the NNSS that are comparable. Another alternative is to establish an additional monitoring/sample collection station near Project 57 that is environmentally similar but not subject to potential transport from the Project 57 Contamination Area. This site would provide control samples from an area that presumably is clean, which could be compared with samples collected adjacent to the Contamination Area.
5. Meteorological and other environmental conditions that potentially affect PM_{10} and $PM_{2.5}$ concentrations and saltation counts should be investigated. Although wind is the dominant force for suspension and transport of airborne dust, other conditions are also likely to have an effect; for example, moist or frozen soil is less likely to be suspended than dry soil. Therefore, an assessment of airborne dust and soil moisture and temperature and perhaps other factors should be performed.
6. The Project 57 monitoring stations were moved in January 2015 to obtain samples downwind of the ground zero and High Contamination Area under the dominant wind conditions. Approximately three years of data were collected at the original

monitoring sites before the stations were moved. Statistical analyses should be performed to determine if the meteorological, environmental, and radiological data from the original and the new monitoring stations can be combined to increase the length of the available data set.

7. Supplementing the BSNE saltation sand traps at P57-3 and P57-4 with additional traps further downwind from the Project 57 ground zero point may provide radiological data useful for estimating the distance contaminated particles may be traveling.
8. An assessment of vegetation density, diversity, and health, may provide insight to the potential local dust generation during wind events. A field survey of vegetation characteristics in the vicinity of the Project 57 monitoring stations was initiated in the spring of 2016. The results of this survey will be completed during the first half of 2017.
9. The gross alpha analysis produces a single concentration value for all alpha producing ions present in the sample. In order to isolate the alpha concentration associated with plutonium isotopes, it is recommended that representative samples of airborne particulate matter be submitted for alpha-spectroscopy analysis on a routine basis. These submissions should be independent of samples submitted because of americium 241 detection by gamma spectroscopy.

REFERENCES

DeSilva, S., 2004. Extended Community: An Oral History of the Community Environmental Monitoring Program (CEMP), 1981 – 2003. Desert Research Institute report number 45209 prepared for the Nevada Field Office of the U.S. Department of Energy, 467 pp.

Friesen, H.N., 1992. Summary of the Nevada Applied Ecology Group and Correlative Programs. DOE/NV-357. Prepared for the U.S. Department of Energy, Nevada Operations Office. Las Vegas, NV.

Misra, M., C. Neve, and A. Raichur, 1993. Characterization and Physical Separation of Radionuclides from Contaminated Soils. Proceedings of the Soil Decon ’93: Technology Targeting Radionuclides and Heavy Metals, Gatlinburg, TN, ORNL-6769, Oak Ridge National Laboratory, Oak Ridge, TN.

Mizell, S.A., G. Nikolich, G. McCurdy, C. Shadel, and J. Miller. 2016. Project 57 Air Monitoring Report: October 1, 2013 through December31, 2014. Desert Research Institute report number 45264 prepared for the Nevada field Office of the U.S. Department of Energy, 87 pp.

Murarik, T.M., T.K. Wenstrang, and L.A. Rogers, 1992. Characterization Studies and Indicated Remediation Methods for Plutonium Contaminated Soils at the Nevada Test Site. Spectrum 1992: Nuclear and Hazardous Waste Management, Boise, Idaho.

Nikolich, G., C. Shadel, J. Chapman, G. McCurdy, V. Etyemezian, J.J. Miller, and S Mizell. 2016. Tonopah Test Range Air Monitoring: CY2015 Meteorological, Radiological, and Airborne Particulate Observations. Desert Research Institute report number 45271 prepared for the Nevada Field Office of the U.S. Department of Energy, 95 pp.

NRC, 2011. Fact Sheet: Biological Effects of Radiation. U.S. Nuclear Regulatory Commission, Office of Public Affairs, p. 4.

NSTec, 2011a. Nevada national Security Site Environmental Report 2010. DOE/NV/25946-1305, 298 pp.

NSTec, 2011b. Nevada national Security Site Environmental Report 2010 Attachment A: Site Description. DOE/NV/25946-1305-ATT A, 80 pp.

NSTec, 2015. Nevada National Security Site Environmental Report 2014. DOE/NV/25946-2566, 276 pp.

NSTec, 2016. Nevada National Security Site Environmental Report 2015. DOE/NV/25946-2950, 270 pp.

Shreve, J.D., Jr., 1958. Operation Plumbbob Summary Report, Test Group 57. Extracted Version prepared by Sandia Corporation for Defense Nuclear Agency 4 June 1982, p. 85.

Tamura, T., 1985. Characterization of Plutonium in Surface Soils, Area 13 of the Nevada Test Site. *The Radioecology of Plutonium and Transuranics in Desert Environments*, HVO, 153, 1973.

Turner, M., M. Rudin, J. Cizdziel, and V. Hodge. 2003. Excess plutonium in soil near the Nevada Test Site, USA. Environmental Pollution 125, p193 – 203.

APPENDIX A: METEOROLOGICAL OBSERVATIONS AT PROJECT 57 MONITORING STATIONS FOR THE REPORTING PERIOD (JANUARY 1, 2015, THROUGH DECEMBER 31, 2015)

Definitions

10-minute average = average of 200 instantaneous observations made every 3 seconds during each 10-minute time period

Daily maximum = maximum of 144 10-minute averages of 3-second observations

Daily minimum = minimum of 144 10-minute averages of 3-second observations

Daily average = average of 144 10-minute averages made during the 24-hour period

Daily period of record maximum = maximum of daily maximums for specific calendar date during the period of record

Daily period of record minimum = minimum of daily minimums for specific calendar date during period of record

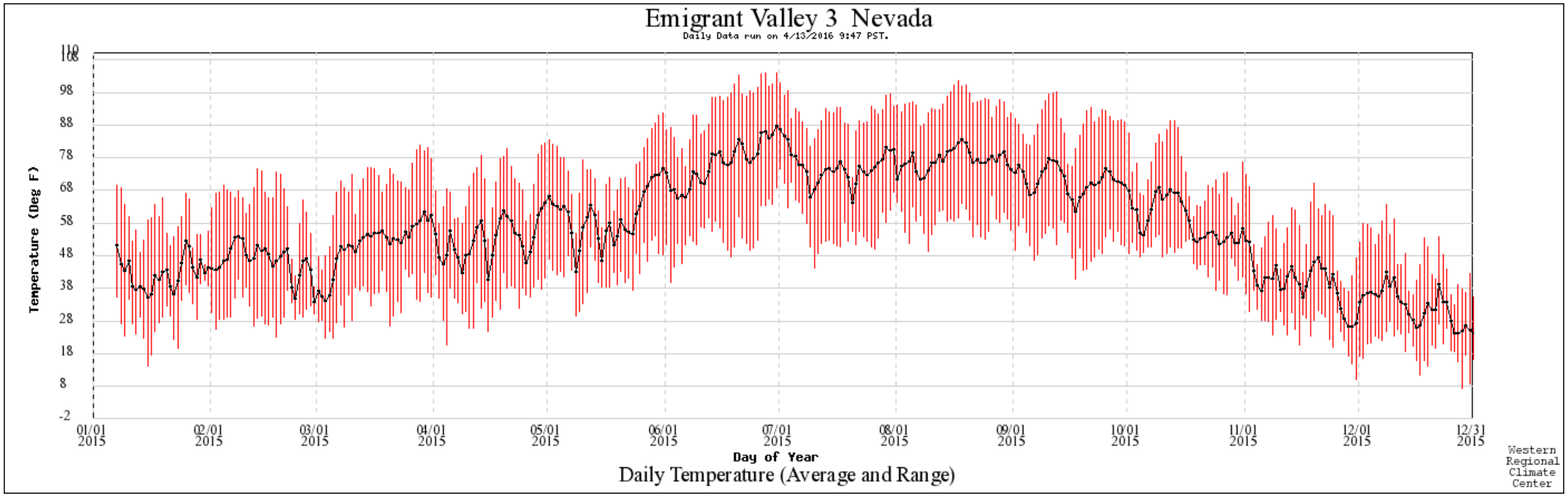

Figure A-1. Daily maximum, minimum, and average air temperature at P57-3 for the reporting period and for the period of record. The black line connects the daily average temperature. The bright red vertical lines connect the maximum and minimum temperature values for each day

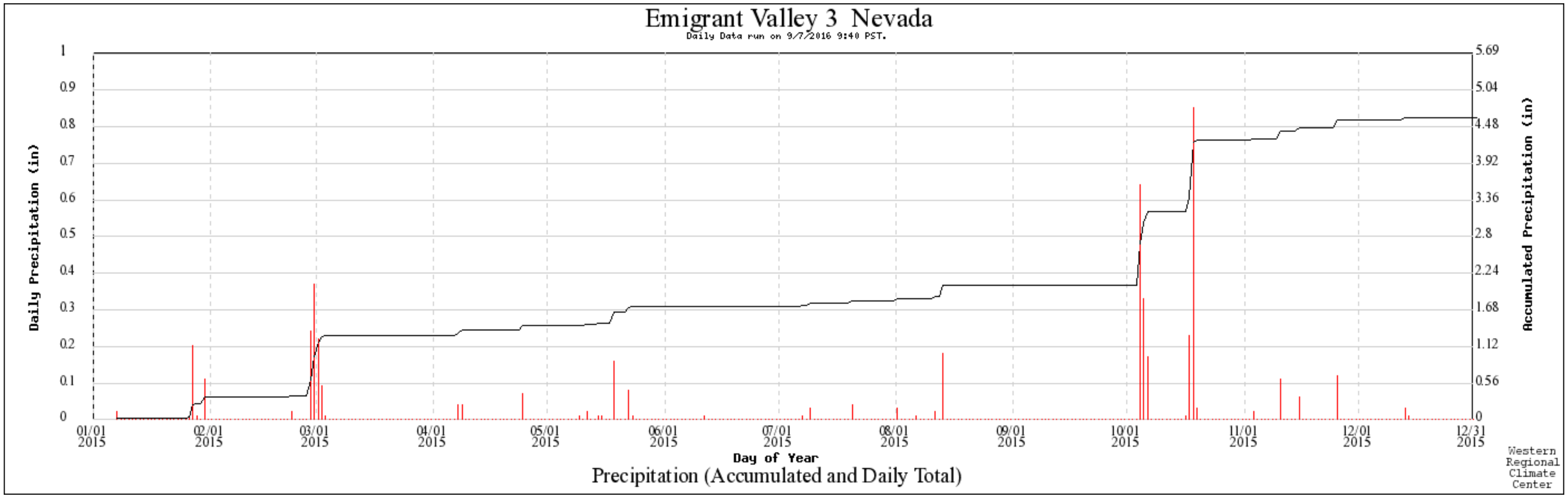

Figure A-2. Total daily precipitation (vertical red lines) and annual accumulated precipitation (black line) at P57-3 for the reporting period.

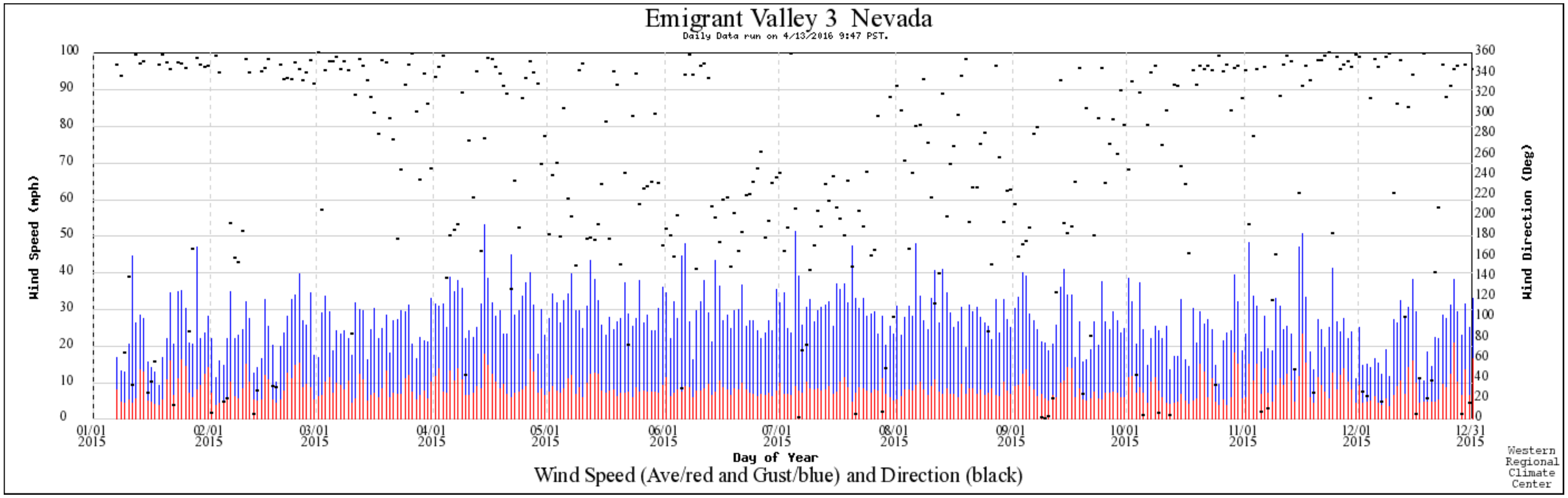

Figure A-3. Daily average (vertical red line) and maximum (vertical blue line) wind speed and daily average wind direction (black dot) at P57-3 for the reporting period.

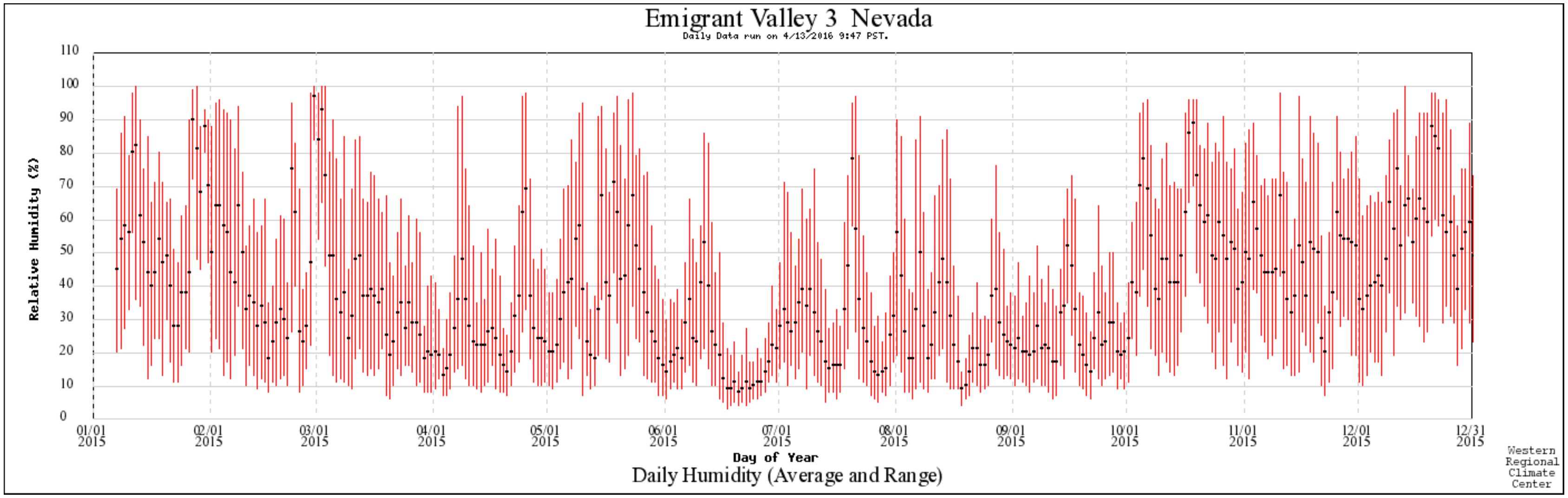

Figure A-4. Daily average relative humidity (black dots) and the daily range of relative humidity indicated by the red vertical lines that connect the daily maximum and minimum values at P57-3 for the reporting period.

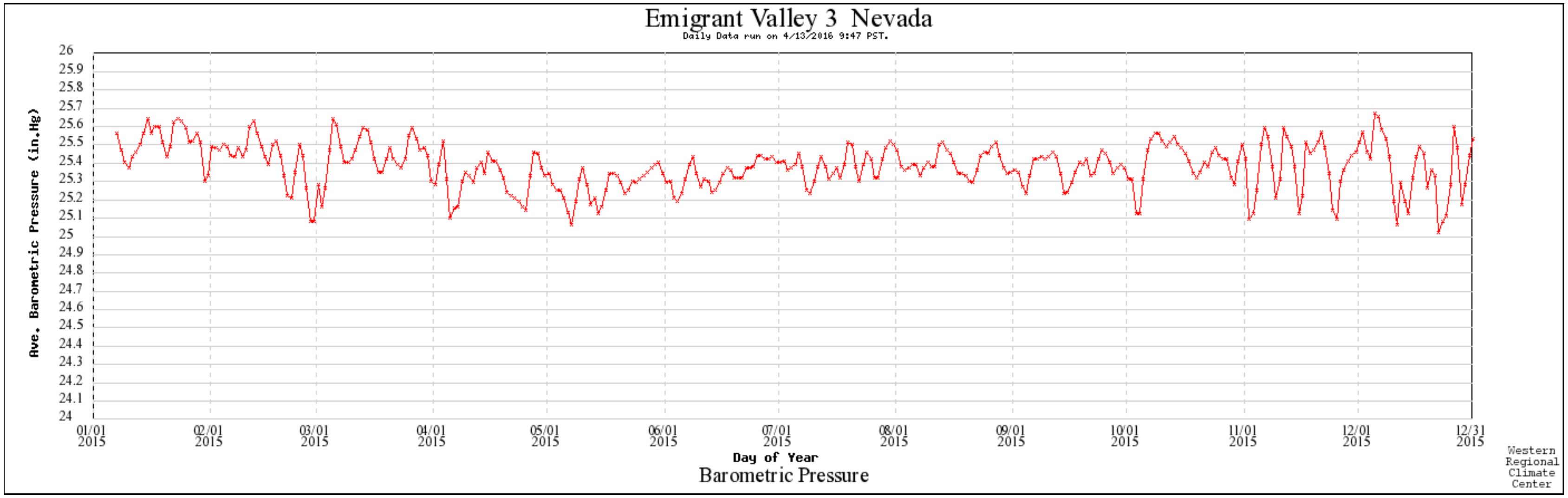

Figure A-5. Daily average barometric pressure at P57-3 for the reporting period.

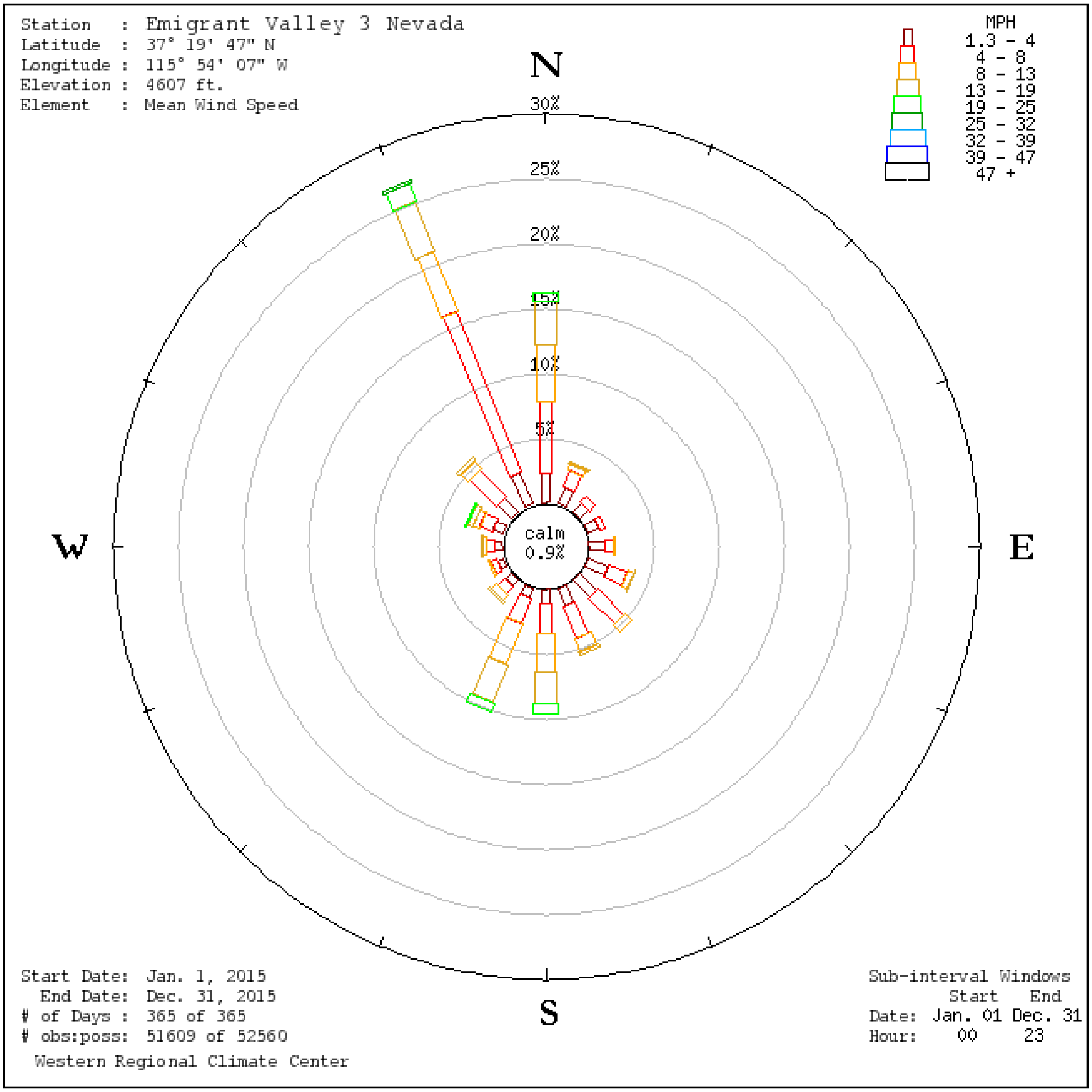

Figure A-6. P57-3 wind rose for the reporting period (January 1, 2015, through December 31, 2015).

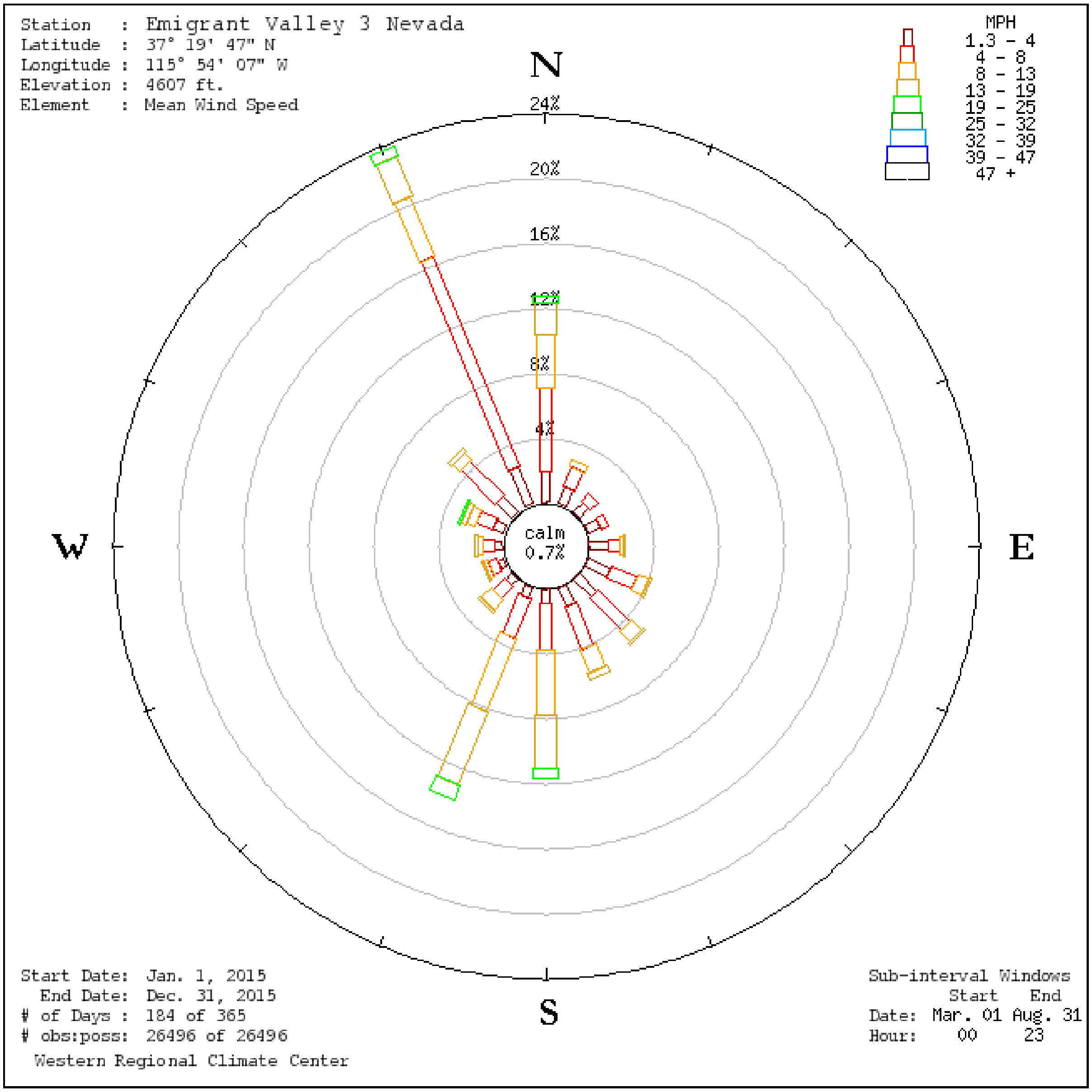

Figure A-7. P57-3 wind rose for the summer season (includes data collected between March 1 and August 31 during the reporting period).

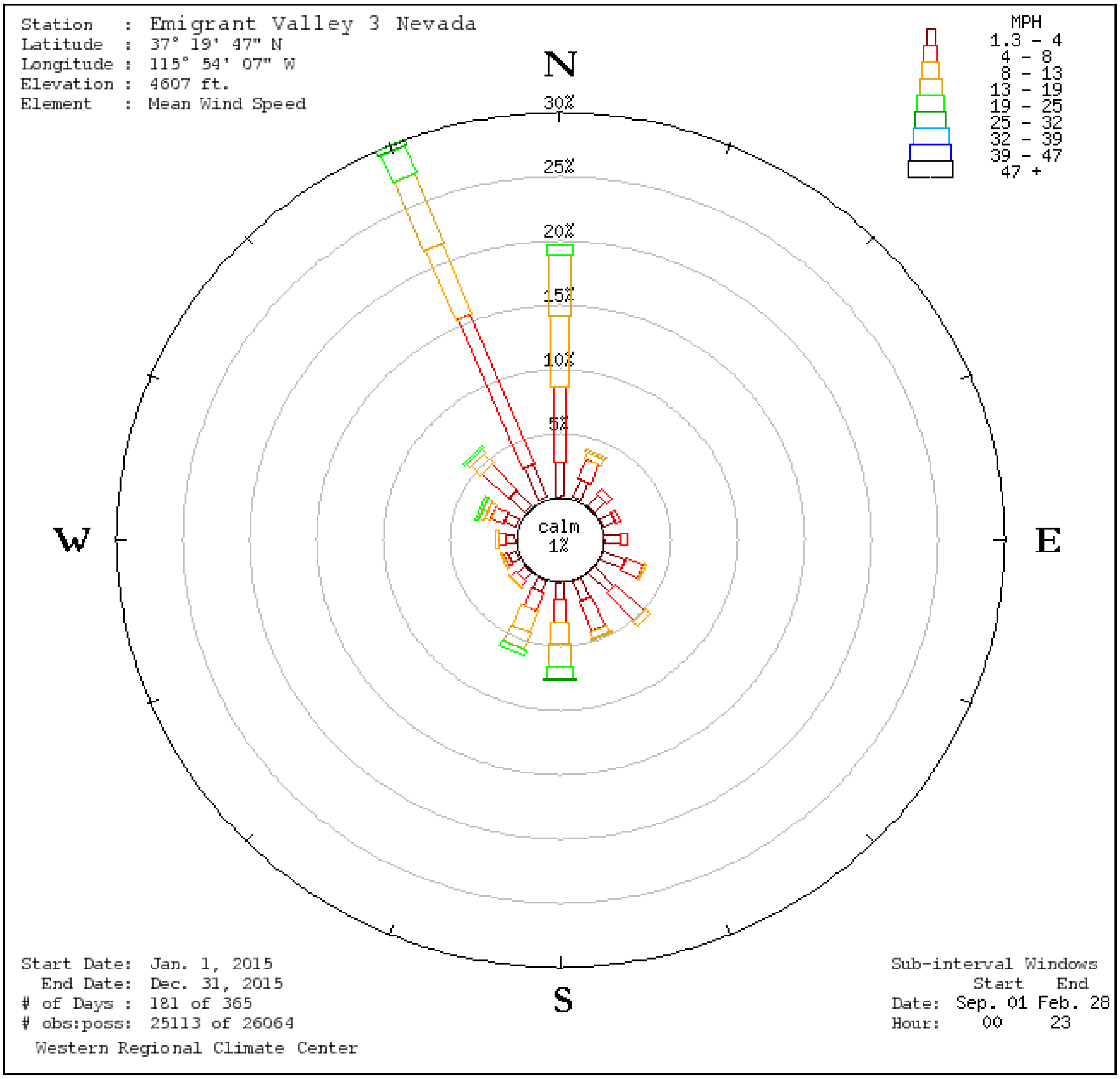

Figure A-8. P57-3 wind rose for the winter season (includes data collected between September 1 and February 28 during the reporting period).

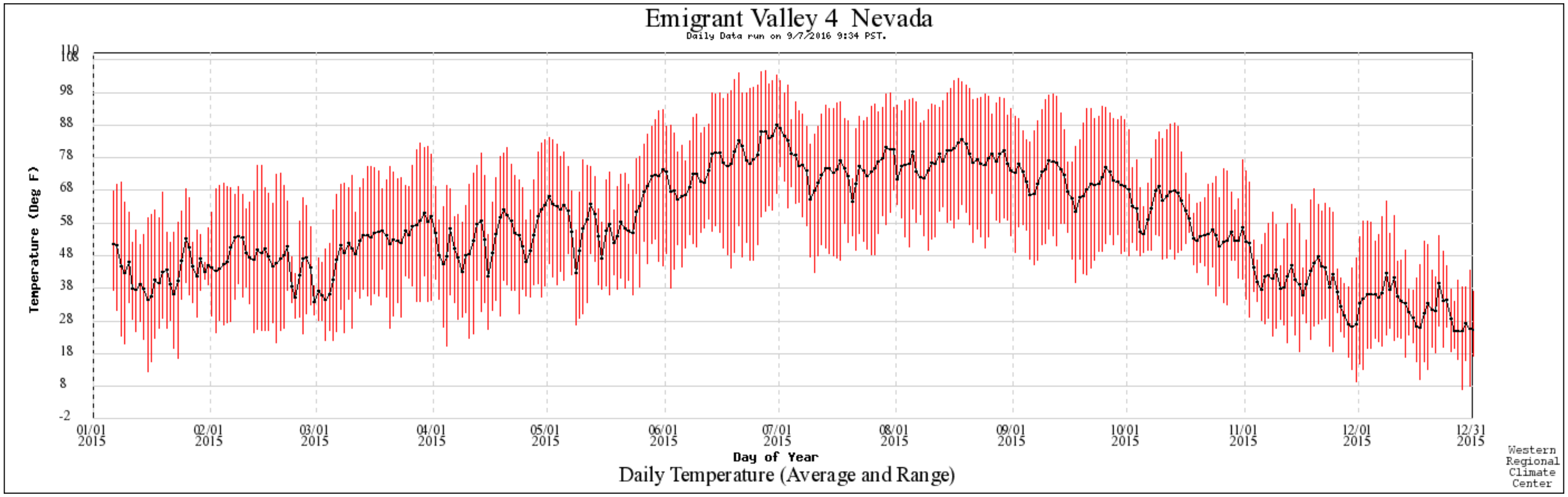

Figure A-9. Daily maximum, minimum, and average air temperature at P57-4 for the reporting period and for the period of record. The black line connects the daily average temperature. The bright red vertical lines connect the maximum and minimum temperature values for each day.

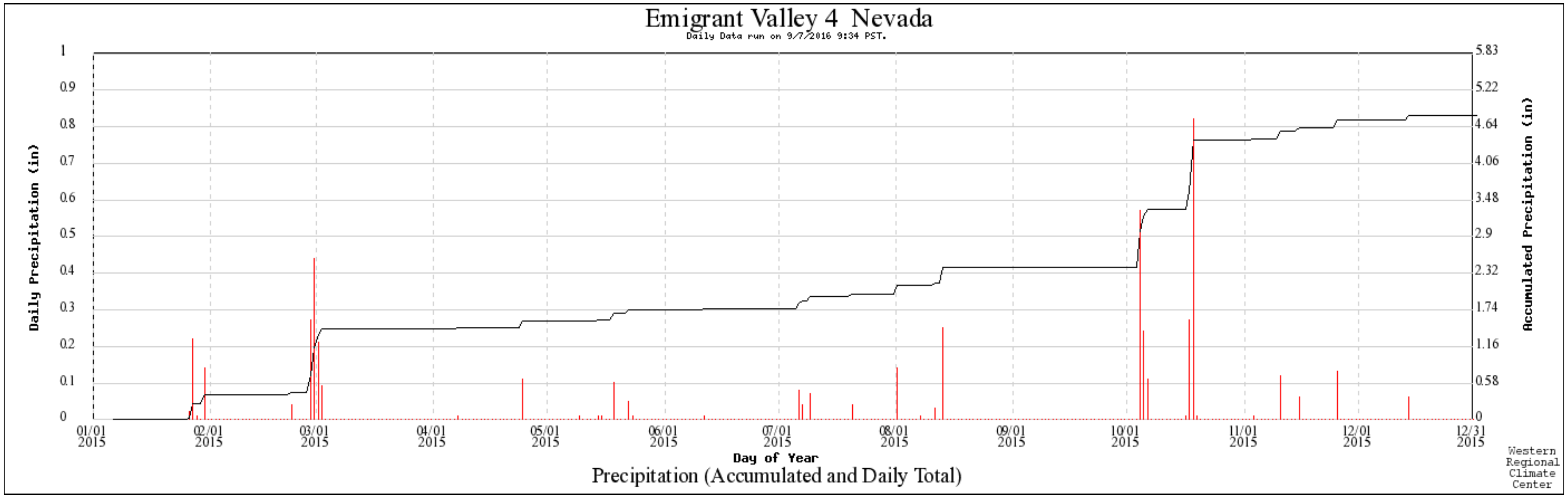

Figure A-10. Total daily precipitation (vertical red lines) and annual accumulated precipitation (black line) at P57-4 for the reporting period.

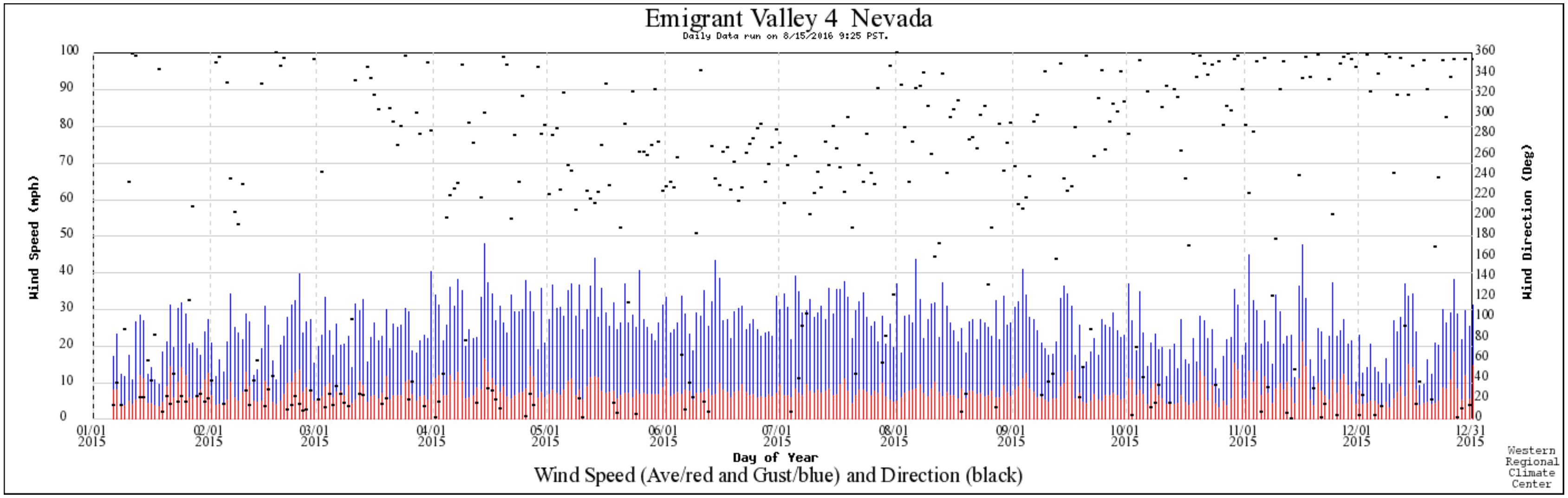

Figure A-11. Daily average (vertical red line) and maximum (vertical blue line) wind speed and daily average wind direction (black dot) at P57-4 for the reporting period.

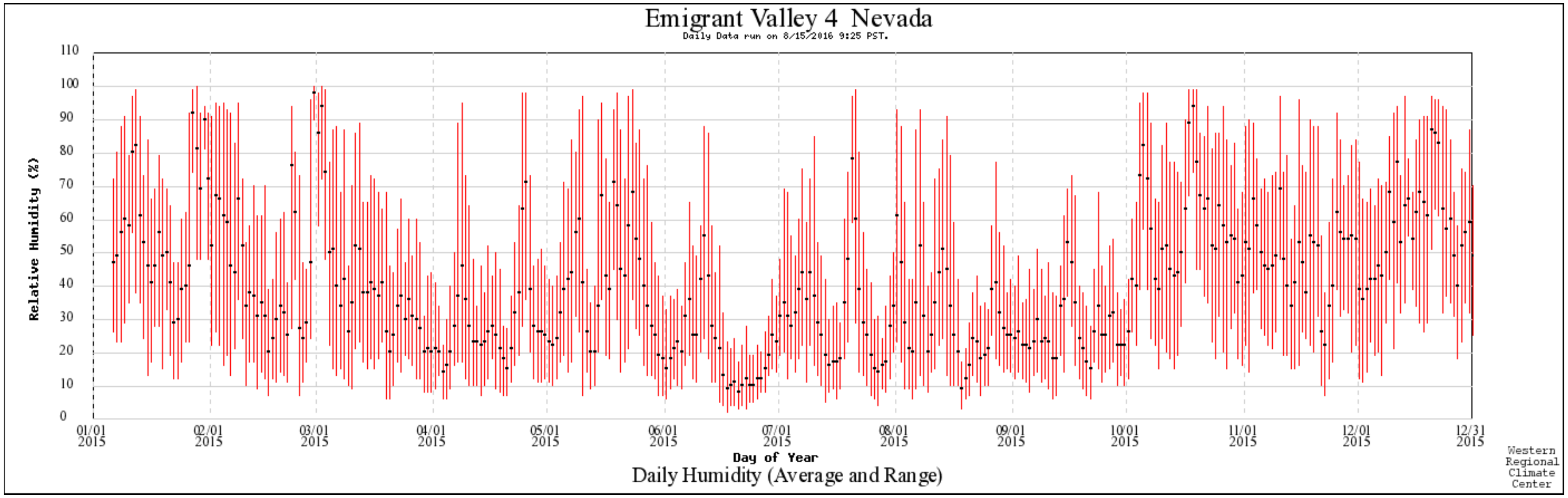

Figure A-12. Daily average relative humidity (black dots) and the daily range of relative humidity indicated by the red vertical lines that connect the daily maximum and minimum values at P57-4 for the reporting period.

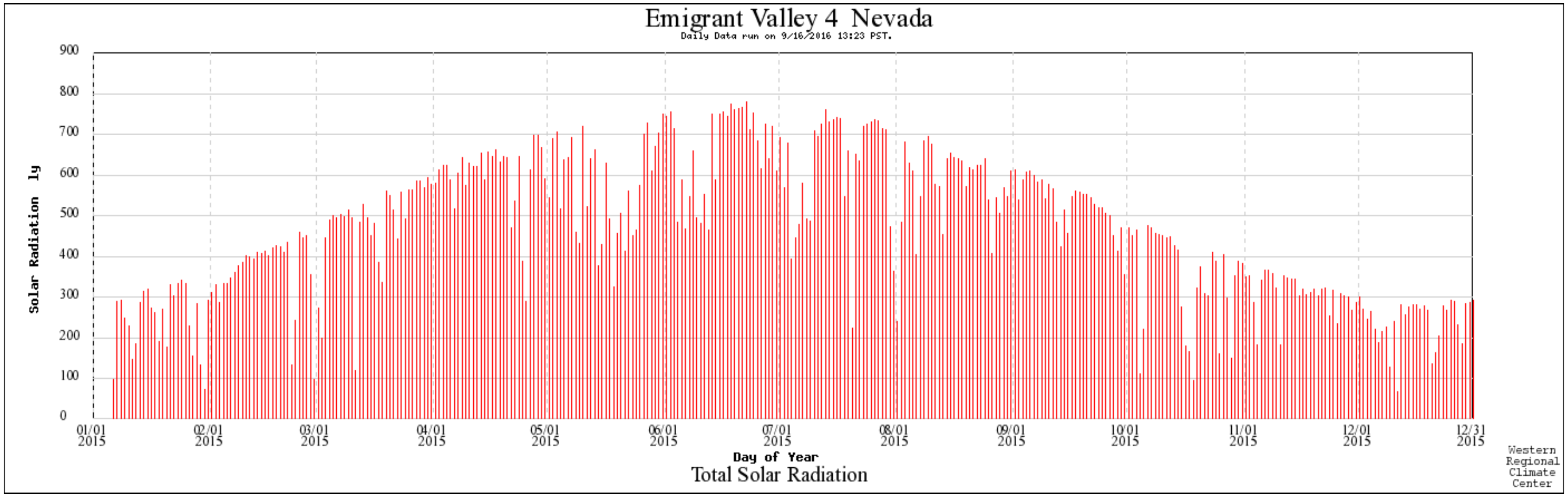

Figure A-13. Daily total solar radiation at P57-4 is indicated by vertical red lines.

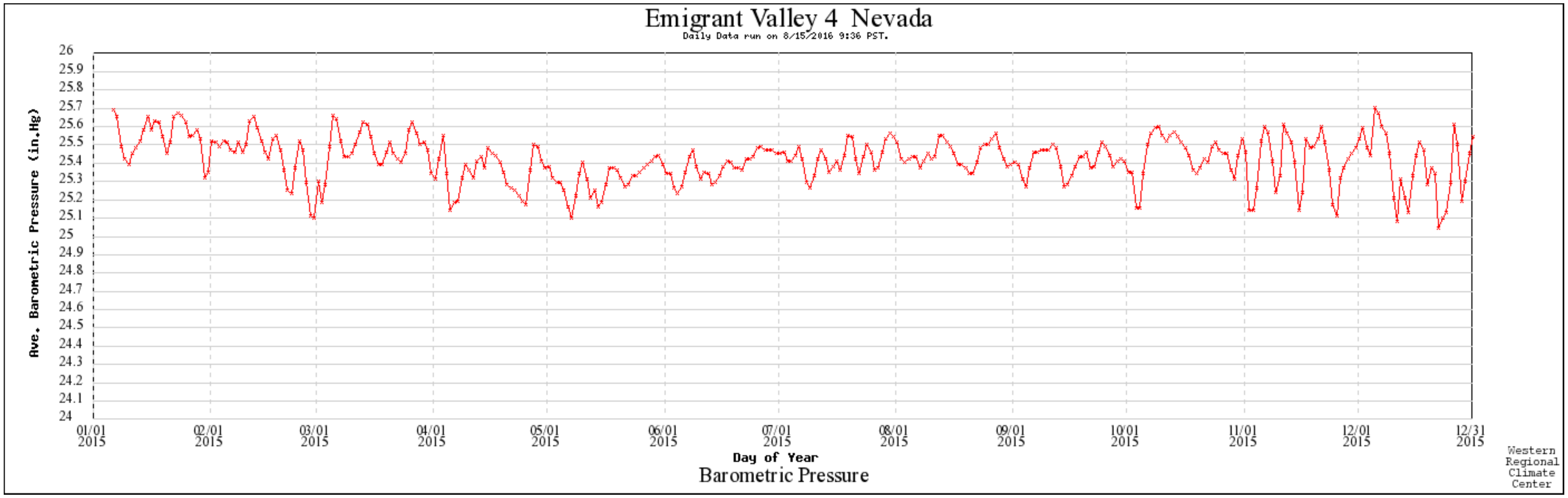

Figure A-14. Daily average barometric pressure at P57-4 for the reporting period.

.

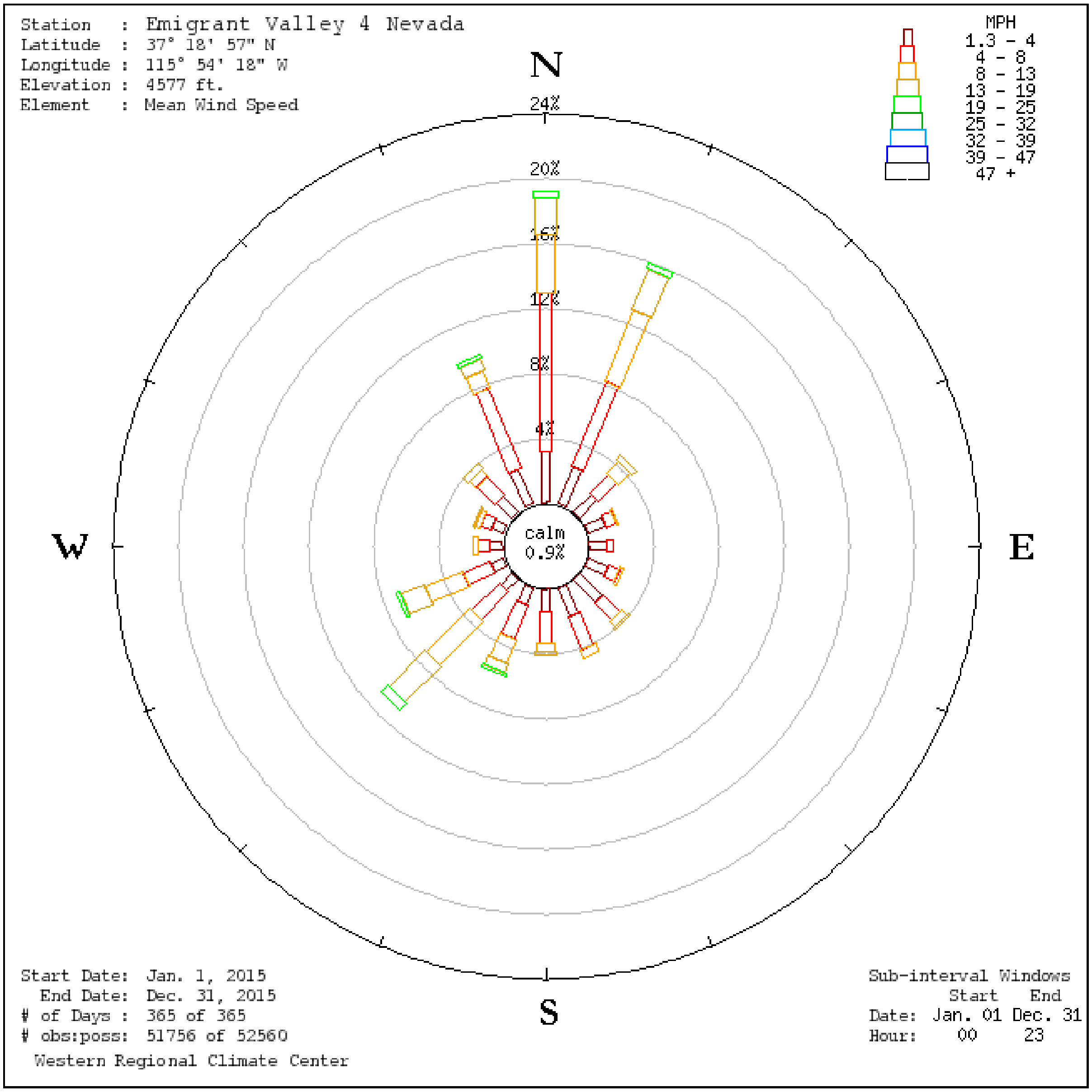

Figure A-15. P57-4 wind rose for the reporting period (January 1, 2015, through December 31, 2015).

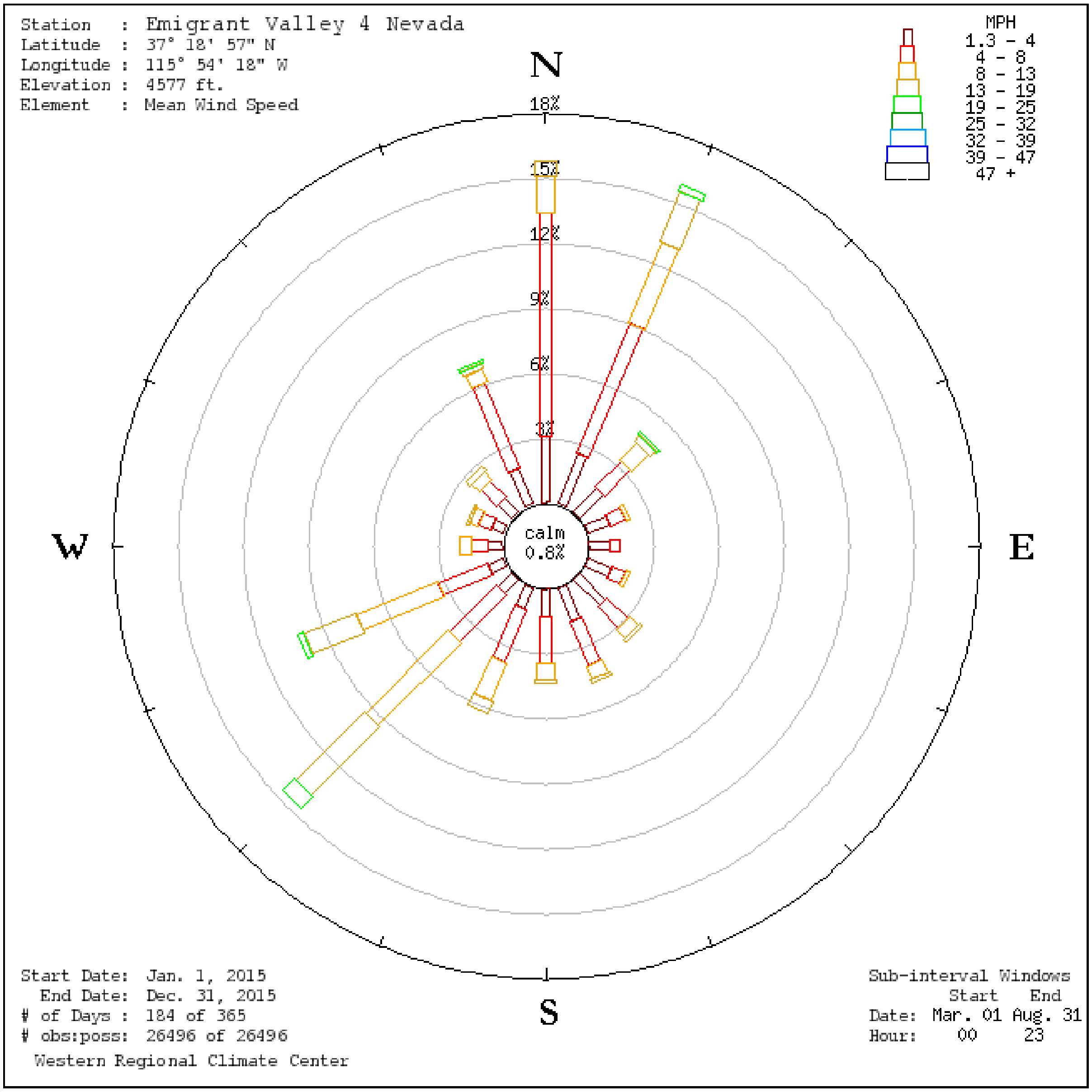

Figure A-16. P57-4 wind rose for the summer season (includes data collected between March 1 and August 31 during the reporting period).

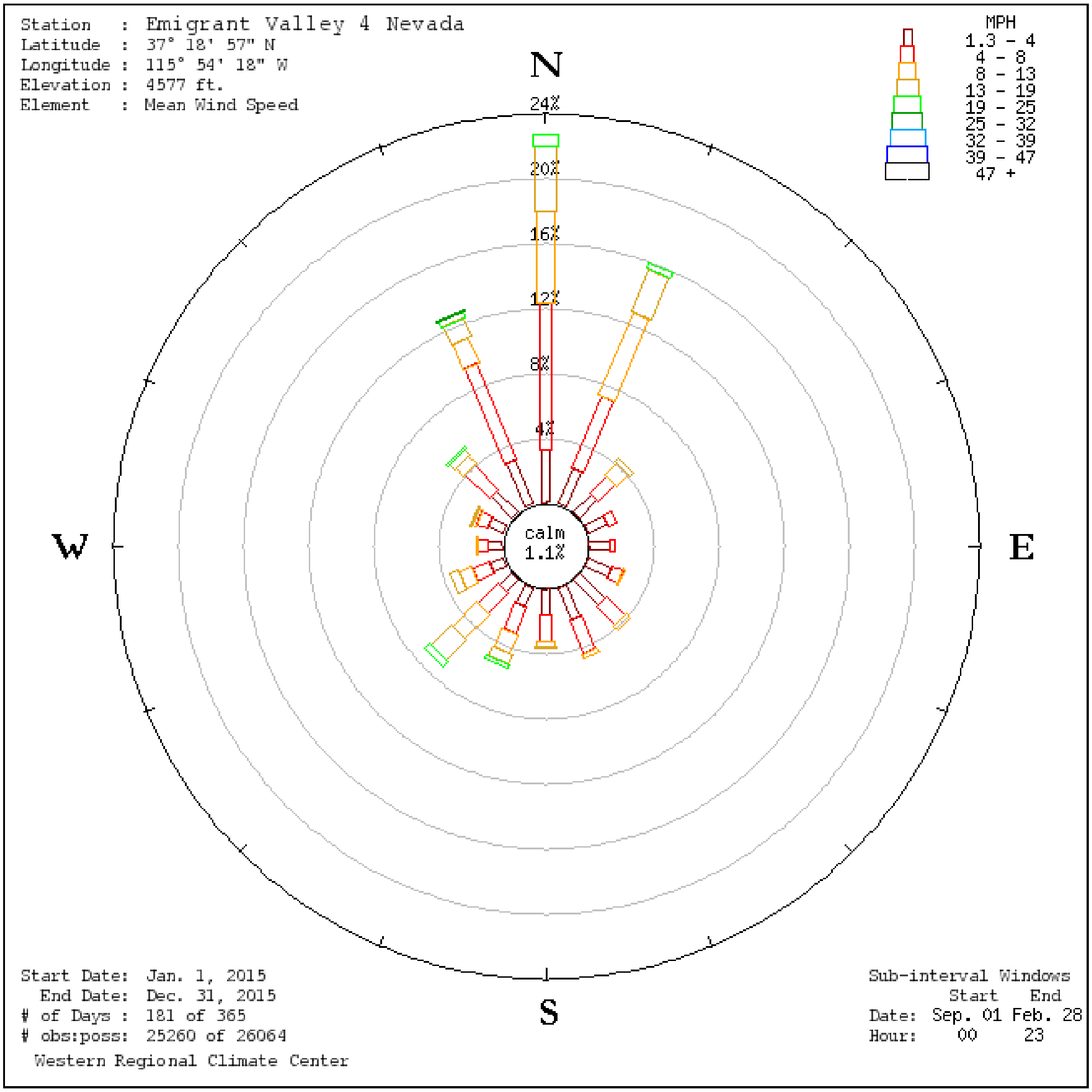

Figure A-17. P57-4 wind rose for the winter season (includes data collected between September 1 and February 28 of each year during the reporting period).

APPENDIX B: SOIL TEMPERATURE AND WATER CONTENT

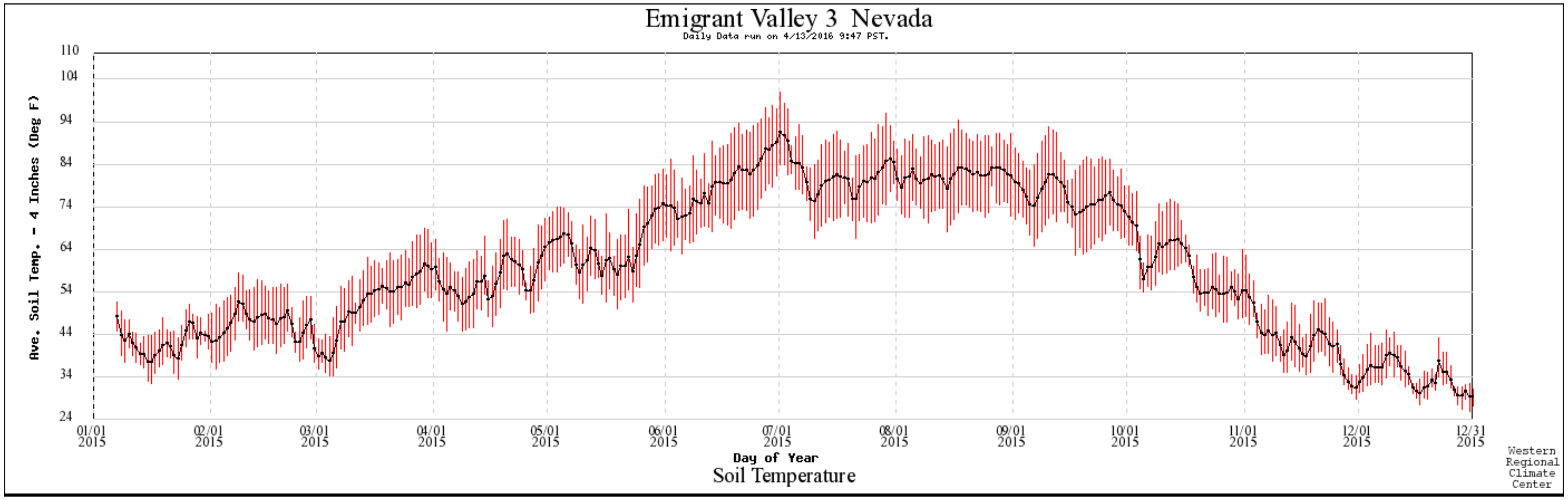

Figure B-1. Daily maximum, minimum, and average soil temperature at P57-3.

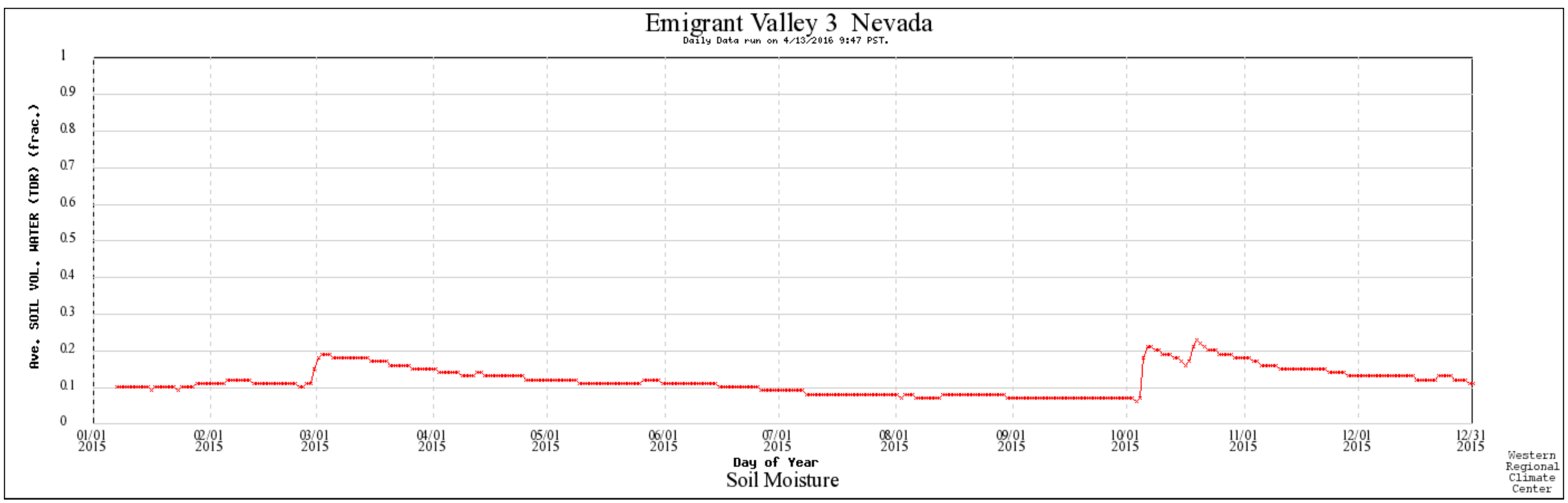

Figure B-2. Daily average soil moisture (volumetric water content [fraction]) at P57-3.

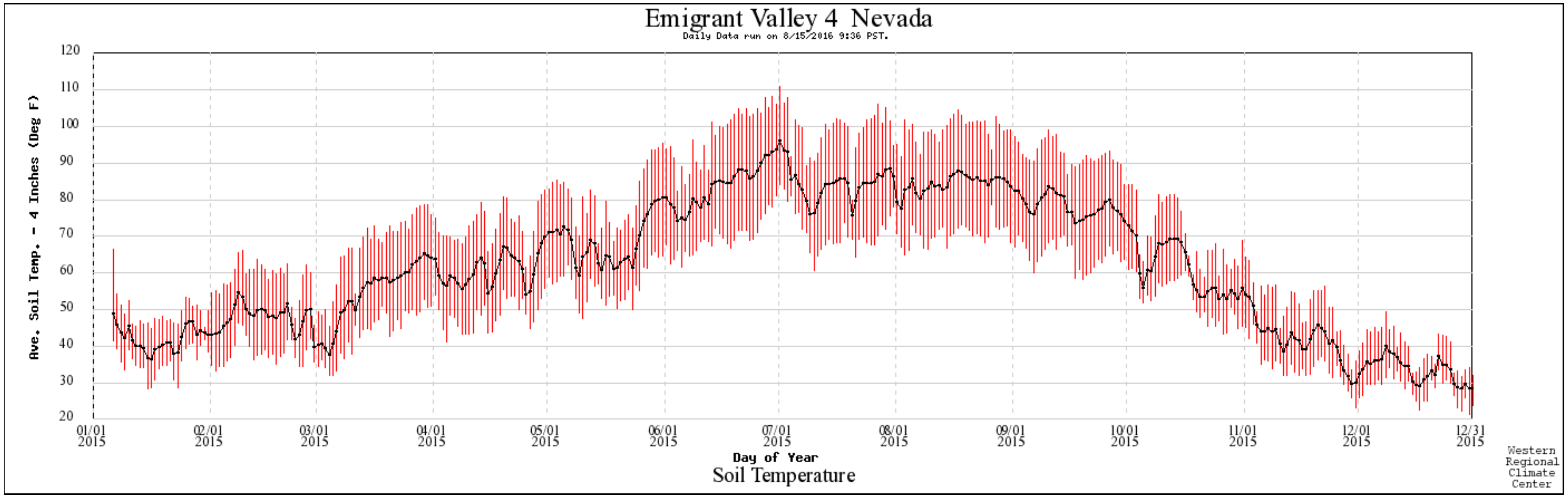

Figure B-3. Daily maximum, minimum, and average soil temperature at P57-4.

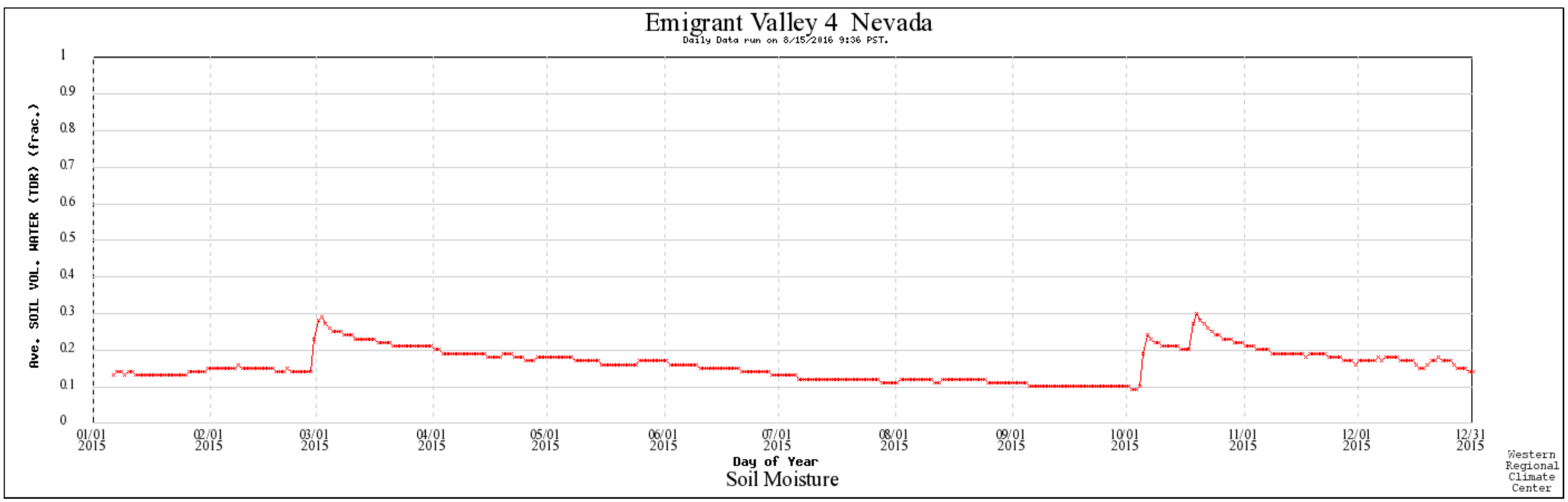

Figure B-4. Daily average soil moisture (volumetric water content [fraction]) at P57-4.

APPENDIX C: AIRBORNE AND SALTATION DUST PARTICLE OBSERVATIONS

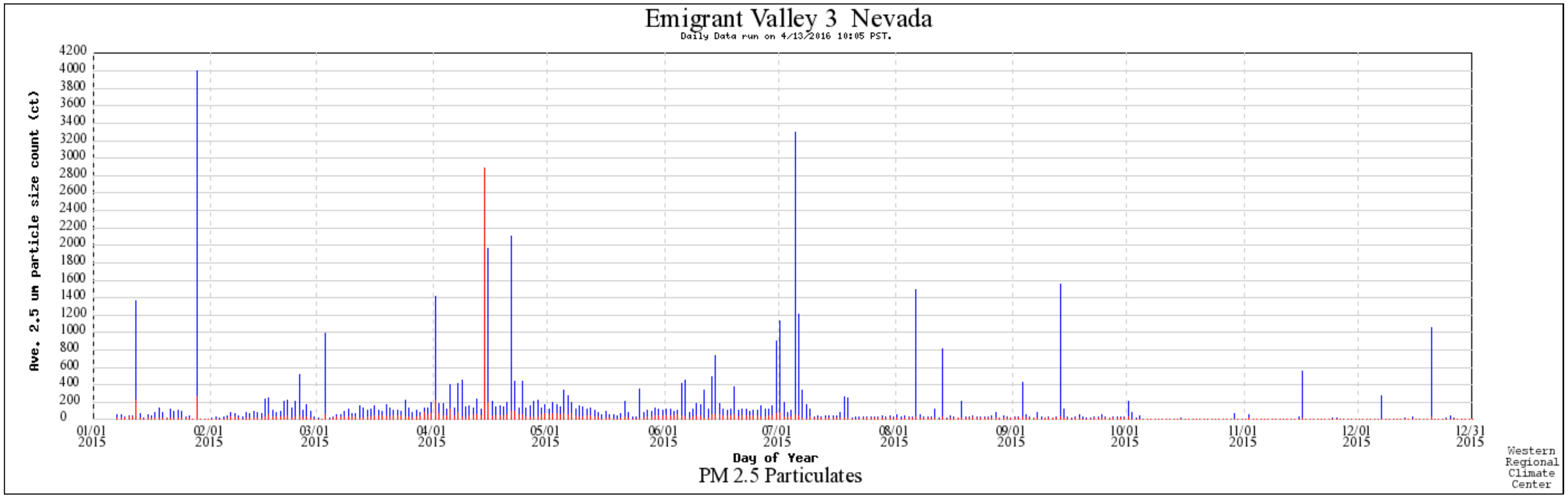

Figure C-1. Daily average and maximum $PM_{2.5}$ counts at P57-3.

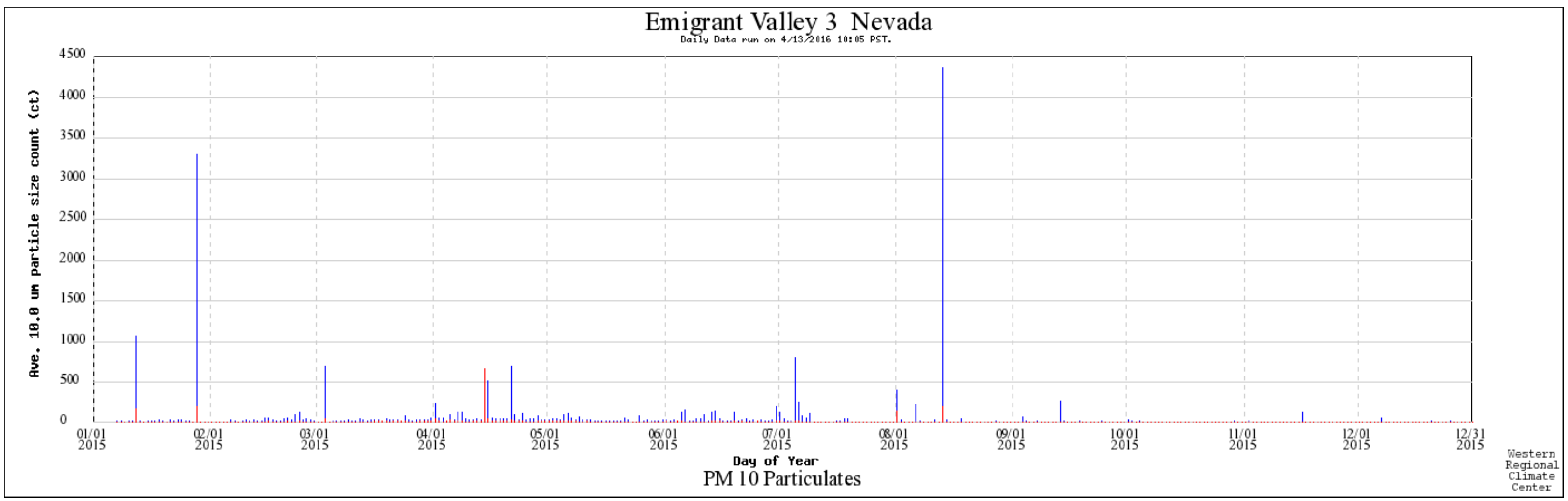

Figure C-2. Daily average and maximum PM_{10} counts at P57-3.

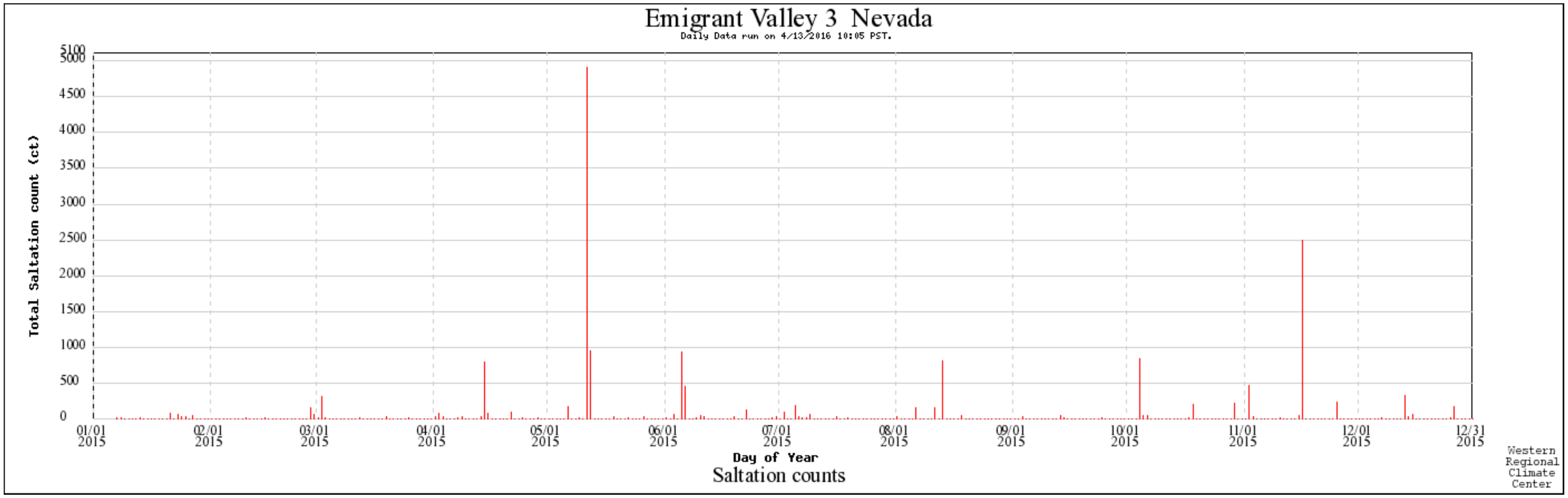

Figure C-3. Daily saltation counts at P57-3.

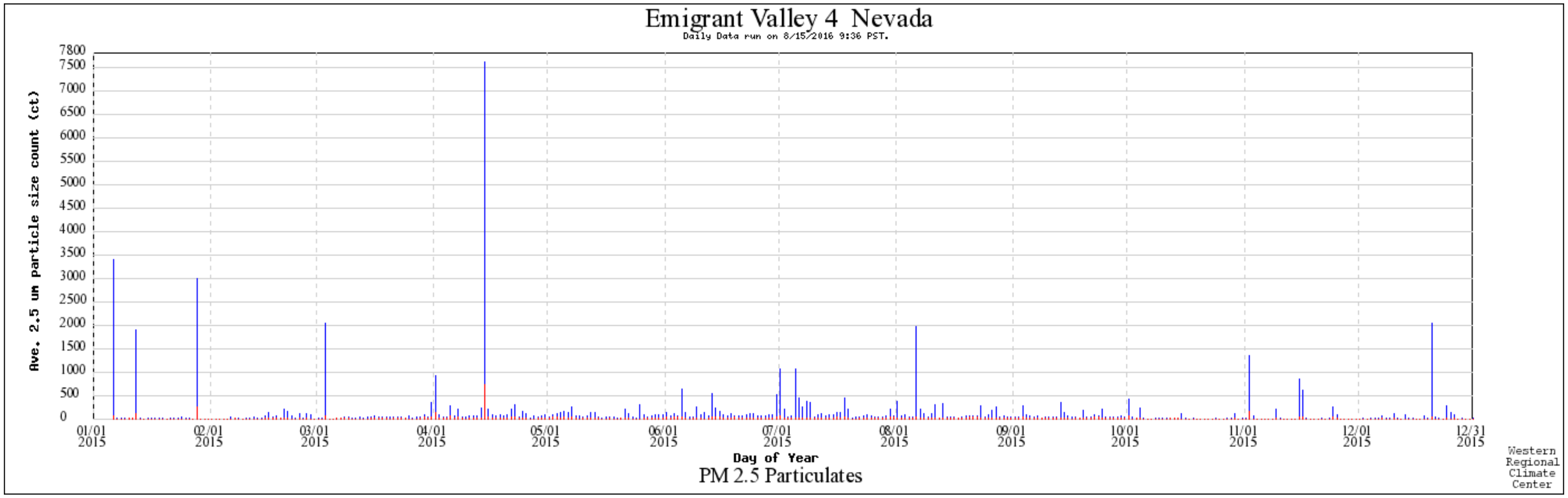

Figure C-4. Daily average and maximum $PM_{2.5}$ counts at P57-4.

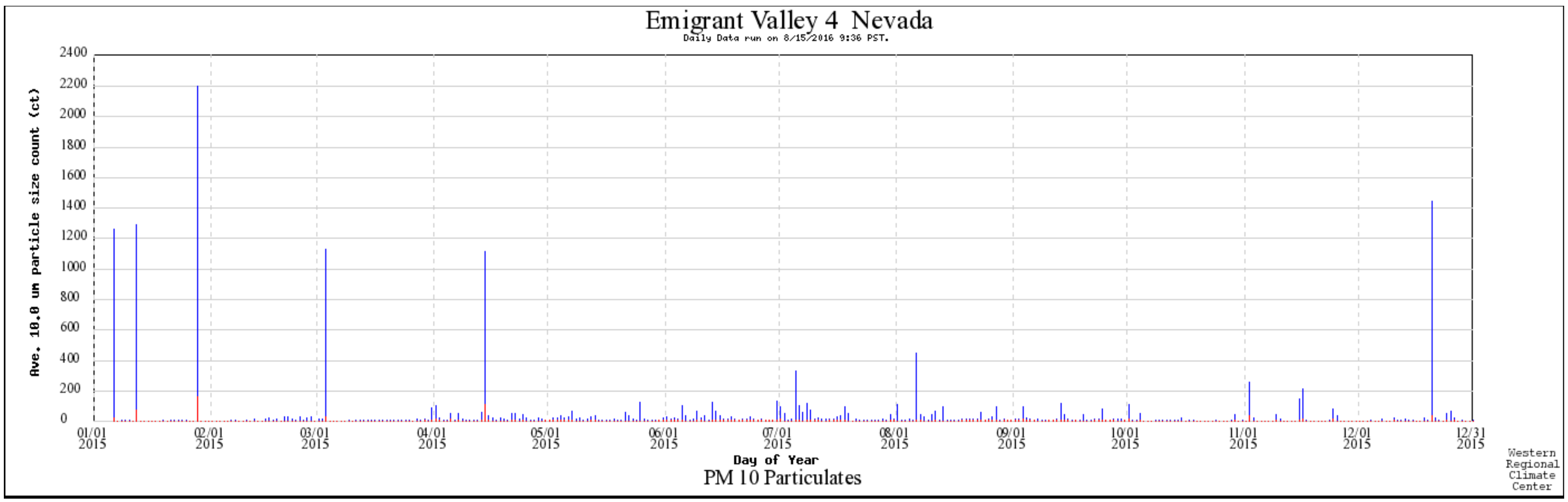

Figure C-5. Daily average and maximum PM_{10} counts at P57-4.

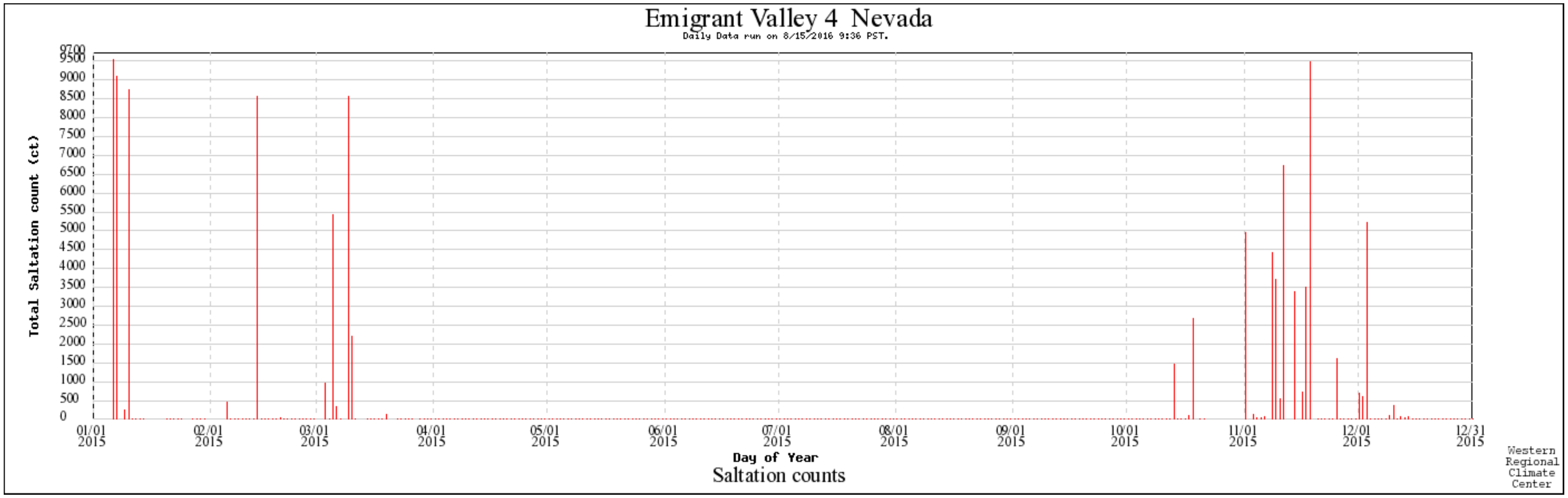

Figure C-6. Daily saltation counts at P57-4.

APPENDIX D: RADIOLOGICAL RESULTS FOR SALTATION SAMPLES

Table D-1. Radionuclide analysis results for saltation samples collected from Project 57 monitoring stations on March 3, 2015.

BSNE # Orientation	**Date**	**Size Fraction**	
		< 63 µm	**63 to 250 µm**
Am-241 (pCi/g)			
P57-1 25-29-35 2 down 1 up	March 3,2015	0.698	0.535
P57-1 27-31-33 1 down 2 up	March 3,2015	0.735	0.303
P57-2 37-41-45 Downwind	March 3,2015	0.414	0.0503
P57-2 39-43-47 Upwind	March 3,2015	0.307	0.0962
Pu-238 (pCi/g)			
P57-1 25-29-35 2 down 1 up	March 3,2015	0.115	0.324
P57-1 27-31-33 1 down 2 up	March 3,2015	0.251	0.125
P57-2 37-41-45 Downwind	March 3,2015	0.233	0.105
P57-2 39-43-47 Upwind	March 3,2015	0.145	0.0426
Pu-239+240 (pCi/g)			
P57-1 25-29-35 2 down 1 up	March 3,2015	3.74	1.94
P57-1 27-31-33 1 down 2 up	March 3,2015	3.57	1.15
P57-2 37-41-45 Downwind	March 3,2015	2.24	0.369
P57-2 39-43-47 Upwind	March 3,2015	1.34	0.279

Radiological analyses by GEL Laboratories, Charleston, South Carolina.

Table D-2. Radionuclide analysis results for saltation samples collected from Project 57 monitoring stations on January 4, 2016.

BSNE # Orientation	Date	Size Fraction	
		< 63	63 to 250 µm
Am-241 (pCi/g)			
P57-3 38-42-46 Downwind	January 4, 2016	6.58	0.203
P57-3 40-44-48 Upwind	January 4, 2016	4.21	0.152
P57-4 26-30-34 Downwind	January 4, 2016	16.6	0.167
P57-4 28-32-36 Upwind	January 4, 2016	14.4	0.188
Pu-238 (pCi/g)			
P57-3 38-42-46 Downwind	January 4, 2016	0.830	0.152
P57-3 40-44-48 Upwind	January 4, 2016	0.664	0.245
P57-4 26-30-34 Downwind	January 4, 2016	2.65	0.0519
P57-4 28-32-36 Upwind	January 4, 2016	1.48	0.0114
Pu-239+240 (pCi/g)			
P57-3 38-42-46 Downwind	January 4, 2016	73.1	0.843
P57-3 40-44-48 Upwind	January 4, 2016	40.3	0.834
P57-4 26-30-34 Downwind	January 4, 2016	338	1.60
P57-4 28-32-36 Upwind	January 4, 2016	247	0.946

Radiological analyses by GEL Laboratories, Charleston, South Carolina.

APPENDIX E: GRAPHICAL PRESENTATION OF WIND AND DUST CONDITIONS DURING MAJOR WIND EVENTS AT P57-NORTH AND SOUTH

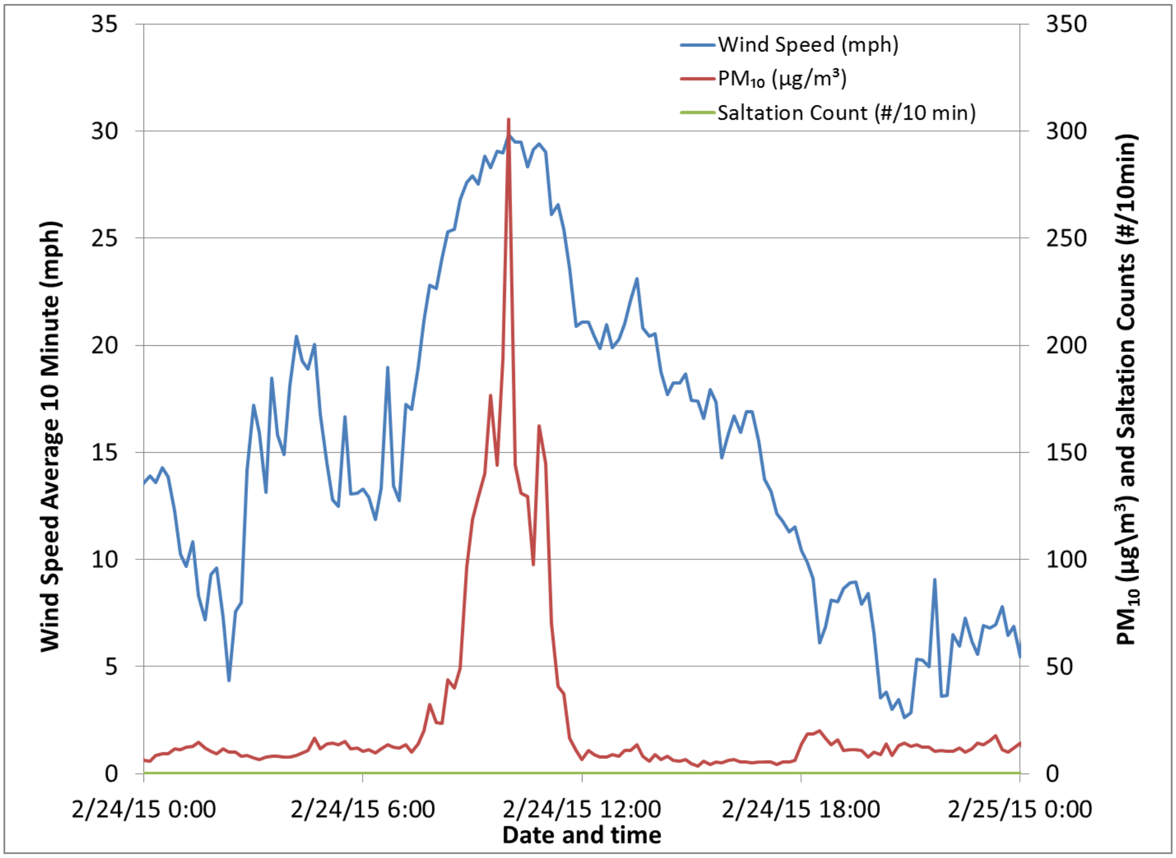

Figure E-1. Wind and dust episode February 24, 2015.

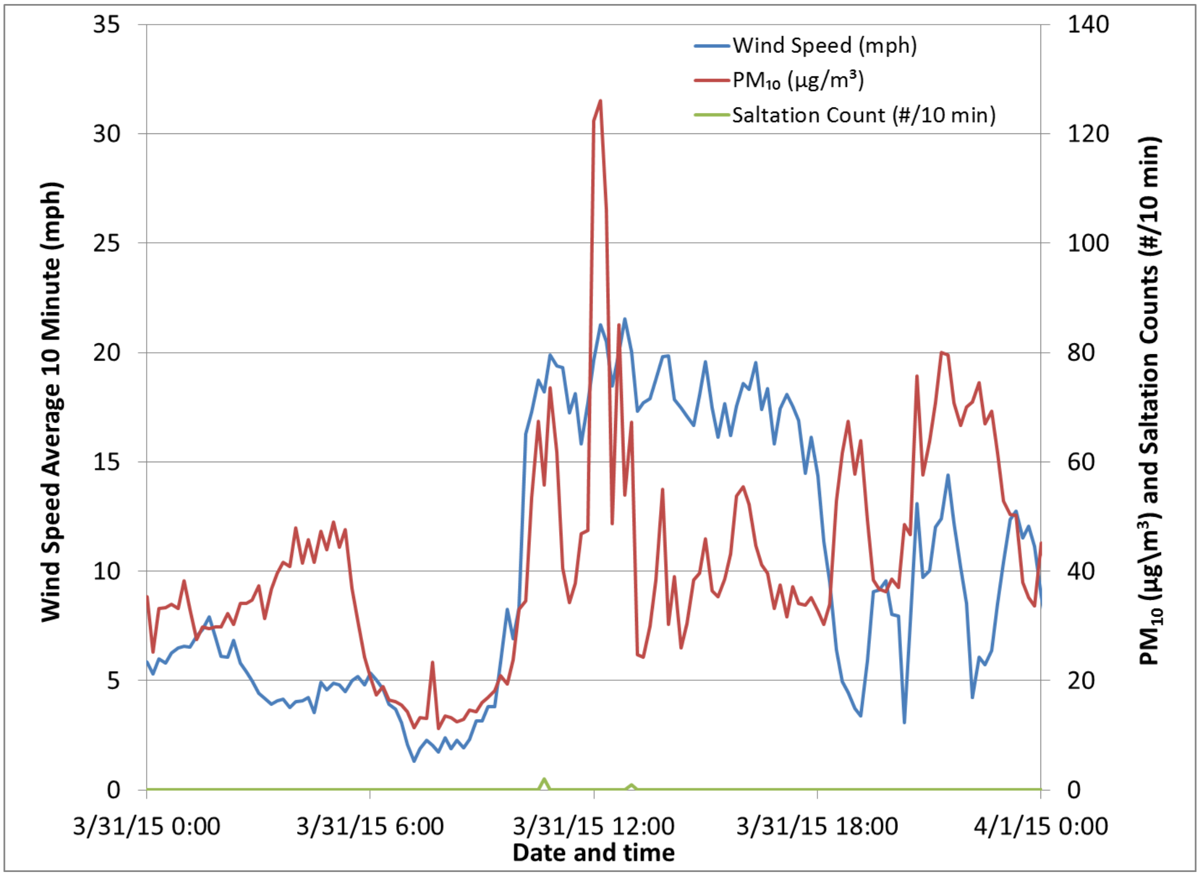

Figure E-2. Wind and dust episode March 31, 2015.

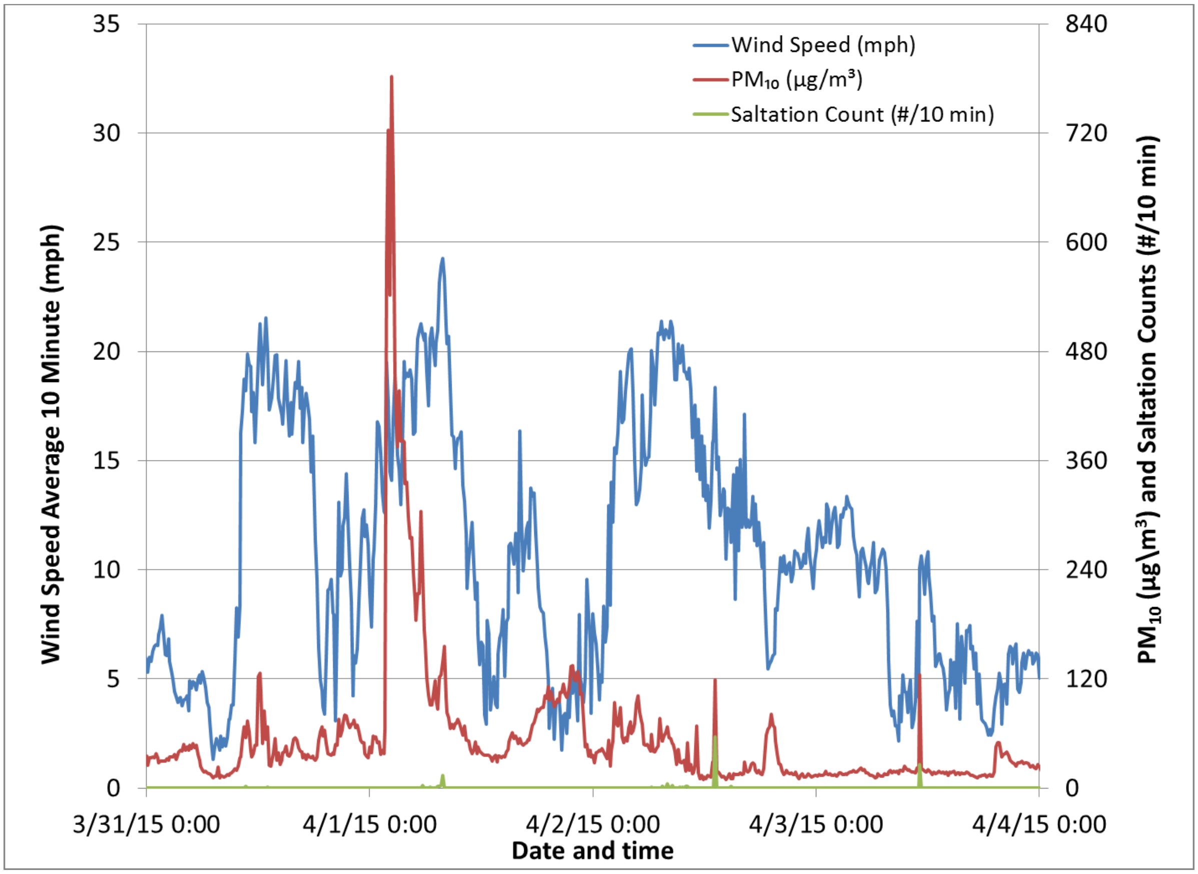

Figure E-3. Wind and dust episode April 1, 2015.

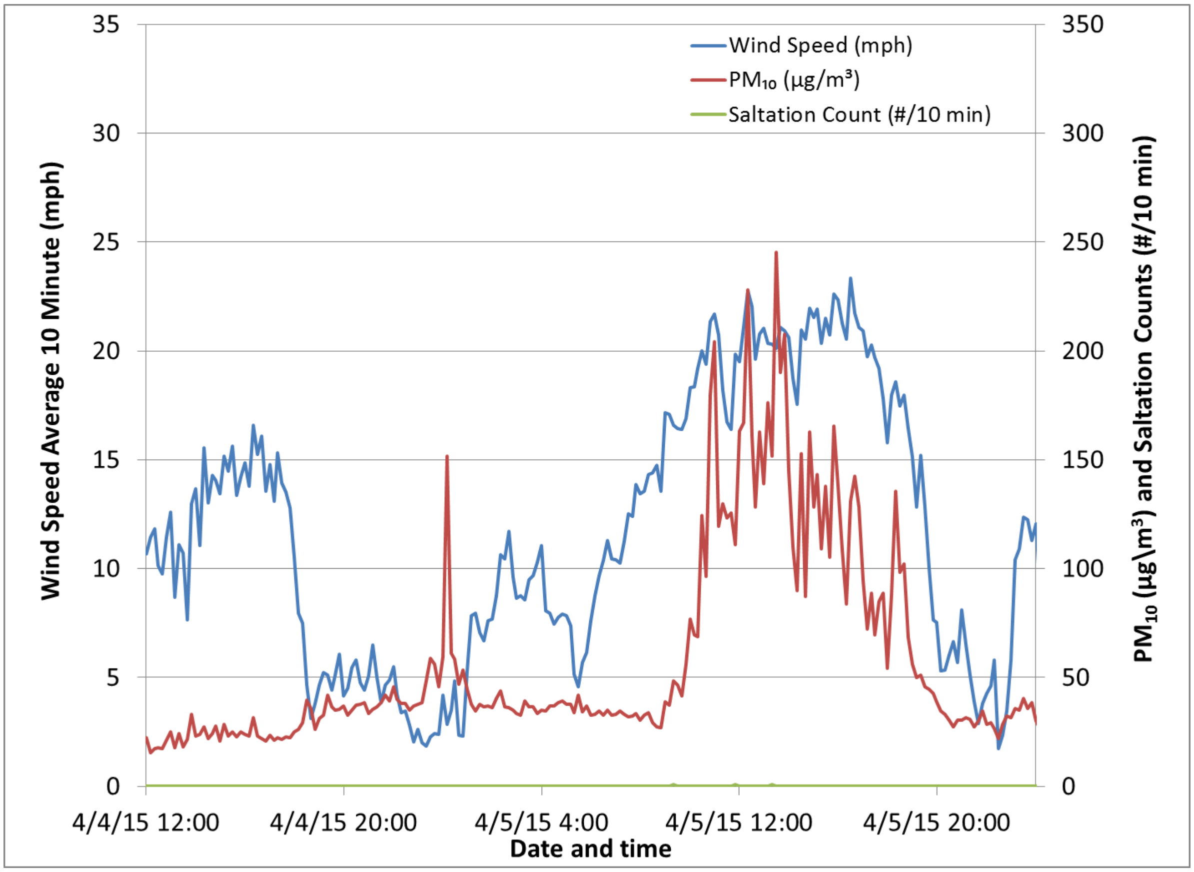

Figure E-4. Wind and dust episode April 5, 2015.

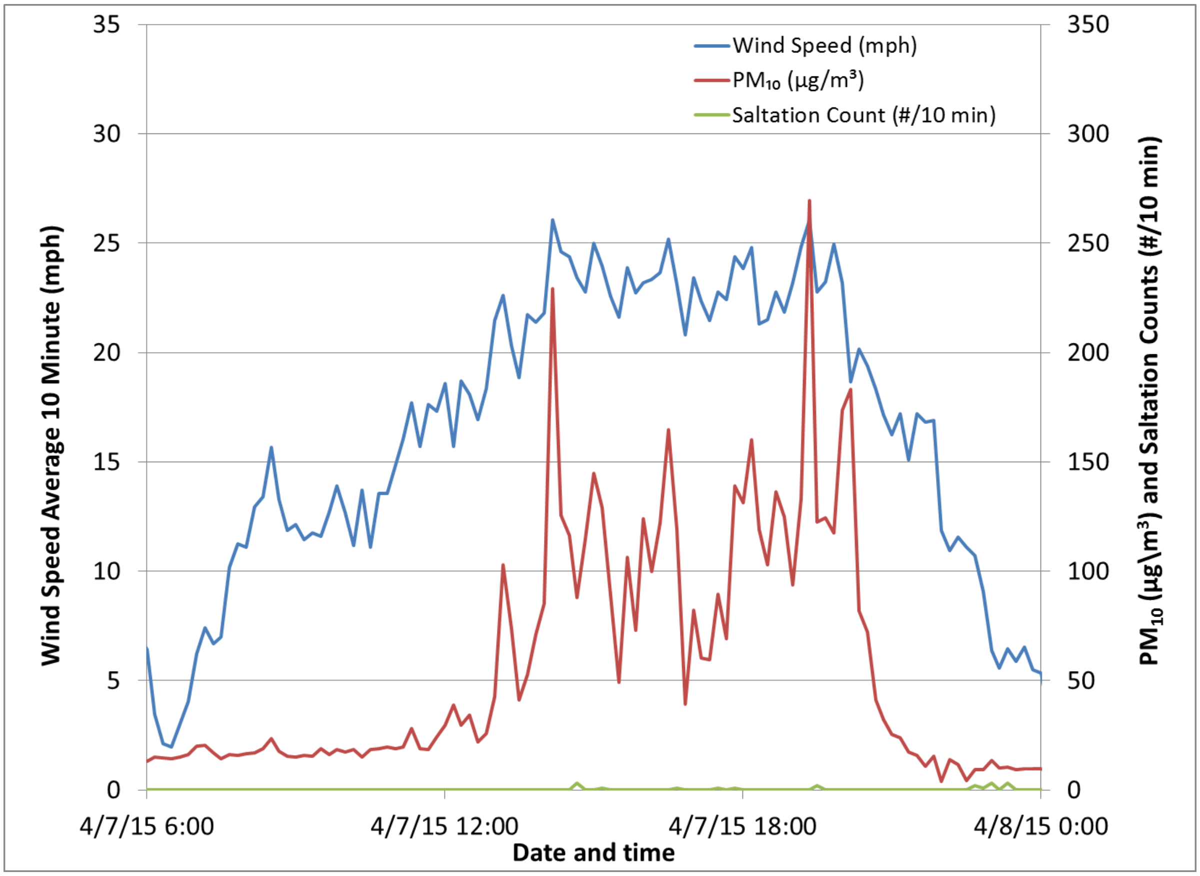

Figure E-5. Wind and dust episode April 7, 2015.

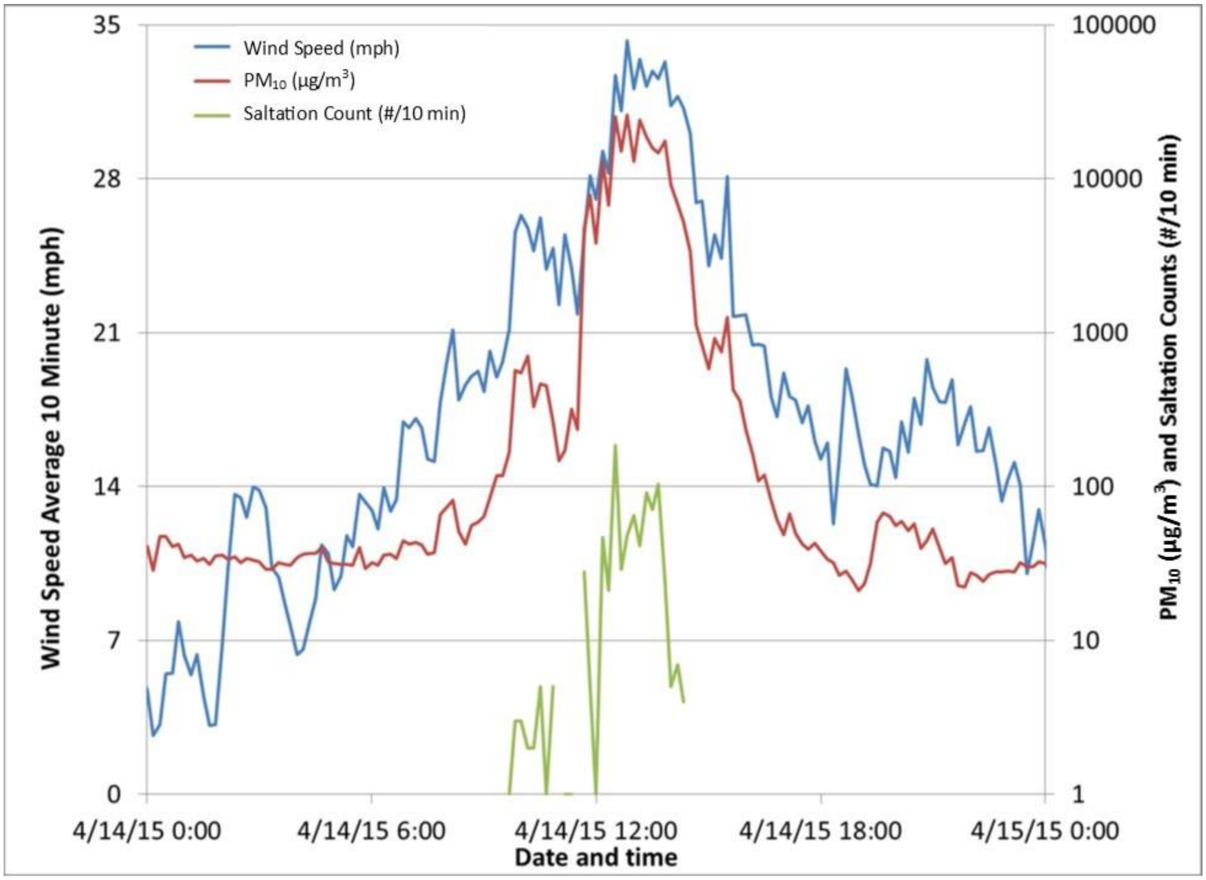

Figure E-6. Wind and dust episode April 14, 2015.

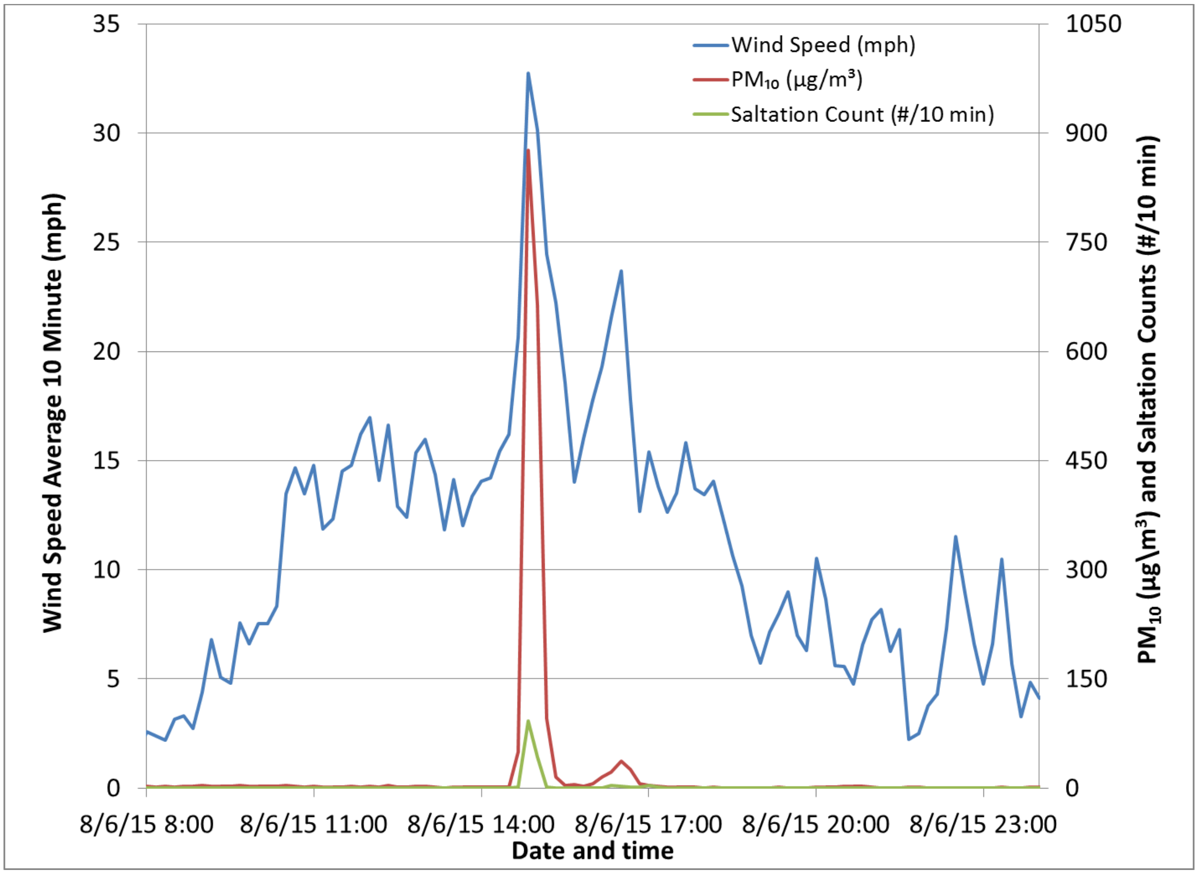

Figure E-7. Wind and dust episode August 6, 2015.

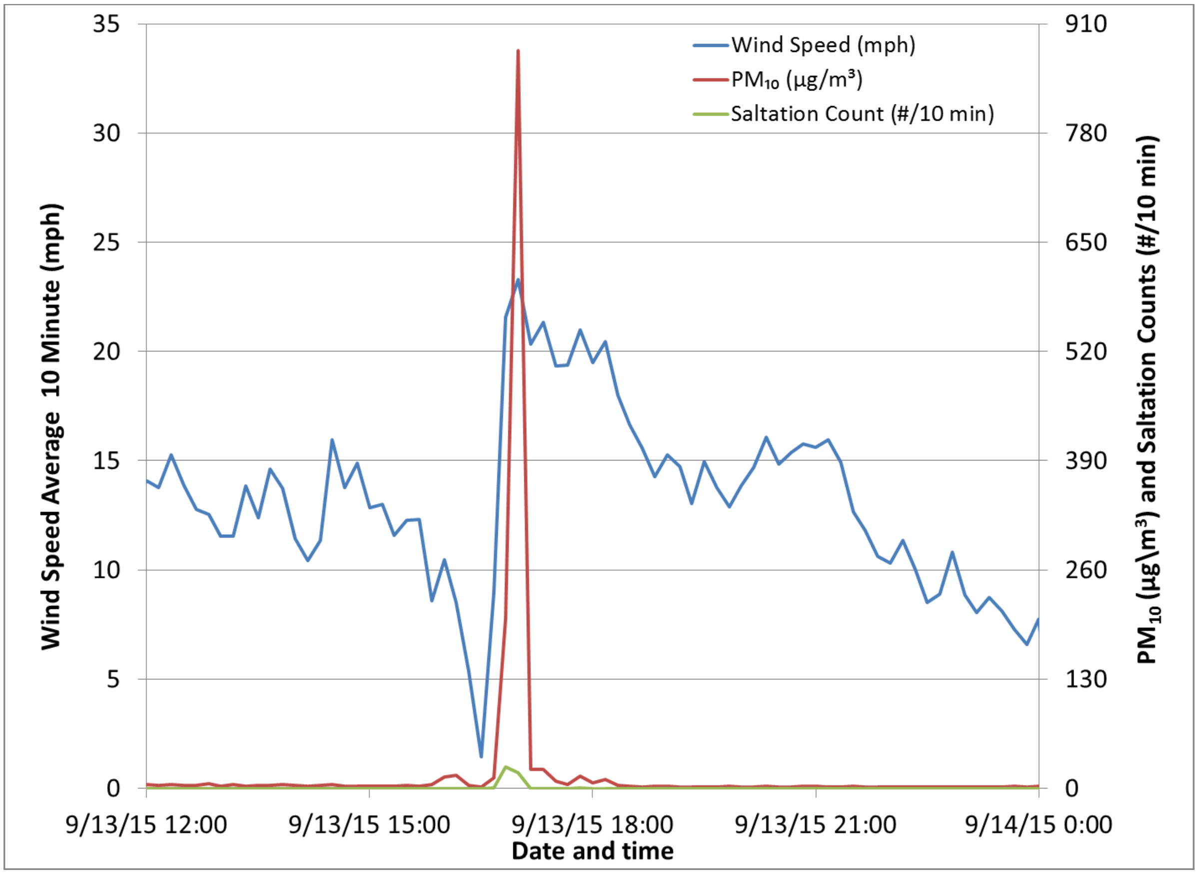

Figure E-8. Wind and dust episode September 13, 2015.

APPENDIX F: MAJOR OPERATIONAL AND OBSERVATIONAL EVENTS DURING DRI SOILS ACTIVITY

Table F-1. Project 57: October 2010 through September 2011

FY2011 (Oct. 2010 – Sept. 2011)	
April 20, 2011*	P57-1 Temporary installation outside CA
May 2011[1]	NSTec RCTs downgraded corridors between the 1957 CA fence and 2007 CA signage to RMAs
July 27 through August 11, 2011*	P57-1 was dismantled and removed from field site at the request of the land management organization
August 11, 2011*	P57-1 was moved up to the 1957 CA fence in the northeast RMA
FY2012 (Oct 2011 – Sept 2012)	
November 18, 2011*	P57-2 was installed adjacent to the 1957 CA fence in the southeast RMA
November 2011	P57-1 and P57-2 Initial deployment of TLDs
December 13, 2011	P57-2 Saltation particle counter installed
January 9, 2012	P57-1 Saltation particle counter installed
January 9, 2012	P57-1 and P57-2 Begin quarterly exchange and analysis of TLDs
January 25, 2012	P57-2 tower was found blown over
April 3, 2012	P57-1 Replaced Met One™ because it was giving inaccurate values
May 29, 2012	Battery imbalance causing power outage, converter replaced
August 20, 2012	P57-1 Split 12v and 24v battery systems
September 17, 2012	P57-2 Split 12v and 24v battery systems

Table F-2. Project 57: October 2012 through September 2014

FY2013 (Oct 2012 – Sep 2013)	
February 11, 2013	P57-1 and P57-2 Hi-Q samplers were removed from the field for manufacturer calibration and maintenance
February 15, 2013	P57-1 and P57-2 Hi-Q samplers were re-installed after manufacturer calibration and maintenance
February 21, 2013	P57-1 Hi-Q blower failed due to fuse failure
March 5 2013	P57-1 Hi-Q returned to service
May 2, 2013	P57-2 Replaced fuse in Hi-Q
May 14, 2013	P57-2 Replaced Hi-Q blower motor and Met One™
June 2013	P57-2 Hi-Q sampler fuse failed due to short in pump; parts were acquired, repairs made, and instrument returned to service
June 25, 2013	P57-2 tower leaning and Hi=Q air sampler laying on the ground
August 5, 213	P57-1 and P57-2 Saltation (Sensit) sensors lowered to 2.5 inches above ground
August 7, 2013	P57-2 Replaced Met One™ for annual calibration
FY2014 (Oct 2013 – Sep 2014)	
November 25, 2013	P57-2 Replaced WXT520 sensor
February 4, 2014	P57-1 and P57-2 Changed from cellulose to fiberglass filters in Hi-Q sampler
February 19, 2014	P57-2 Re-set wind speed output from m/s to MPH
April 14, 2014	**P57-1 and P57-2 Initial deployment of BSNE Saltation Sand Traps installed**
April 15, 2014	P57-2 Removed Sensit and swapped Met One™
August 18 2014	P57-2 Install new Sensit
August 21, 2014	P57-1 Swapped Met One™

Table F-3. Project 57: October 2014 through July 2016

FY2015 (Oct 2014 – Sep 2015)	
January 7, 2015	**P57-1 and P57-2 decommissioned and relocated P57-3 and P57-4 established**
March 3, 2015	P57-1 and P57-2 BSNE saltation sand traps recovered P57-3 and P57-4 clean BSNE traps deployed
April 13, 2015	P57-3 and P57-4 installed new Hi-Q blower motors
April 15, 2015	P57-3 and P57-4 collected 2-day sample to evaluate impact of observed wind storm
May 11 2015	P57-3 Met One^{TM} (K14481) recovered for annual manufacturer calibration (K13708) installed
June 23, 2015	P57-4 Hi-Q sample reported Am-241 detection, sample required additional analyses
July 30, 2015	P57-4 Data review indicates Sensit saltation sensor failed beginning in April or May
September 14, 2015	P57-3 Hi-Q not running, returned to manufacturer for repair
FY2016 (Oct 2015 – Sep 2016)	
October 13, 2015	P57-3 and P57-4 rain gage calibrated, P57-4 Sensit replaced
October 22, 2015	P57-3 Hi-Q reinstalled after repair
November 9, 2015	P57-3 Hi-Q tipped over on face, intake on the ground, discarded sample 10/27/15 – 11/9/15
November 23, 2015	P57-3 Hi-Q tipped over on back, intake on the ground, discarded sample 11/9/15 – 11/23/15
January 4, 2016	P57-3 and P57-4 BSNE Saltation Sand Traps recovered and clean traps deployed
March 2, 2016	P57-3 replaced station tower, transferred all equipment and sensors to new tower
May 10, 2016	P57-4 Met One^{TM} (SN K14481) removed for annual calibration replaced with spare (SN M5276)
June 7, 2016	P57-4 Batteries in 24v system not holding adequate charge, Hi-Q shutting down overnight, Sensit failed
June 21, 2016	P57-4 batteries for 24v system replaced, Hi-Q operating 24/7
July 6, 2016	P57-3 Hi-Q not running blower/fuse may have failed
July 18, 2016	P57-3 Hi-Q removed from field for manufacturer repair; Met One^{TM} (Sn K13708) removed for manufacturer calibration, Met One^{TM} (Sn K14481) returned from calibration and installed

1 Historical notes for May 2011 through January 2012 were obtained from Miller 2012a.

2 Thermoluminescent dosimeters (TLDs) are retrieved and replaced quarterly beginning in January 2012.

APPENDIX G: QUALITY ASSURANCE PROGRAM

Although the current data collected for the Project 57 Air Monitoring study are considered for informational purposes to support conceptual models or guide investigations, the U.S. Department of Energy National Nuclear Security Administration Nevada Field Office (DOE/NNSA/NFO) Soils Activity Quality Assurance Plan (QAP) (2012) was used as a guideline for the collection and analysis of the airborne radiological data presented in the section of this report titled, “Radiological Assessment of Airborne Particulate Matter.” This QAP as well as the Desert Research Institute Quality Assurance Program Manual for the DOE Program (2010) ensures compliance with U.S. Department of Energy (DOE) Order DOE O 414.1D, “Quality Assurance”, which implements a quality management system to ensure the generation and use of quality data. The following items are addressed by the aforementioned QA documents:

- Data quality objectives (DQOs)
- Sampling plan development appropriate to satisfy the DQOs
- Environmental health and safety
- Sampling plan execution
- Sample analyses
- Data review
- Continuous improvement

Data Quality Objectives (DQOs)

The DQO process is a strategic planning approach that is used to plan data collection activities. It provides a systematic process for defining the criteria that a data collection design should satisfy. These criteria include when and where samples should be collected, how many samples to collect, and the tolerable level of decision errors for the study. The DQOs are unique to the specific data collection or monitoring activity and their defined level of use (in this case, for informational purposes).

Measurement Quality Objectives (MQOs)

The MQOs are basically equivalent to DQOs for analytical processes. The MQOs provide direction to the laboratory concerning performance objectives or requirements for specific method performance characteristics. Default MQOs are established in the subcontract with the laboratory but may be altered to satisfy changes in the DQOs. The MQOs for the Project 57 Air Monitoring study are described in terms of precision, accuracy, representativeness, completeness, and comparability requirements. These terms are defined and discussed in the DOE/NNSA/NFO (QAP).

Sampling Quality Assurance Program

Quality Assurance (QA) in field operations for the Project 57 Air Monitoring study includes sampling assessments, surveillances, and oversight of the following supporting elements:

- The sampling plan, DQOs, and field data sheets accompanying the sample package
- Database support for field and laboratory results, including systems for long-term storage and retrieval
- Qualified personnel who are available and able to perform required tasks
- Sample packages include the following items:
- Sample collectors field notes confirming all observable information pertinent to sample collection
- An Air Surveillance Network Sample Data Form that documents air sampler parameters, collection dates and times, and total sample volumes collected
- Chain-of-custody forms that also include some of the elements of the field notes

This managed approach to sampling ensures that the sampling is traceable and enhances the value of the final data available to the project manager. The sample package also ensures that the personnel responsible for sample collection have followed proper procedures for sample collection.

Data obtained in the course of executing field operations are entered in the documentation that accompany the sample package during sample collection and in the Project 57 Study database along with analytical results on their receipt and evaluation.

Completed sample packages are kept as hard copy in file archives. Analytical reports are kept as hard copy in file archives as well as in a dedicated and secure archival systems that are protected and maintained in accordance with the Desert Research Institute's Computer Protection Program.

Laboratory QA Oversight

Although the data for the Project 57 Air Monitoring study is for informational purposes, the main aspects of the DOE O 414.1D requirements are used as guidelines to evaluate laboratory services through review of the vendor laboratory policies formalized in a Laboratory Quality Assurance Plan (LQAP). The Project 57 study is assured of obtaining quality data from laboratory services through a multifaceted approach that involves specific procurement protocols, the conduct of quality assessments, and requirements for selected laboratories to have an acceptable QA Program. These elements are discussed below.

<u>Procurement</u>

Laboratory services are procured through subcontracts that establish the technical specifications required of the laboratory to provide the basis for determining compliance with those requirements and evaluating overall performance. A subcontract is usually awarded on a best-value basis as determined by pre-award audits, but because of the specific requirement requested for gamma spectroscopy analysis (24 hour count duration) for the Project 57 study, the laboratory was procured on a sole-proprietor basis. The laboratory was required to provide a review package that included the following items:

- All procedures pertinent to subcontract scope
- Environment, Safety, and Health Plan
- LQAP
- Example deliverables (hard copy and/or electronic)
- Proficiency testing (PT) results from the previous year from recognized PT programs
- Résumés
- Accreditations and certifications
- Licenses

Continuing Assessment

A continuing assessment of a selected laboratory involves the ongoing monitoring of a laboratory's performance against the contract terms and conditions, of which technical specifications are a part. The following tasks support continuing assessment:

- Tracking schedule compliance
- Reviewing analytical data deliverables
- Monitoring the laboratory's adherence to the LQAP
- Monitoring for continued successful participation in approved PT programs

Data Review

Essential components of process-based QA are data checks, verification, validation, and data quality assessment to evaluate data quality and usability.

Data Checks: Data checks are conducted to ensure accuracy and consistency of field data collection operations prior to and on data entry into Project 57 databases and data management systems.

Data Verification: Data verification is defined as a compliance and completeness review to ensure that all laboratory data and sample documentation are present and complete. Sample preservation, chain-of-custody, and other field sampling documentation shall be reviewed during the verification process. Data verification ensures that the reported results entered in Project 57 databases correctly represent the sampling and/or analyses performed and includes evaluation of quality control (QC) sample results.

Data Validation: Data validation is the process of reviewing a body of analytical data to determine if it meets the data quality criteria defined in operating instructions. Data validation ensures that the reported results correctly represent the sampling and/or analyses performed, determines the validity of the reported results, and assigns data qualifiers (or "flags") if required. The process of data validation consists of the following:

- Evaluating the quality of the data to ensure that all project requirements are met
- Determining the impact on data quality of those requirements if they are not met
- Verifying compliance with QA requirements
- Checking QC values against defined limits
- Applying qualifiers to analytical results in the Project 57 databases for the purposes of defining the limitations in the use of the reviewed data

Operating instructions, procedures, applicable project-specific work plans, field sampling plans, QA plans, analytical method references, and laboratory statements of work may all be used in the process of data validation. Documentation of data validation includes checklists, qualifier assignments, and summary forms.

Data Quality Assessment (DQA): The DQA is the scientific evaluation of data to determine if the data obtained from environmental data operations are of the right type, quality, and quantity to support their intended use. The DQA review is a systematic review against preestablished criteria to verify that the data are valid for their intended use.

2015 Sample QA Results

The QA assessments were performed by the Project 57 Air Monitoring study, including the laboratory responsible for sample analyses. These assessments ensure that sample collection procedures, analytical techniques, and data provided by the subcontracted laboratory comply with Project 57 study requirements. Data were provided by the University of Nevada, Las Vegas, Radiation Services Laboratory (gross alpha/beta and gamma spectroscopy data), and Mirion Technologies (TLD data). A brief discussion of the 2015 results for laboratory duplicates, control samples, blank analyses, and interlaboratory comparison studies is provided along with summary tables within this section.

<u>Laboratory Duplicates (Precision)</u>

A laboratory duplicate is a sample that is handled and analyzed following the same procedures as the primary sample analysis. The relative percent difference (RPD) between the initial result and the corresponding duplicate result is a measure of the variability in the analytical process of the laboratory, mainly overall measurement uncertainty. The average absolute RPD, expressed as a percentage, was determined for the calendar year 2015 samples and is listed in Table G-1. An RPD of zero indicates a perfect duplication of results of the duplicate pair, whereas an RPD greater than 100 percent generally indicates that a duplicate pair falls beyond QA requirements and is not considered valid for use in data interpretation. These samples are further evaluated to determine the reason for QA failure and if any corrective actions are required. Overall, the RPD values for all analyses indicate very good results with no samples exceeding an RPD of 100 percent.

Table G-1. Summary of laboratory duplicate samples for the Project 57 Air Monitoring study in 2015.

Analysis	**Matrix**	**Number of Samples Reported[(a)]**	**Number of Samples Reported above MDC[(b)]**	**Average Absolute RPD of those above MDC (%)[(c)]**
Gross Alpha	Air	11	11	25.3
Gross Beta	Air	11	11	5.9
Gamma – Beryllium 7	Air	9	8	10.4
Gamma – Lead 210	Air	9	1	2.5
TLDs	Ambient Radiation	12	NA	1.5

a) Represents the number of laboratory duplicates reported for the purpose of monitoring precision. If an associated field sample was not processed, the field duplicate was not included in this table.

b) Represents the number of laboratory duplicate sets reported above the minimum detectable concentration (MDC) (MDC is not applicable for TLDs). If either the original laboratory analysis or its duplicate was reported below the detection limit, the precision was not determined.

c) Reflects the average absolute RPD calculated for those field duplicates reported above the MDC.

The absolute RPD calculation is as follows:

$$Absolute\ RPD = \frac{|LD - LS|}{(LD + LS)/2} \ X \ 100\%$$

Where: LD = Laboratory duplicate result
LS = Laboratory sample result

Laboratory Control Samples (Accuracy)

Laboratory control samples (LCSs) (also known as matrix spikes) are performed by the subcontract laboratory to evaluate analytical accuracy, which is the degree of agreement of a measured value with the true or expected value. Samples of known concentration are analyzed using the same methods as employed for the project samples. The results are determined as the measured value divided by the true value, expressed as a percentage. To be considered valid, the results must fall within established control limits (or percentage ranges) for further analyses to be performed. The LCS results obtained for 2015 are summarized in Table G-2. The LCS results were satisfactory with all samples falling within control parameters for the air sample matrix.

Table G-2. Summary of laboratory control samples for the Project 57 Air Monitoring study in 2015.

Analysis	Matrix	Number of LCS Results Reported	Number Within Control Limits[(a)]
Gross Alpha	Air	12	12
Gross Beta	Air	12	12
Gamma	Air	8	8

a) Control limits are as follows: 78 percent to 115 percent for gross alpha, 87 percent to 115 percent for gross beta, 90 percent to 115 percent for gamma (137Cs, 60Co, 241Am).

Laboratory Blank Analysis

Laboratory blank sample analyses are essentially the opposite of LCSs discussed above. These samples do not contain any of the analyte of interest. Results of these analyses are expected to be zero, or more accurately below the MDC of a specific procedure. Blank analysis and control samples are used to evaluate overall laboratory procedures, including sample preparation and instrument performance. The laboratory blank sample results obtained for 2015 are summarized in Table G-3. The laboratory blank results were satisfactory with all of the alpha and beta blank samples falling within control parameters for the air sample matrix.

Table G-3. Summary of laboratory blank samples for the Project 57 Air Monitoring study in 2015.

Analysis	Matrix	Number of Blank Results Reported	Number within Control Limits[(a)]
Gross Alpha	Air	12	12
Gross Beta	Air	12	12
Gamma	Air	8	8

a) Control limit is less than the MDC.

Interlaboratory Comparison Studies

Interlaboratory comparison studies are conducted by the subcontracted laboratories to evaluate their performance relative to other laboratories providing the same service. These types of samples are commonly known as blind samples, in which the expected values are known only to the program conducting the study. The analyses are evaluated and if found satisfactory, the laboratory is certified that its procedures produce reliable results. The interlaboratory comparison sample results obtained for 2015 are summarized in Tables G-4 and G-5.

Table G-4 shows the summary of interlaboratory comparison sample results for the subcontract radiochemistry laboratory. The laboratory participated in the QA Program administered by Mixed Analyte Performance Evaluation Program (MAPEP) for gross alpha, gross beta, and gamma analyses. The subcontractors performed very well during the year by passing all of the parameters analyzed.

Table G-4. Summary of interlaboratory comparison samples of the radiochemistry laboratory for the Project 57 Air Monitoring study in 2015.

		MAPEP Results	
Analysis	**Matrix**	**Number of Results Reported**	**Number Within Control Limits[(a)]**
Gross Alpha	Air	2	2
Gross Beta	Air	2	2
Gamma	Air	2	2

a) Control limits are determined by the individual inter-laboratory comparison study.

Table G-5 shows the summary of the in-house performance evaluation results conducted by the subcontract dosimetry group. This internal evaluation was based on National Voluntary Laboratory Accreditation Program (NVLAP) criteria and was performed biannually. The dosimetry group performed very well during the year by passing 12 out of 12 of the TLDs analyzed.

Table G-5. Summary of interlaboratory comparison TLD samples of the subcontract dosimetry group for the Project 57 Air Monitoring study in 2015.

Analysis	**Matrix**	**Number of Results Reported**	**Number Within Control Limits[(a)]**
TLDs	Ambient Radiation	12	12

a) Based upon NVLAP criteria; absolute value of the bias plus one standard deviation < 0.3.

References

Desert Research Institute, 2010. *Desert Research Institute Quality Assurance Program Manual for the DOE Program*, October 2010.

U.S. Department of Energy, 2011. DOE O 414.1D, *Quality Assurance*, April 2011.

U.S. Department of Energy, 2013. *Soils Activity Quality Assurance Plan,* May 2012.

APPENDIX H: INSTRUMENTATION MODELS AND MANUFACTURERS

Instrument/Measurement	Model	Manufacturer
Wind speed	WXT-510	Vaisala Louisville, CO
Wind direction	WXT-510	Vaisala Louisville, CO
Precipitation	TE-525	Texas Electronics Dallas, TX
Temperature	WXT-510	Vaisala Louisville, CO
Relative humidity	WXT-510	Vaisala Louisville, CO
Solar radiation	CS-300	Apogee Instruments Logan, UT
Barometric pressure	WXT-510	Vaisala Louisville, CO
Soil temperature	Type T thermocouple	Omega Norwalk, CT
Soil moisture content	CS-616	Campbell Scientific Logan, UT
Ambient Particulate Profiler	Model 212	Met One Instruments Grants Pass, OR
Sensit H11-LINTM		Sensit, Inc. Redlands, CA
Datalogger		Campbell Scientific Logan, UT
Airborne particle collector		Hi-Q San Diego, CA
Thermoluminescent dosimeters		
BSNE Saltation Sand Traps	Big Spring Number Eight	Custom Products and Consulting LLC Big Spring, Texas

STANDING DISTRIBUTION LIST

Scott A. Wade
Assistant Manager for Environmental Mgmt
Nevada Field Office
National Nuclear Security Administration
U.S. Department of Energy
P.O. Box 98518
Las Vegas, NV 89193-8518
Scott.Wade@nnsa.doe.gov

Robert Boehlecke
Nevada Field Office
National Nuclear Security Administration
U.S. Department of Energy
P.O. Box 98518
Las Vegas, NV 89193-8518
Robert.Boehlecke@nnsa.doe.gov

Tiffany Lantow
Nevada Field Office
National Nuclear Security Administration
U.S. Department of Energy
P.O. Box 98518
Las Vegas, NV 89193-8518
Tiffany.Lantow@nnsa.doe.gov

Peter Sanders
Nevada Field Office
National Nuclear Security Administration
U.S. Department of Energy
P.O. Box 98518
Las Vegas, NV 89193-8518
Peter.Sanders@nnsa.doe.gov

Sarah Hammond, Contracting Officer
Office of Acquisition Management
NNSA Service Center
Pennsylvania and H Street, Bldg. 20388
P.O. Box 5400
Albuquerque, NM 87185-5400
Sarah.Hammond@nnsa.doe.gov

Jenny Chapman
DOE Program Manager
Division of Hydrologic Sciences
Desert Research Institute
755 E. Flamingo Road
Las Vegas, NV 89119-7363
Jenny.Chapman@dri.edu

Julianne Miller
DOE Soils Activity Manager
Division of Hydrologic Sciences
Desert Research Institute
755 E. Flamingo Road
Las Vegas, NV 89119-7363
Julie.Miller@dri.edu

Pat Matthews
Navarro, LLC
P.O. Box 98952
M/S NSF167
Las Vegas, NV 89193-8952
Patrick.Matthews@nv.doe.gov

Reed Poderis
National Security Technologies, LLC
P.O. Box 98521
M/S NLV082
Las Vegas, NV 89193-8521
poderirj@nv.doe.gov

*****Nevada State Library and Archives
State Publications
100 North Stewart Street
Carson City, NV 89701-4285

Archives Getchell Library
University of Nevada, Reno
1664 N. Virginia St.
Reno, NV 89557
dcurtis@unr.edu

DeLaMare Library
262
University of Nevada, Reno
1664 N. Virginia St.
Reno, NV 89557
dcurtis@unr.edu

Document Section, Library
University of Nevada, Las Vegas
4505 Maryland Parkway
Las Vegas, NV 89154
sue.wainscott@unlv.edu

†Library
Southern Nevada Science Center
Desert Research Institute
755 E. Flamingo Road
Las Vegas, NV 89119-7363

‡Nuclear Testing Archive
ATTN: Martha DeMarre
National Security Technologies, LLC
Mail Stop 400
PO Box 98521
Las Vegas, NV 89193-8521
demarrme@nv.doe.gov
(2 CDs)

∫Office of Scientific and Technical Information
U.S. Department of Energy
P.O. Box 62
Oak Ridge, TN 37831-9939

All on distribution list receive one electronic PDF copy, unless otherwise noted.

***** 12 paper copies
† 3 paper copies; CD with pdf (from which to print)
‡ compact disc only
∫ electronic copy (pdf) only